

# **Trigger mechanisms for sand intrusions**

Inferences from published data and investigation of 3D  
seismic data from the northern North Sea

**Iselin Torland Tjensvold**

Master thesis in Petroleum Geology



Department of Earth Science

University of Bergen

February 2018



## **Abstract**

Numerous publications have addressed subsurface sediment remobilization, in terms of geometries of the intrusions, where the intrusions occur, the parent unit of the intrusions and trigger mechanisms. Several authors have suggested different trigger mechanisms. The most frequently suggested trigger mechanism is earthquake induced liquefaction, but the suggestion is rarely well supported by evidence.

This thesis has investigated the possibility of a link between trigger mechanisms and the tectonic setting of the basin where sand intrusions occur. Several basins worldwide were investigated, and revealed an overrepresentation of subsurface sediment remobilization at convergent margins (including transform margins) and inverted passive margins. Convergent margins tend to show a relatively steep slope, and hence lateral pressure transfer was proposed as an important trigger mechanism at this type of tectonic setting. The subduction of the oceanic plate causes a step-wise compression of the deep sediments, and consequently the fluids are forced to escape rapidly, causing lateral fluid transfer to shallower strata. This process can result in rapid build-up of fluid pressures exceeding the lithostatic stress in the shallowest positions of the dipping (and permeable) strata, and trigger sand injections here.

Investigations of 3D seismic data from the northern North Sea was carried out to examine trigger mechanisms of sand intrusions at inverted passive margins. One phase of subsurface sediment remobilization was recognized within the Early Oligocene to Mid Miocene succession. Several evidence point towards one alternative to a trigger mechanism causing subsurface sediment remobilization in the northern North sea: 1) remobilization took place along the basin-flank transition, but not in the basin center, 2) a detachment surface was interpreted along the base of the subsurface sediment remobilization, and pose a good candidate as the slide plane, 3) mounds are arranged in N-S trending ridges along the basin-flank transition, and are hence parallel to the eastern margin and a potential headwall scarp, 4) liquefaction of mud and sand are triggered by shearing, 5) the interpreted slide plane is parallel to the bedding. Accordingly, shearing along the slope caused by a submarine slab slide was suggested as the main trigger mechanism of subsurface sediment remobilization in the northern North Sea. Submarine slab slides represent sedimentary processes that are common on inverted passive margins. Consequently, the interpretation is considered at least partly applicable to other inverted passive margins worldwide.



## Acknowledgements

The study was conducted at the Department of Earth Science, at the University of Bergen. Several persons have been important during the work of this thesis, and deserves to be acknowledged.

First, I would like to show my greatest gratitude to my supervisor Christian Hermanrud, for his genuine interest in the topic of my master thesis, his rapid and constructive feedback, and our good discussions. Thanks to everyone in the PESTOH-group, for valuable discussions.

I also want to thank my supervisor for giving me the opportunity to attend and present at a Sand Injectite conference in London. At the conference I got in touch with Antonio Grippa and Professor Andrew Hurst (both from the University of Aberdeen), who invited me to be their field assistant on a field trip to Panoche and Tumey Hills in California. I gratefully acknowledge the two, for giving me the opportunity to observe sand intrusions in the field, valuable discussions and explaining me different aspects of the sand intrusion networks when we were in the field. I also want to thank Statoil for funding my tickets to London, and SUCCESS for funding my tickets to California.

I would like to thank CGG and Statoil ASA, for providing the broadband seismic and well data that was necessary to complete this thesis.

A big thank you goes to Theodor Lien, Erlend Torland Tjensvold, Vilde Dimmen, David Peacock, Kristine Sleen Jensen, Jonas Aas Torland, Mads André Mæland and Karoline Thu Skjærpe for proof reading parts of my thesis and giving me constructive feedback. I would like to thank Marthe Fenne Vestly for assisting me in matlab. I would also like to thank my friends at the University of Bergen, especially Martin Kjenes, Karoline Thu Skjærpe, Theodor Lien, Ida Marie Gabrielsen and my fellow students working at Grotten for great company the last months.

Last, but not least, I would like to thank my family, for always thinking of me, being supportive and reminding me that there is a world outside the University too. It means a lot to me. The greatest thank you goes to my boyfriend Espen Tangnes. Thank you for always being motivating when I needed an extra push, always being cheerful and patient when I needed it the most. These two years would not have been the same without you.

Bergen, February 2018

Iselin Torland Tjensvold



## Table of contents

Abstract .....	I
Acknowledgements .....	III
1. Introduction .....	1
2. Geological Background of the northern North Sea .....	5
2.1 Pre-Cenozoic .....	5
2.1.1 The Paleozoic (542-251 Ma) .....	5
2.1.2 The Mesozoic (251-66 Ma) .....	6
2.2 The Cenozoic (66 Ma – today) .....	8
2.2.1 Palaeocene .....	9
2.2.2 Eocene .....	9
2.2.3 Oligocene .....	10
2.2.4 Miocene .....	11
2.2.5 Pliocene and Pleistocene .....	13
3. Remobilization of sand .....	15
3.1 The sand remobilization process .....	15
3.2 Trigger mechanisms .....	16
3.2.1 Shearing caused by large magnitude earthquakes .....	17
3.2.2 Shearing caused by meteorite impacts .....	17
3.2.3 Tectonic stress in tectonic active areas .....	17
3.2.4 Rapid fluid migration of hydrocarbons or pore fluids into an unconsolidated sand body .....	18
3.2.5 Build-up of excessive pore pressure due to depositional processes .....	18
3.2.6 Formation of polygonal faults .....	19
3.2.7 Rapid compaction and subsidence linked to glaciation .....	19
3.2.8 Lateral pressure transfer .....	19
3.2.9 Experiments for triggering of sand remobilization .....	19
3.3 Pore fluid pressure and the centroid concept .....	21
3.4 Submarine slides .....	22
3.5.1 Geometries and seismic identification of remobilized sand .....	24
3.5.2 Seismic identification of extrusive sands .....	25
3.5.3 Seismic signatures and geometries of intrusive sands .....	25
4. Data and methods .....	29
4.1 Basinal setting of remobilized sands worldwide .....	29
4.1.1 Limitations .....	30

4.1.2	Workflow .....	31
4.2	Northern North Sea seismic data.....	32
4.2.1	Seismic interpretation and workflow .....	33
4.2.2	Surface maps .....	38
4.2.3	Seismic attributes .....	38
4.2.4	Uncertainties.....	38
4.3	Well analyses.....	39
4.4.	Workflow for inverted passive margins .....	41
5.	Basinal setting of remobilized sands worldwide.....	43
5.1	Basins at convergent and strike-slip margins .....	44
5.2	Basins at inverted passive margins (flank and toe of slope) .....	56
5.3.	Occurrence of remobilized sand linked to basinal setting: summary.....	61
6.	Observations from the northern North Sea .....	67
6.1	Seismic observations in area 1A .....	70
6.1.1	Shapes of mounds.....	71
6.1.3	Distribution of mounds.....	76
6.1.4	Seismic observations outside the mounds .....	78
6.2	Seismic observations in area 1B.....	81
6.3	Seismic observations in area 1C.....	83
6.4	Seismic observations in area 2 .....	85
6.4.1	Shapes and distribution of mounds .....	85
6.4.2	Unmounded areas .....	87
6.5	Seismic observations in area 3A .....	88
6.5.1	Shapes and distribution of mounds .....	89
6.5.2	Unmounded area .....	92
6.6	Seismic observations in area 3B.....	95
6.7	Lithology distribution in mounds and in unbounded areas.....	99
6.7.1	Lithology distribution in mounds vs. unbounded areas in the basin.....	99
6.7.2.	Distribution of sand in unbounded areas at the flank.....	102
6.7.3	Uplift vs. sand thickness.....	104
7.	Interpretation .....	107
7.1	Suggested trigger mechanisms for sand intrusions at convergent and transform margins .....	107
7.2	Post-depositional subsurface remobilization at inverted passive margins, based on the case study from the northern North Sea .....	111
7.2.1	Evidence of subsurface remobilization in the northern North Sea.....	112



7.2.2 Slope failure and submarine slab slides .....	112
7.2.3. Distribution of mounds.....	114
7.2.4 Lithology distribution in CSS-4 to CSS-6.....	116
7.2.5 Formation of sand intrusions in the northern North Sea basin.....	118
8. Future work .....	123
8.1 The literature study.....	123
8.2 The case study from the northern North Sea.....	123
9. Conclusion.....	124
References .....	127
Appendix .....	141
Appendix A: Field report .....	141
Appendix B: Complete version of Table 5-1 .....	147



## 1. Introduction

Sand intrusions were described for the first time in 1827 (Murchison, 1827), but the importance of the subject was not appreciated until Dixon et al. (1995) discovered their influence on hydrocarbon reservoirs. Since then sand intrusions have been described in numerous publications, based on locations from all over the world. Several trigger mechanisms have been proposed in the literature, e.g. earthquakes, meteoritic impacts and rapid fluid migration. The most frequently suggested trigger mechanism is earthquake induced liquefaction. What is a common trend when different authors are proposing trigger mechanisms, is that evidence that explains the proposed trigger mechanism is rarely well documented.

Jolly and Lonergan (2002) divided occurrences of sand intrusions into groups based on the sedimentary environment where the subsurface sand remobilization occurred. They evaluated already proposed trigger mechanisms, but they did not link the trigger mechanisms to processes that are typical for the specific basin settings that they addressed. Jonk et al. (2005b) also presented a short overview of six locations where sand intrusions occur. Similar to Jolly and Lonergan (2002) they linked the location of the sand intrusions to the sedimentological settings, but not to the physical processes characteristic for these specific settings. Further on, they described fluid flow through the sand injectites. Huuse et al. (2010) presented a table displaying locations worldwide where sand remobilization, mud remobilization, gas hydrates and surface seeps occur. In the table they linked the different phenomena to i.a. the tectonic setting, the driver and the trigger mechanism. However, the link between trigger mechanisms and basinal setting were not further described in the text. The mud and sand remobilization were by Huuse et al. (2010) described as phenomena occurring during separate events.

The widespread occurrence of sand injections in the geological settings where sand intrusions occur frequently, demonstrate that trigger mechanisms that are characteristic for such settings are comparatively common. The understanding of what these mechanisms are is still debated.

The North Sea basin pose a good example of large scale subsurface sediment remobilization. Here, sand intrusions most frequently occur in Eocene to Oligocene strata (Jolly and Lonergan, 2002; Hurst and Cartwright, 2007). Previous studies that addressed sand intrusions in the North Sea, focused on local areas. Apparently, the distribution of remobilized sand in the North Sea basin has not yet been described on a regional scale. Christensen (2015) observed evidence of two phases of remobilization within the Early Oligocene to Mid Miocene succession, and suggested that the remobilization was related to sliding along a detachment surface, due to uplift

of the eastern basin flank. This suggestion was based on observations from the Johan Sverdrup area in the North Sea, i.e. only a limited area.

The sedimentary processes that occur in the northern North Sea are characteristic of inverted passive margins in general, and hence the observations from the area are considered applicable to other inverted passive margins. One would therefore expect that observations from the northern North Sea, even if it is based on a limited time interval, is at least partly applicable to other inverted passive margins.

The aim of this thesis was to investigate the possible link between trigger mechanisms and the tectonic setting of the basin where sand intrusions occur. Hence, it was large scale subsurface sediment remobilization that was addressed, although smaller scale sand intrusions also are described in the literature. This thesis focuses on sand intrusions at both convergent and inverted passive margins, but with different approaches.

The tectonic setting and sandstone geometries at the time of subsurface sand remobilization was compared to a number of different basins at convergent and transform margins. This thesis advocates a trigger mechanism that is common for these sand intrusion provinces, and that is linked to the specific tectonic setting. For convergent and transform margins the trigger mechanism was suggested on the basis of published data.

The Panoche and Tumey hills is an area that shows the best exposed parent-intrusion network in the world (Cartwright, 2010). Due to the well exposed sand intrusion networks, the Panoche and Tumey hills are frequently used as analogues to large-scale sand intrusions observed in seismic, independent of the tectonic setting of the basin. A fieldtrip to the Panoche and Tumey hills was attended to learn more about sand intrusions at convergent margins. A report from this fieldtrip is included in Appendix A.

In comparison to the convergent margins, the trigger mechanism associated to inverted passive margins was suggested on the basis of published data and a case study from the northern North Sea. To analyze regional characteristics of the sand intrusions in the study area in the northern North Sea, a 3D seismic dataset that covers an area from 60°N to 62°N was interpreted. Reflectors were interpreted within an interval that consist of Early Oligocene to Mid Miocene strata (top CSS-3 to top CSS-6). To verify the work, the interpretation from this project was compared to interpretations displayed in Faleide et al. (2002). The upper Hordaland Group was investigated in terms of how mounds, chaotic reflectors and continuous reflectors were

distributed within the study area. 34 wells were analyzed to investigate the total amount of sand in the study area and the amount of uplift of the mounds.



## 2. Geological Background of the northern North Sea

Remobilization of sand is a phenomenon mainly recognized within the Cenozoic succession (Figure 2-1), and hence the Cenozoic era represents the focus of this master project. The pre-Cenozoic period is important for the development of today's North Sea basin, and will thus be briefly described, focusing on the most important events. The Cenozoic era will be described in more detail.

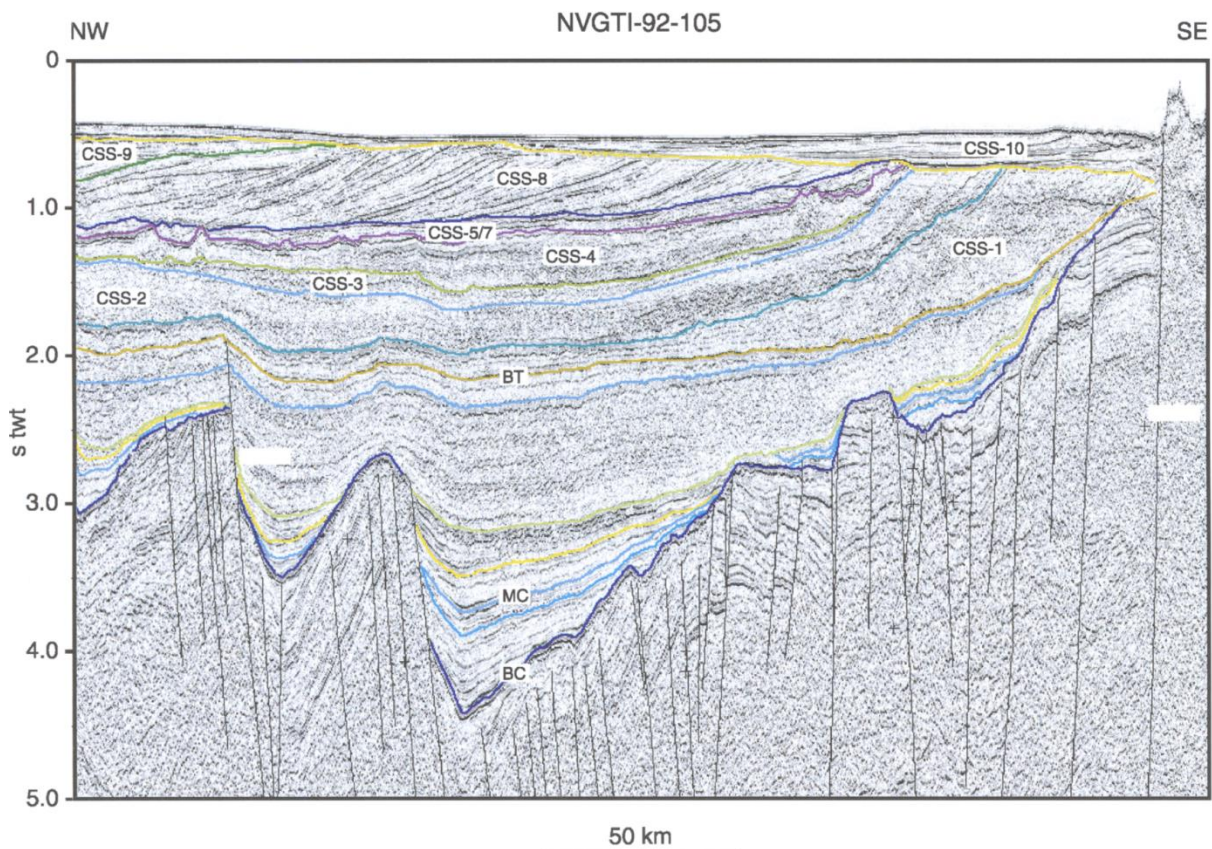


**Figure 2-1:** Regional seismic line NVGTI-92-105, from Faleide et al. (2002). The seismic line goes through well 35/12-1 and 34/07-1. BT marks Base Tertiary, MC marks Mid Cretaceous and BC marks base Cretaceous. The seismic sequences are annotated by the CSS-sequences, which will be introduced in chapter 2.2.

### 2.1 Pre-Cenozoic

#### 2.1.1 The Paleozoic (542-251 Ma)

The Paleozoic era encompasses the Cambrian, Ordovician, Silurian, Devonian, Carboniferous and Permian periods, respectively. The main event in the North Sea area during the Palaeozoic was the formation of the Caledonian Orogeny. It occurred in Late Silurian to Early Devonian time when Laurentia and Baltica collided. Approximately 60 million years later, Avalonia entered the collision zone. As Figure 2-2 shows, Baltica was situated in the east, Laurentia approached from the west, and Avalonia from the south. The latter started as a magmatic arc

and was originally part of Gondwana, until it broke loose from the super continent during Early Ordovician. The collision between the continents occurred as a response to the closing of the northern and southern Iapetus oceans (Coward et al., 2003).

In the North Sea the collision involved Laurentia and Scandinavia (part of Baltica) and commenced already in Ordovician, when island arc material was pushed onto the accretionary prism. The convergence continued as south-easterly trending overthrusting onto Baltica, which persisted until Silurian time (Coward et al., 2003).

The collapse of the Caledonian Orogeny occurred in Devonian to Carboniferous, and is also an important part of the North Sea Basin evolution. Pull-apart basins developed, and created grabens, in addition to a drastic increase of the sediment influx linked to the collapse and erosion of the mountain range (Coward et al., 2003).

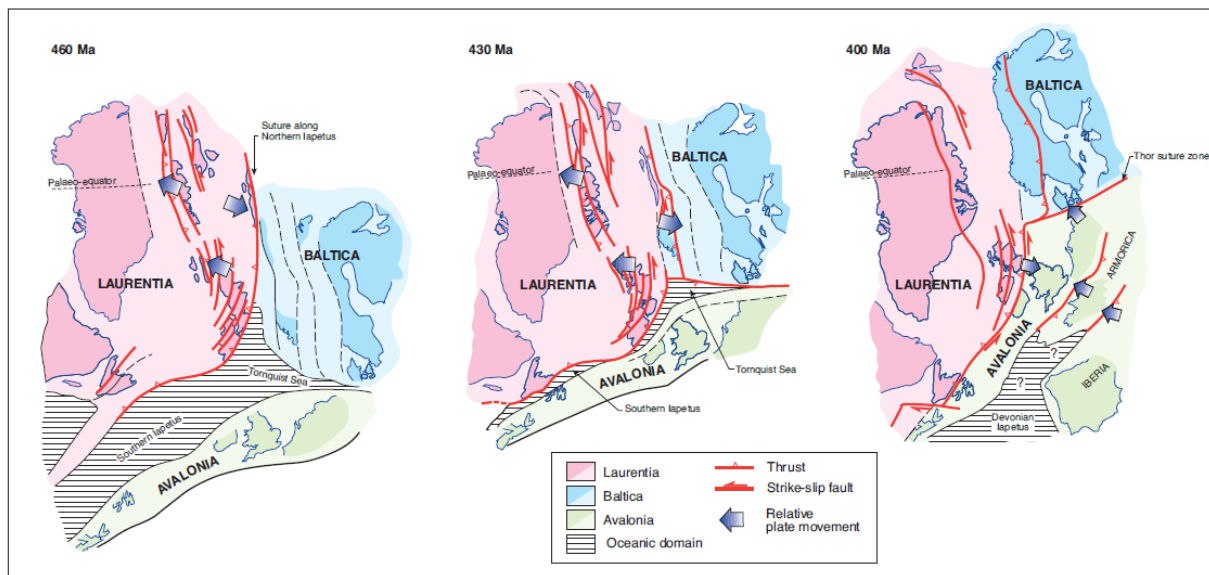


**Figure 2-2:** Illustration the formation of the Caledonian orogeny (Coward et al., 2003).

### 2.1.2 The Mesozoic (251-66 Ma)

The Mesozoic era is divided into three periods, Triassic, Jurassic and Cretaceous. Two major rifting episodes characterize the pre-Cenozoic era, the first occurred in Permo-triassic and the second in Mid to Late Jurassic. Each rifting episode was followed by a period recognized by thermal relaxation and subsidence (Færseth, 1996; Whipp et al., 2014).

The Permo-Triassic rifting event represent the break-up of the supercontinent, Pangea (Færseth, 1996). The rifting resulted in tilting of fault blocks and tilted half grabens, which became sedimentary basins. The sedimentary basins represented a major depocenter, bound by faults that probably continued through the entire crust (Færseth, 1996; Whipp et al., 2014). During



Triassic, the half-grabens were filled and draped by alluvial, fluvial and lacustrine sediments, which represent the Hegre Group (Whipp et al., 2014). The continental environment persisted until Early Jurassic time, and during this period the Staffjord Group was deposited. The Staffjord Group represents an important hydrocarbon reservoir in the northern North Sea. The Dunlin Group overlies the Staffjord group, and consists of a marine shale deposited during a transgressive period (Steel, 1993).

In Mid Jurassic, the northern North Sea was characterized by tectonic uplift, and hence a relative sea level fall. As a result of the relative sea level fall, followed by relative sea level rise, the Brent delta developed as a regressive-transgressive delta system, representing the Brent Group. The Brent Group represents important hydrocarbon reservoirs in the North Sea (Helland-Hansen et al., 1992).

The second rifting event during the Mesozoic took place from Mid to Late Jurassic, and was initiated simultaneously as the deposition of the Brent Group. The extension caused reactivation of the faults that were formed during the Permo-Triassic rifting, in addition to generating new faults (Færseth, 1996). The rifting mainly caused a deepening of the basin, and consequently drowning of the Brent delta, and deposition of the Viking Group. The Viking Group is solely characterized by marine sediments (Ziegler, 1975; Gautier, 2005; Whipp et al., 2014).

During the Late Kimmeridgian to Late Berriasian (Late Triassic to Early Cretaceous) a major flooding occurred, creating an anaerobic marine environment. The marine anoxic conditions, together with high organic productivity, developed favourable conditions for generation of hydrocarbon source rocks. The deep-marine mudstone, represented by the Draupne Formation, was deposited throughout this period and posed an important source rock in the North Sea (Gautier, 2005).

In summary, the North Sea basin developed as a result of three major rifting episodes, each followed by a period of thermal relaxation and subsidence (Ziegler and Van Hoorn, 1989; Nøttvedt et al., 1995):

1. Devonian extension in an intermontane basinal setting.
2. Permo-Triassic rifting, characterized by low relief and alluvial plain settings. This rifting episode marks the breakup of the supercontinent Pangea.
3. Late Jurassic-Cretaceous rifting, characterized by deep marine conditions.

The three rifting phases above caused thinning of the crust, and hence lowering of the crustal surface relief, causing changes in the accommodation space and sediment supply (Nøttvedt et al., 1995; Ravnås et al., 2000).

### 2.2 The Cenozoic (66 Ma – today)

The tectonically passive Cenozoic is the youngest geological era, characterized by several uplift and subsidence episodes above the pre-existing rift basin. The era consists of the epochs: Palaeocene, Eocene, Oligocene, Miocene, Pliocene and Pleistocene, respectively, and they will be addressed in the text in the same order. Jordt et al. (1995) divided the Cenozoic succession into 10 seismic sequences based on the stratigraphic framework of the North Sea (Figure 2-1). The division of the Cenozoic seismic stratigraphic sequences (CSS-sequences) was based on biostratigraphic data from a selection of key wells, presented by Eidvin and Riis (1992); Galloway et al. (1993); Gradstein and Backstrøm (1996); Martinsen et al. (1999); Eidvin et al. (2000). The division was later improved by Jordt et al. (2000) and Faleide et al. (2002).

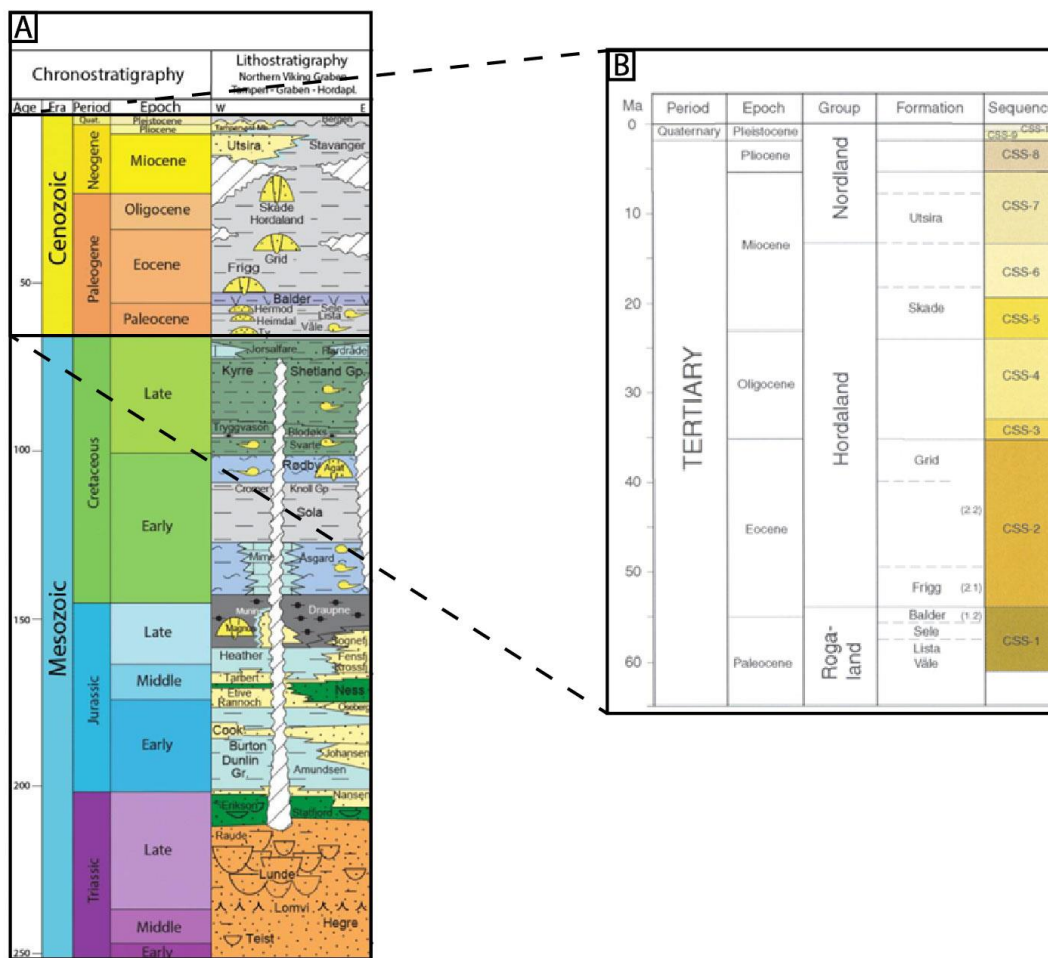


**Figure 2-3:** A) Displays the lithostratigraphy of the northern North Sea (from Lien (2017), modified after Gradstein et al. (2010)). B) Displays a zoom-in of the lithostratigraphy of the Cenozoic succession, put into context with the CSS-sequences (from Faleide et al. (2002)).

### **2.2.1 Palaeocene**

One of the two main uplift episodes are registered in Palaeocene, and Faleide et al. (2002) argue that it is related to the arrival of the Iceland Plume, which initiated the break-up of the northeast Atlantic Ocean. The tectonic uplift caused erosion of the provenance area, generating sand rich clinofolds building out into the North Sea basin. The clinofolds form sediment wedges, most likely due to subsidence of the basin in combination with increased sediment supply. As a result of the sediment infill of the North Sea basin, the relative sea level decreased. The sediments deposited in the North Sea basin during Palaeocene constitute the Rogaland Group (Isaksen and Tonstad, 1989). The main provenance area was located on the East Shetland Platform and the Scottish Highlands in the west. Other provenance areas were located at the eastern part of the Scandinavian continental platform (Jordt et al., 1995; Faleide et al., 2002).

The Mesozoic sediments deposited in the rift basin and on the platform were exposed to differential compaction, caused by reactivation of the Mesozoic graben faults, especially along the margin of the West Shetland Basin. The syn-depositional faulting occurred as a result of regional subsidence (Milton et al., 1990).

During the Paleocene–Eocene transition, the North Sea experienced a regional transgression, which is observed in the Late Paleocene–Early Eocene succession as aggradational and uniform layers. The transgression was onset by volcanism in the west, continued by uplift of the Atlantic continental margin and regional tectonic subsidence in the east (Jordt et al., 1995). The source area of the Late Paleocene–Early Eocene succession was most likely the Basaltic province formed in relation to the North Atlantic rift zone (Faleide et al., 2002).

### **2.2.2 Eocene**

The deposition of the Rogaland Group persisted until the Early Eocene. At this time, the North Sea basin was still subsiding, and the opening of the North Atlantic Ocean was complete (Ziegler, 1975; Isaksen and Tonstad, 1989). Volcanic activity occurred as a response to the opening of the North Atlantic Ocean, and hence volcanic material appear in the upper part of Rogaland Group (the Balder Formation) (Isaksen and Tonstad, 1989).

The transition from CSS-1 to CSS-2 marks a break in deposition. CSS-2 is characterized by a major transgression event, where the flooding caused deposition of mud in the North Sea basin. The initiation of CSS-2 coincides with the base of the Hordaland Group (Figure 2-3). After the break, there was a shift in deposition to a more basinward direction, which is observed as onlapping onto the basin margins (Faleide et al., 2002). Deepwater and slope processes were the main depositional feature in the formation of the Eocene succession, e.g. the deposition of

Lower Eocene Frigg Formation deposited as a submarine fan, sourced from the East Shetland Platform (Faleide et al., 2002).

The sediments that were deposited during Mid Eocene time and onwards consist of mud and silt, whilst sand was deposited episodically at the fringe of the basin (Faleide et al., 2002). During Late Eocene, the northern North Sea was exposed to tectonic uplift and relative sea level fall, which caused erosion and starvation in large parts of the northern North Sea basin, but it also promoted delta systems to build out from west into the North Sea (Jordt et al., 1995; Faleide et al., 2002). The sandy Grid Formation was deposited during this period, and consist of sand interbedded with claystone sourced, from the East Shetland Platform (Isaksen and Tonstad, 1989).

The transition between Eocene and Oligocene marks a major global climate shift, from greenhouse to icehouse conditions and hence a drop in bottom water temperatures (4-5°C) (Rundberg and Eidvin, 2005). Rundberg (1989) observed changes in the clay mineralogy in the northern North Sea, and based on similar observations made in other parts of the world, it was suggested that the changes were linked to the global cooling of the climate (at this time). The mineralogical changes involved initiation of siliceous-rich sedimentation in the northern North Sea. Based on biostratigraphical data, a hiatus is recognized between Eocene and Oligocene, which also marks the boundary between CSS-2 and CSS-3 (Jordt et al., 2000).

### **2.2.3 Oligocene**

CSS-3 represents the Early Oligocene succession (Figure 2-3). Though Faleide et al. (2002) describe thinning of the Oligocene succession towards east and west, they also emphasize the East Shetland Platform as the main provenance area of the North Sea basin during Oligocene. During Early Oligocene, the first major accumulation of sand was fed to the northern North Sea, sourced by the East Shetland Platform (Rundberg and Eidvin, 2005; Eidvin et al., 2014). Rundberg and Eidvin (2005) suggest that the high sediment influx was caused by a compressive tectonic episode, linked to development of a new plate-configuration. The accumulated sand is in some areas measured to a maximum thickness of 400m. Consequently, it is assumed that the compressive regime have generated major uplift episodes and erosion of the East Shetland Platform to generate such large volumes of sand (Figure 2-4; Rundberg and Eidvin, 2005). Apart from the sandy pulses derived from the East Shetland Platform during uplift episodes, the Oligocene sedimentation was dominated by mud in the northern North Sea (Eidvin et al., 2014).

The boundary between CSS-3 and CSS-4 is marked by the intra-Oligocene unconformity formed as a result of uplift of Fennoscandia together with parts of the North Sea basin, which caused a relative sea level fall (Jordt et al., 2000; Faleide et al., 2002). The regression was closely followed by a minor relative sea level rise, and hence the Late Oligocene succession was dominated by aggradation of silt and clay, with occasional uplift episodes generating accumulation of sand in the basin. By the end of Oligocene, the North Sea had become a narrow and relatively shallow basin, due to compressional tectonics causing uplift and sediment infill (Faleide et al., 2002).

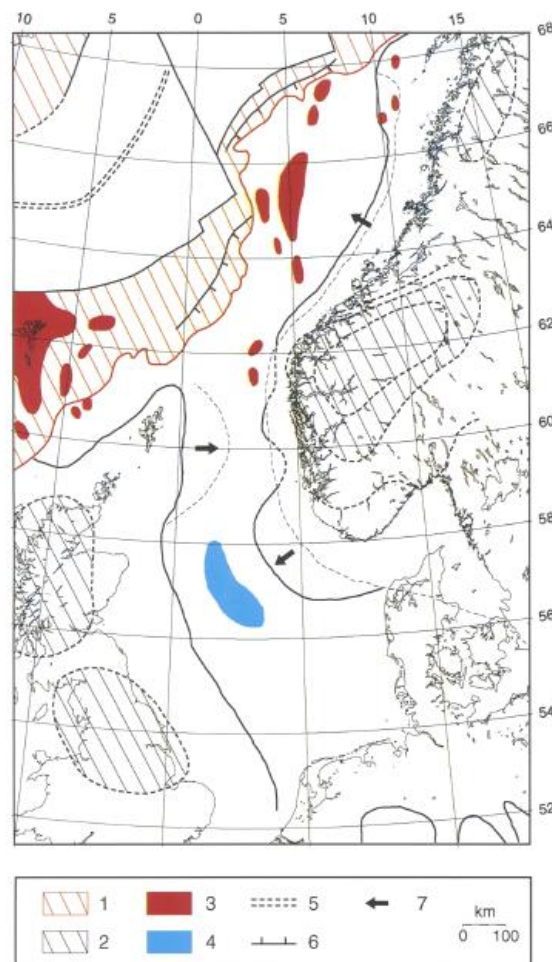


**Figure 2-4:** The figure displays the regional setting of the North Sea basin during Early Oligocene. 2) Areas exposed to uplift, 4) main depocenters and 7) outbuilding directions (Figure 15 in Faleide et al., 2002).

### 2.2.4 Miocene

The Miocene succession is divided into three sequences: CSS-5, CSS-6 and CSS-7 (Figure 2-3). According to Faleide et al. (2002) the Miocene sequences are present in the northern North Sea. However, because the depocenters are located in the south, the sequences thin towards north and are in some areas absent. In other areas the thickness of the sequences are below

seismic resolution, which makes it hard to distinguish the different sequences within the Oligocene-Miocene succession.

The sedimentation pattern during Early Miocene resembles the one in Late Oligocene. What separates them is a change in depocenter, from the Tampen area to the Viking Graben (Faleide et al., 2002). A new major sand influx episode occurred in Early Miocene, and deposited what today is recognized as the Skade Formation (maximum thickness 300m). The Skade Formation was sourced from the East Shetland Platform, deposited in an open marine environment and consists of sand interbedded with claystone (Isaksen and Tonstad, 1989; Rundberg and Eidvin, 2005; Eidvin et al., 2014). It is probably a continuation of the Hutton sands at UK sector (Gregersen and Johannessen, 2007). Except from the high sediment influx during the deposition of the Skade Formation, the deposition rate during Early to Mid Miocene was characterized by a low accumulation rate (Faleide et al., 2002).

The boundary between the Hordaland Group and the Nordland Group is characterized by a mudstone sequence, most likely formed in a distal part of a submarine fan, possibly the Frigg fan (Eidvin et al., 2013). The Mid Miocene Unconformity is located on the top of this mudstone sequence (Faleide et al., 2002; Rundberg and Eidvin, 2005). During the hiatus, the top Hordaland Group was re-worked by post-depositional processes, and hence parts of the surface do not display primary depositional features (Løseth et al., 2003; Løseth et al., 2013).

There are uncertainty linked to how the hiatus was formed, e.g. if it was formed submarine or subaerial (e.g. Jordt et al. (1995) and Rundberg and Eidvin (2005)). Rundberg and Eidvin (2005) have not observed any subaerial evidence in the wells they examined, but instead they found evidence suggesting a shallowing of the basin due to a relative sea level fall. Faleide et al. (2002) also suggest that the hiatus was triggered by a glacio-eustatic sea level fall, together with regional uplift. In contrast, Martinsen et al. (1999) and Løseth et al. (2013) propose that the entire North Sea was uplifted and then subaerially eroded during the formation of the Mid Miocene Unconformity.

During Late Miocene (CSS-7), the North Sea basin was almost closed due to tectonic uplift of surrounding landmasses. At this time, the shallow northern North Sea basin operated as a link between the deeper central North Sea and the Norwegian – Greenland Sea (Faleide et al., 2002; Rundberg and Eidvin, 2005).

The Cenozoic era is characterized by three major episodes with significantly sand rich sediment influx to the North Sea basin, and the third episode occurred in Mid Miocene to Early Pliocene

time. The large sand deposit is recognized as the Utsira Formation (Rundberg and Eidvin, 2005; Gregersen and Johannessen, 2007). It was deposited in a shallow marine environment, on top of the Mid Miocene unconformity, mainly sourced from the East Shetland Platform (Galloway et al., 1993; Gregersen et al., 1997; Martinsen et al., 1999; Rundberg and Eidvin, 2005).

### **2.2.5 Pliocene and Pleistocene**

Sediments derived from the Norwegian landmasses, prograded westwards and downlapped onto the Utsira Formation. The glaciation processes were initiated as a continuation of the uplift and subsidence episodes during Miocene-Pliocene, and became the main sediment source (Jordt et al., 1995; Faleide et al., 2002). The controlling factor affecting the westward progradation was the variation in eustatic sea level, causing changes in accommodation space, which resulted in the high-frequency sequences (Sørensen et al., 1997).

A new major uplift phase occurred in Late Pliocene to Early Pleistocene time, partly resulting from isostatic uplift due to unloading caused by glacial erosion. Metamorphic phase changes in the mantle, intra-plate stress, erosion and flexural effects also amplified the uplift episode (Jordt et al., 1995; Faleide et al., 2002).

CSS-9 and CSS-10 are of Pleistocene age (Figure 2-3). In short, Pleistocene is a continuation of the trends described in Late Pliocene, with erosion and progradation of glacial derived material. The Pleistocene succession is deposited on top of the Late Pliocene progradational strata forming an angular unconformity. Pleistocene deposits is reworked by glacial processes, which were intensified during this epoch (Faleide et al., 2002).





### 3. Remobilization of sand

Some background knowledge about remobilization of sand, and the different processes linked to the phenomenon is essential to get a good understanding of the topics discussed in this thesis. The concepts of slope failure and the centroid effect will also be described, as these may be closely linked to trigger mechanisms of subsurface sand remobilization. The following chapter will also provide information on recognition of sand intrusions from seismic data.

Sand intrusions were first described by Murchison (1827), but the importance of the phenomenon was not appreciated until Dixon et al. (1995) showed that sand injectites can be important in petroleum exploration and production. Sediment remobilization occur as a result of pore fluid flow processes in the subsurface, at relatively shallow depths (<1km burial; Lonergan et al., 2000; Jonk, 2010). Sand remobilization is characterized as a syn- or post-depositional phenomenon, which moves sand away from where it was originally deposited. (Lonergan et al., 2000; Hurst et al., 2003a; Hurst et al., 2003b; Szarawarska et al., 2010). Here, post-depositional sand remobilization will be addressed. In this thesis, the term “remobilized sand” and “subsurface sand remobilization” are used to describe liquefied or fluidized sand that is either injected into surrounding strata (sand injectites/intrusions or extrusive sand/extrudites) or remobilized within the layer. The sand injection may happen upwards, downwards or lateral, depending on the easiest migration route (Parize and Friès, 2003; Jonk et al., 2007b; Beyer, 2015). If the remobilized sand reaches the seafloor it is known as “extrusive sand” or a “sand extrudite” (Hurst et al., 2006).

#### 3.1 The sand remobilization process

When a sand is remobilized, it retains its density, but the viscosity is reduced to the viscosity of the fluid. Two different mechanisms can cause this situation, fluidization and liquefaction. Fluidization is the process where an external fluid is injected into the sediment. If the velocity of the fluid is higher than the sinking velocity of sand grains in water, the fluid flow will carry the grains. In contrast, liquefaction occurs due to reorganisation of the grains, causing the grain framework to collapse and expulsion of excessive pore fluids (Lowe, 1979; Maltman and Bolton, 2003). In this thesis, sand remobilization includes both liquefaction and fluidization mechanisms, and are together referred to as liquidization (Allen, 1982).

For sediment remobilization to be possible, there are certain prerequisites that needs to be fulfilled. First, a *parent sand* (the source of the sand) must be present. The parent sand is an unconsolidated sand body, and is therefore capable of being remobilized. Sand injectites are commonly detached from its source, which makes it hard to identify parent beds (Diller, 1890; Peterson, 1966; Parize, 1988).

Secondly, the parent bed must be overlain by a cohesive and *low permeable seal* (e.g. claystone), thus acting as a pressure barrier (Cartwright et al., 2007). Consequently, some of the pore fluids entrapped in the sand during deposition will remain in the pores despite the weight of the overburden, thereby generating overpressure (Jonk, 2010).

Build-up of fluid overpressure in the unconsolidated sand body is crucial in the process to make sediment remobilization possible (Jolly and Lonergan, 2002). Overpressure is reached when the fluid pressure exceeds the hydrostatic pressure, which constitutes the weight of the water column (Maltman, 1994; Swarbrick and Osborne, 1998). In addition to the presence of overpressure fluids, a *trigger mechanism* is necessary to initiate the remobilization. Different trigger mechanisms are presented and evaluated in section 3.2.

To summarize, the remobilization process is dependent of three prerequisites:

1. A parent sand, which is the source of the remobilized sand.
2. A seal represented by a low permeable rock, to make overpressure build-up possible.
3. A trigger mechanism is necessary to initiate fluidization or liquefaction, which thereby result in sand remobilization.

### 3.2 Trigger mechanisms

The trigger mechanism needed to initiate sand remobilization is, in this thesis, defined as a relatively rapid event that creates a steep overpressure gradient between the unconsolidated sand body and shallower strata. A steep pressure gradient may also develop internally in a layer, e.g. by local grain rearrangement. Grain rearrangement results in a denser grain packing and thereby an excess fluid volume. This fluid volume will be overpressured unless it can be drained as rapid as the compaction caused by the grain rearrangement.

Several different trigger mechanisms have been proposed in the literature, but the chain of events from trigger to remobilization is rarely well proved and explained. The different suggested mechanisms include: 1) shearing caused by large-scale earthquakes, 2) shearing

caused by meteoritic impacts, 3) tectonic stress in tectonic active areas, 4) rapid migration of hydrocarbon or pore fluids into the unconsolidated sand body, 5) build-up of excessive pore pressure due to depositional processes, 6) formation of polygonal faults, 7) rapid compaction and subsidence linked to glaciation, and 8) lateral pressure transfer. These mechanisms are all explained in the following subchapters.

### **3.2.1 Shearing caused by large magnitude earthquakes**

Shearing caused by large magnitude earthquakes as a trigger mechanism for remobilization of sand, is the most commonly proposed trigger mechanism in the literature (Fuller, 1912; Gill and Kuenen, 1957; Reimnitz and Marshall, 1965; Hesse and Reading, 1978; Obermeier, 1989; Saucier, 1989; Sims and Garvin, 1995; Galli, 2000; Jolly and Lonergan, 2002; Briedis et al., 2007; Huuse et al., 2007; Cartwright, 2010; Huuse et al., 2010; Szarawarska et al., 2010; Wild and Briedis, 2010). Large magnitude earthquakes are capable of fluidizing sand at shallow depths (approximately 10m). Whereas, on greater depths liquidization of sand by seismic activity is unlikely. At greater depths the strata are exposed to larger overburden stress, but still shallow enough for pore pressures to be stable. Sand injection occur at 500-1000m depth, and this implies that even the largest magnitude earthquakes are incapable of triggering sand remobilization at these depths (Jackson, 2007).

### **3.2.2 Shearing caused by meteorite impacts**

Shearing caused by meteorite impacts was a frequently proposed trigger mechanism in the past (Huuse et al., 2007; Huuse et al., 2010; Szarawarska et al., 2010; Hurst et al., 2011). Meteorite impacts are rare events, and they are randomly distributed across the globe. While such impacts may have resulted in sand remobilization some places, they cannot be a main trigger mechanism for sand injectites worldwide: a) because sand injectites are a common phenomenon, and b) because they do not occur randomly, but are confined to certain basin types and time periods.

### **3.2.3 Tectonic stress in tectonic active areas**

Winslow (1983) proposed tectonic stress in tectonic active areas to be a possible trigger mechanism for remobilization of sand. The suggestion is based on fieldwork carried out in the Southern Patagonia and Tierra del Fuego (the southern Andes) fold and thrust belt, where it was observed clastic dike swarms that had been injected into the Cenozoic foreland fold and thrust belt. Dike swarms occur at the toe of thrust faults, intruding into the hanging wall. Based on these observations, sand remobilization seems to be related to the tectonic compression, and hence this type of trigger mechanism is only relevant for tectonic active margins. Other authors

have also proposed tectonic stress as a as an important trigger mechanism (e.g. Peterson, 1966; Huang, 1988).

### **3.2.4 Rapid fluid migration of hydrocarbons or pore fluids into an unconsolidated sand body**

Rapid fluid migration of hydrocarbons or pore fluids into an unconsolidated sand body as a trigger mechanism for sand remobilization have been suggested by several authors (Jenkins, 1930; Brooke et al., 1995; Cole et al., 2000; Lonergan et al., 2000; Yardley and Swarbrick, 2000; Jolly and Lonergan, 2002; Davies et al., 2006). This proposal involves migration of hydrocarbon or pore fluids into an unconsolidated sand body to increase the overpressure, resulting in fluidization of the sand. If migration of hydrocarbons would pose an important trigger mechanism, sand intrusions would be expected to occur more frequently above hydrocarbon reservoirs and reservoirs that reveal shows of hydrocarbons, e.g. in the North Sea.

Davies et al. (2006) have suggested the mineral transformation from opal A to CT as an external fluid source, and hence a source to generate overpressure and fluidization. The basis of their suggestion is that the mineral transformation from opal A to opal CT occurs at depths of less than 500m. In the transformation process the porosity is reduced and water is released rapidly.

Expansion of hydrothermal fluids due to igneous intrusions was suggested as a trigger mechanism for sand intrusions by e.g. Moreau et al. (2012); Hartmann et al. (2013); Pinto et al. (2015). The process is onset by heating of pore fluids, causing the pore fluid pressure to rise and potentially migrate into or within an unconsolidated sand body. This type of trigger mechanism is capable of fluidizing large volumes of sand (Moreau et al., 2012).

Tidal pumping (Taj et al., 2014) is a trigger mechanism associated to coastal plains. This process is only capable of remobilizing small amounts of sand, and hence it will not be further described in this thesis.

### **3.2.5 Build-up of excessive pore pressure due to depositional processes**

Build-up of excessive pore pressure due to depositional processes includes passage of storm waves (Allen, 1985; Martel and Gibling, 1993), slumping (Gill and Kuenen, 1957; Truswell, 1972), and channel switching (Hiscott, 1979). This trigger mechanism refers to small scale sand remobilization, and will hence not be evaluated further in this thesis.

### **3.2.6 Formation of polygonal faults**

Formation of polygonal faults has also been suggested as a trigger mechanism for the formation of sand intrusions and extrudites (Lonergan and Cartwright, 1999; Cosgrove and Hillier, 2000; Gras and Cartwright, 2002; Hillier and Cosgrove, 2002; Cartwright et al., 2003; Hurst et al., 2003a; Cartwright, 2007). Polygonal faults are recognized as normal faults with moderate throw in a seismic cross-section. The formation process is not yet fully understood, but Cartwright et al. (2003) suggested that the polygonal faults may be generated by density inversion, gravity collapse, syneresis or compactional loading. Sand intrusions have been observed along the fault plane of polygonal faults, but despite the previous mentioned observation, Jackson (2007) exclude the phenomenon as a trigger mechanism and controlling factor for sand intrusions. This conclusion was substantiated by: 1) dikes are offset by polygonal faults, which implies that in some cases the sand remobilization happens prior to the formation of faults, 2) if the sand injectites were related to the polygonal faults, the distribution of sand intrusions should have exposed a polygonal pattern in plan-view, which is disproved. The arguments are based on observations from the North Sea.

### **3.2.7 Rapid compaction and subsidence linked to glaciation**

Rapid compaction and subsidence linked to glaciation (Dreimanis and Rappol, 1997; Hyam et al., 1997; Passchier, 2000; Le Heron and Etienne, 2005; Løseth et al., 2013; Parnell et al., 2013) are also a proposed trigger mechanism of sand remobilization. The glacier apply pressure to the underlying sediments, allowing build-up of overpressure. As the glacier moves, it cause shearing and consequently grains are reorganized which may cause liquefaction of sand.

### **3.2.8 Lateral pressure transfer**

Lateral pressure transfer, caused by the centroid effect (Yardley and Swarbrick, 2000) is also suggested as a trigger mechanism for sand injectites (Stump and Flemings, 2000; Flemings et al., 2002; Cartwright, 2010). The centroid effect will be further described in section 3.3.

### **3.2.9 Experiments for triggering of sand remobilization**

Several experiments have been conducted to demonstrate and understand how sand remobilization is triggered. Rodrigues et al. (2009) succeeded in triggering sand injectites in the laboratory using layers of sand, glass microspheres and silica powder. The sand and the glass microspheres were the components capable of being fluidized, and the silica powder represented the properties of a claystone. To fluidize and remobilize the sediments, they added compressed air from below (external fluid source) to build up overpressure and eventually trigger remobilization (Figure 3-1).

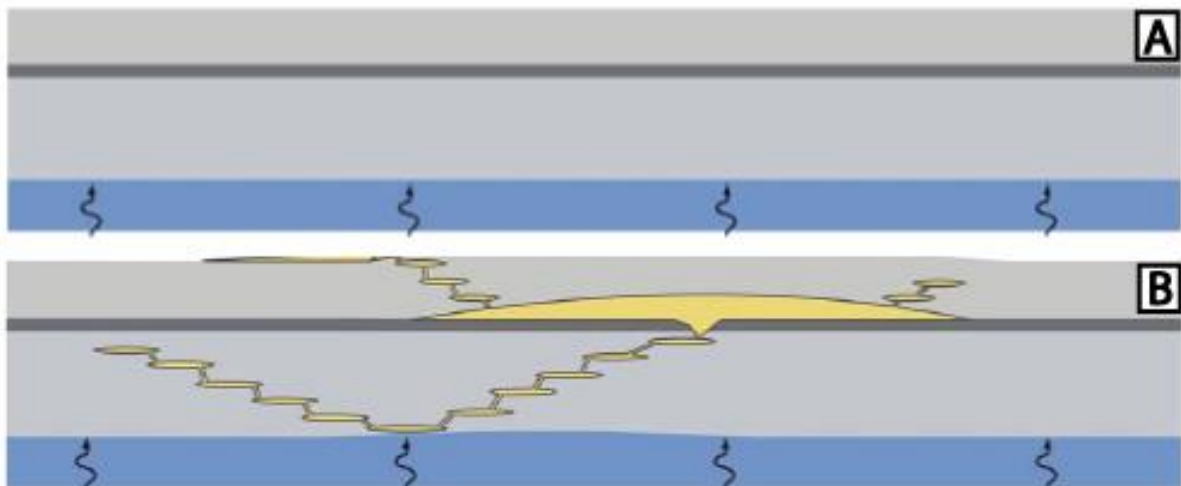


**Figure 3-1:** Illustration of the setup (A) and results (B) of the experiment conducted by Rodrigues et al. (2009).

Hermanrud et al. (2010) conducted another lab experiment, using a tube filled with water and supplied sand and then kaolin powder, to simulate unconsolidated sand covered by a caprock. Instead of triggering sediment remobilization with an external water source, they tilted the tube and hit the tube repeatedly with a hammer, followed by rotation of the tube relatively fast from clockwise to counter-clockwise. The different movements were carried out to provoke reorganization of the sand grains, and thereby sediment compaction. The compaction and reorganization of the sand grains resulted in excessive pore fluid that needed to escape and hence sand was liquefied (Figure 3-2).

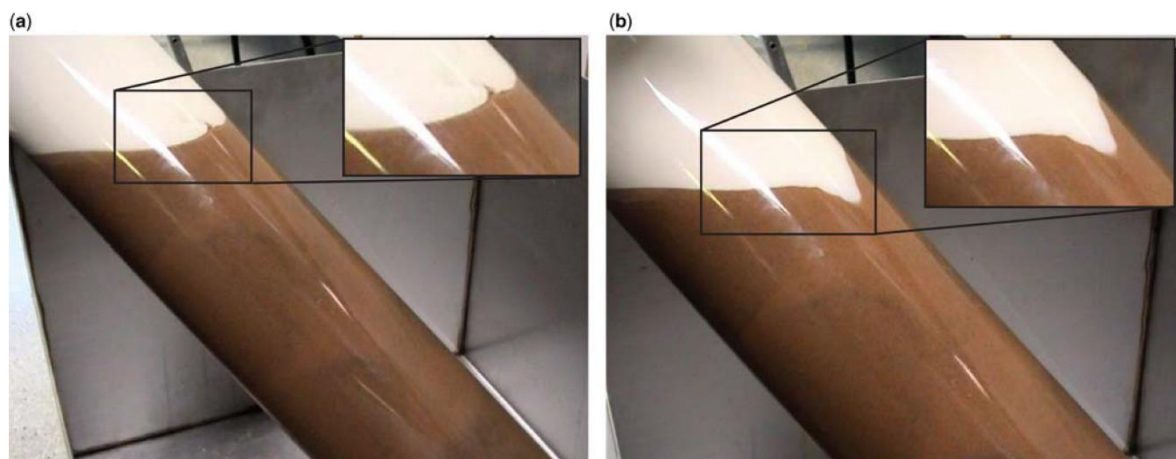


**Figure 3-2:** Experiment conducted by Hermanrud et al. (2010), where a) shows water starting to intrude into the kaolin layer, and b) shows how the kaolin collapses into the sand when the liquefaction process stops.

### 3.3 Pore fluid pressure and the centroid concept

To understand the sediment remobilization process, it is important with knowledge about subsurface fluid behavior. Pore pressure is a fundamental component in the understanding of subsurface fluid flow, and hence the understanding of the formation process of sand injectites.

*Pore fluid pressure* describes the fluid pressure in the pore space (Bruce and Bowers, 2002). Pore pressures versus depth relationships are often separated into two different regimes. The upper regime is characterized by normal pressure, and the fluids are in pressure communication with the surface. Hence, pressure in the upper sequence follows a hydrostatic pressure gradient. The lower sequence is divided into different compartments with fluid pressures that are not in pressure communication with the surface, i.e. non-hydrostatic (Shaker, 2002).

*The centroid concept* was first defined in 1997 (Traugott, 1997). It describes how the pore pressure in reservoirs and seals are dependent of the structural relief and overburden weight. The fundamental idea behind the centroid concept is that along an inclined structure, composed of seals (e.g. shale) and reservoirs (e.g. sand), there is a midpoint where the pore pressure is in equilibrium between the seal and the reservoir (Yardley and Swarbrick, 2000; Shaker, 2005). As displayed in Figure 3-3, the pore pressure gradient of the sand follows the hydrostatic gradient, while the pore pressure gradient of the shale is parallel to the lithostatic gradient (Yardley and Swarbrick, 2000).

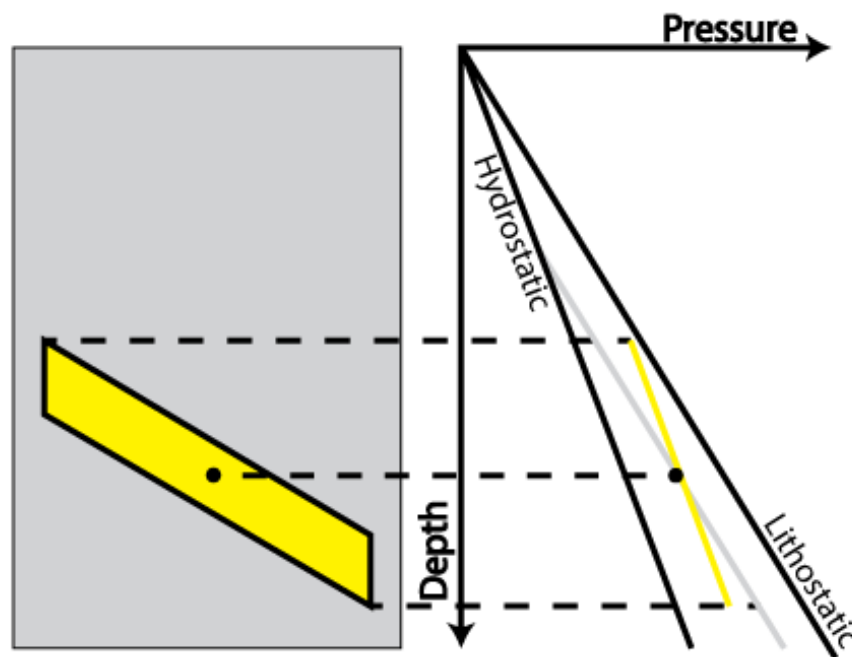


**Figure 3-3:** Model that explains the centroid concept based on the pressure relationships in a sequence that consist of shale and sand. The pressure gradient of the sand (marked with yellow) is parallel to the hydrostatic gradient,

and the pressure gradient of the shale (marked with grey) is parallel to the lithostatic pressure, and hence the centroid appears at the midpoint of the sand layer. This is the only place where the pressure of the sand and the shale are equal (slightly modified from Yardley and Swarbrick, 2000).

Lateral pressure transfer from deep to shallower strata are caused by the centroid effect, and is by Yardley and Swarbrick (2000) and Cartwright (2010) suggested as a possible trigger mechanism for sand remobilization (Figure 3-4). Jonk (2010) on the other hand, propose that lateral pressure transfer does not generate high enough fluid flow velocities to remobilize sand.

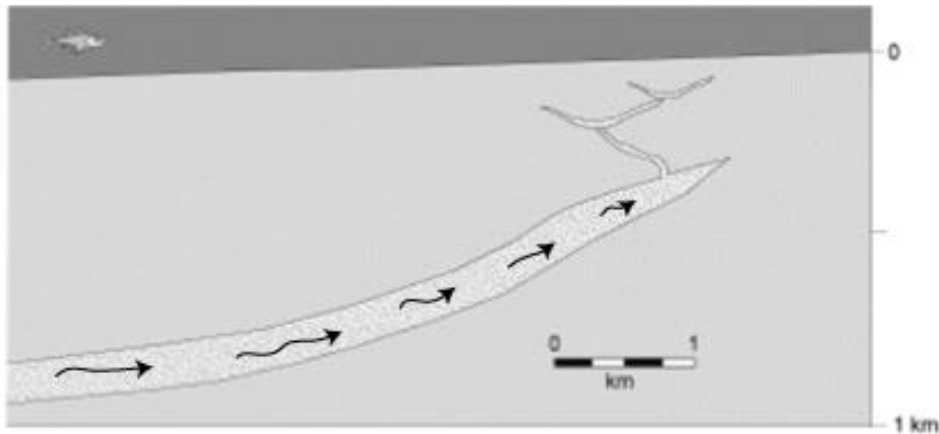


**Figure 3-4:** Lateral pressure transfer triggering sand remobilization in an inclined unconsolidated sand body (slightly modified from Cartwright, 2010).

### 3.4 Submarine slides

Unstable slopes are recognized at both passive and active margins, and at both low- and high angled slopes. Unstable slopes may be exposed to slope failure (also called submarine slides and submarine mass failures), triggered by an external event, e.g. oversteepening caused by flank uplift (Huvenne et al., 2002), earthquakes (Moore and Shannon, 1991), seepage (e.g. gas and dissociation of hydrates) and high sedimentation rates (Gardner et al., 1999). Slope failure is usually caused by a combination of several trigger mechanisms and occur when the internal shear strength of the sediment layer is exceeded (Lee et al., 1999; Huvenne et al., 2002).

Nardin et al. (1979) define two subclasses of slides; glides and slumps. The main difference between the two are that slumps are characterized by rotational movements along a discrete surface, but little internal deformation. Whereas, glides slide along a horizontal surface (without rotational movements), also with little internal deformation. The sedimentary structures linked to glides are generally recognized as undeformed bedding, though some plastic deformation at toe of slope or at the base of the slide might occur (Nardin et al., 1979).



Slumps can be identified on seismic as a unit with a deformed slope and base-of-slope component. Rotated blocks can be observed in seismic sections (Nardin et al., 1979). What characterizes both glides and slumps in seismic data are that the reflectors are generally continuous and undisturbed, though the deposits may show a certain grade of distortion in some parts of the deposit (Nardin et al., 1979). Often the headwall scarp is visible in seismic, both in map view and profile view. The headwall scarp marks the sharp boundary where the slide was released (Olafiranye et al., 2013).

Huvenne et al. (2002) describes a feature in the western Porcupine Basin (offshore Ireland), where a thin (~85m) but laterally extensive (>750 km<sup>2</sup>) slab of sediments was transformed into a slide (Figure 3-5). Once the slope failure has been triggered, the overpressured and hence weak layer at the base of the slab is liquefied and collapses. It is recognized as the detachment surface. Consequently, the liquefied sediments were interpreted to form a slide, and the detachment surface acted as the slide plane. In this case the slide stopped before it got to the toe of slope, but if the slide had continued, compression and over-thrusting at the toe of slope most likely would have occurred (Hampton et al., 1996; Huvenne et al., 2002). The Porcupine basin is located at the same tectonic setting as the North Sea basin, and hence the Porcupine basin will be used as a reference for interpretation of seismic observations in the northern North Sea.

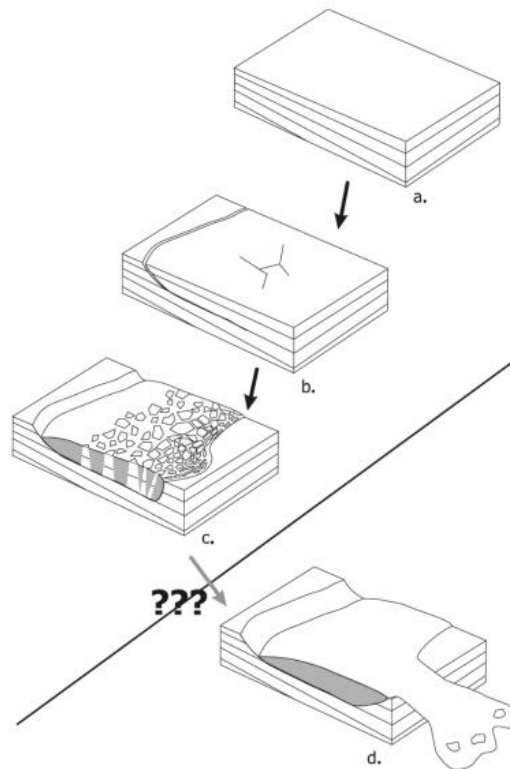


**Figure 3-5:** Simple sketch of the slope failure process described in Huvenne et al. (2002), a) The slope is in its initial, b) illustrates the first stage after the slope failure has been triggered, c) the sediment slab has started to slide down the slope. This is when the sand layer liquefies as a result of reorganization of the grains due to the shear movements. d) Huvenne et al. (2002) suggests a hypothetical last stage of the slide, describing over-thrusting of sliding material. The squares illustrate blocks of undisturbed sediments (Figure 8 in Huvenne et al., 2002).

### 3.5.1 Geometries and seismic identification of remobilized sand

Indications of remobilized sand have been observed in both outcrop and on seismic data. The outcrops in e.g. Panoche and Tumey Hills (Figure 3-6) are commonly used as analogues to try to understand sand intrusion networks from observations in seismic data. If seismic data was acquired from the outcrop displayed on Figure 3-6, most of the sand intrusions would not have been visualized, since the size are below seismic resolution. Hence, inferences about fluid pressure variations within injection complexes are uncertain. Even dikes that are tens of metres wide may be hard to resolve on seismic data if they are steep (A. Grippa, pers. comm. 2017).

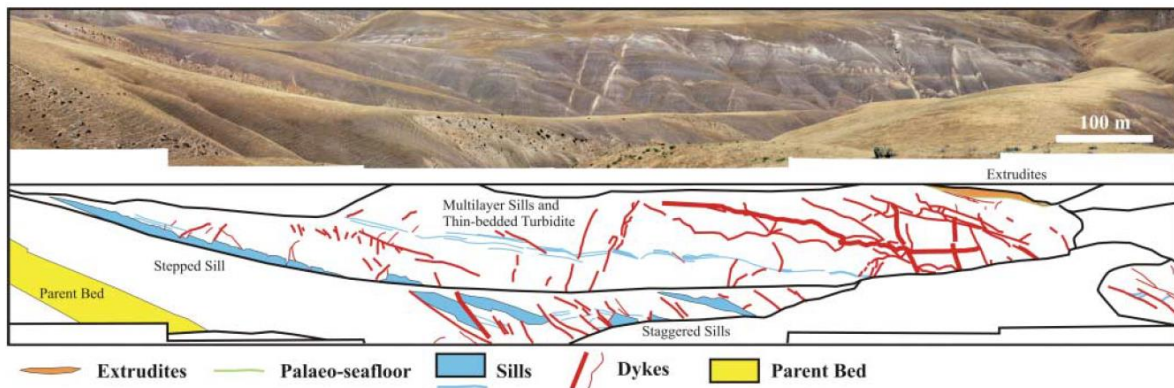


**Figure 3-6:** Overview of the eastern part of Panoche Giant Injection Complex, Marca Canyon. If seismic data was acquired from this outcrop, most of the intrusions would be too small to be visualized (Figure 2 in Vigorito et al., 2008).

### 3.5.2 Seismic identification of extrusive sands

Extrusive sand (referred to as extrudites, by Hurst et al. (2006)) is defined as remobilized sand that has reached the surface. The most common examples are sand volcanoes, which are recognized on seismic data as conical features (Hurst et al., 2011). Extrudites also occur as thick and lateral extensive sheets, wedging out in all directions from its feeder (Figure 3-7). These extensive sheets may be misinterpreted as intrusive sills or depositional sand bodies (Hurst et al., 2006; Løseth et al., 2012). Sheet-like extrudites can be identified as downlapping features onto the seafloor and onlapping features onto a high, e.g. a mound (Løseth et al., 2012).

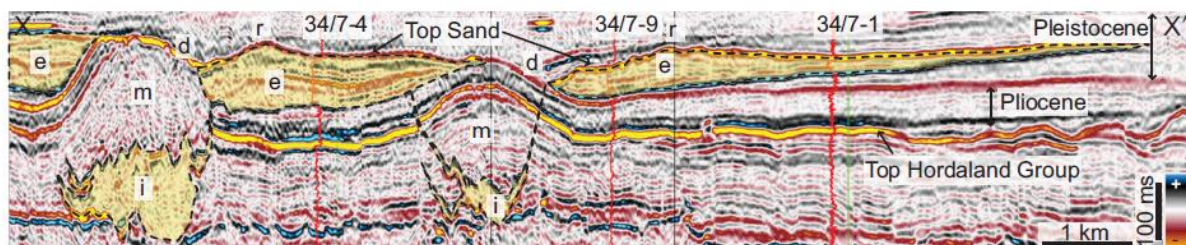


**Figure 3-7:** Seismic profile cross-cutting the Snorre Field in the North Sea. The figure shows extrusive sand bodies that onlap onto the mounds (m), and fills the ditches (d) created by the mounds. Intrusive sands (i) are located below the mounds. The top of the extrusions are represented by a ridge (R) (Figure 2 in Løseth et al., 2012).

### 3.5.3 Seismic signatures and geometries of intrusive sands

Intrusive sands can have a variety of geometries, influenced by rheology of the host rock, the properties of the parent sand and the stress rate when the remobilization occurred (Pollard and Johnson, 1973; Jolly and Lonergan, 2002). The geometries of the sand injectites can be divided into sills, high- and low- angled dikes and sometimes also irregular geometries that together constitute the “building blocks” in larger geometries, like conical intrusions and saucer-shapes

(Figure 3-8). Mounds (also referred to as forced folds or jack-up folds) can develop as a result of the sediment remobilization (Thompson et al., 1999; Lonergan et al., 2000; Thompson et al., 2007; Scott et al., 2009).

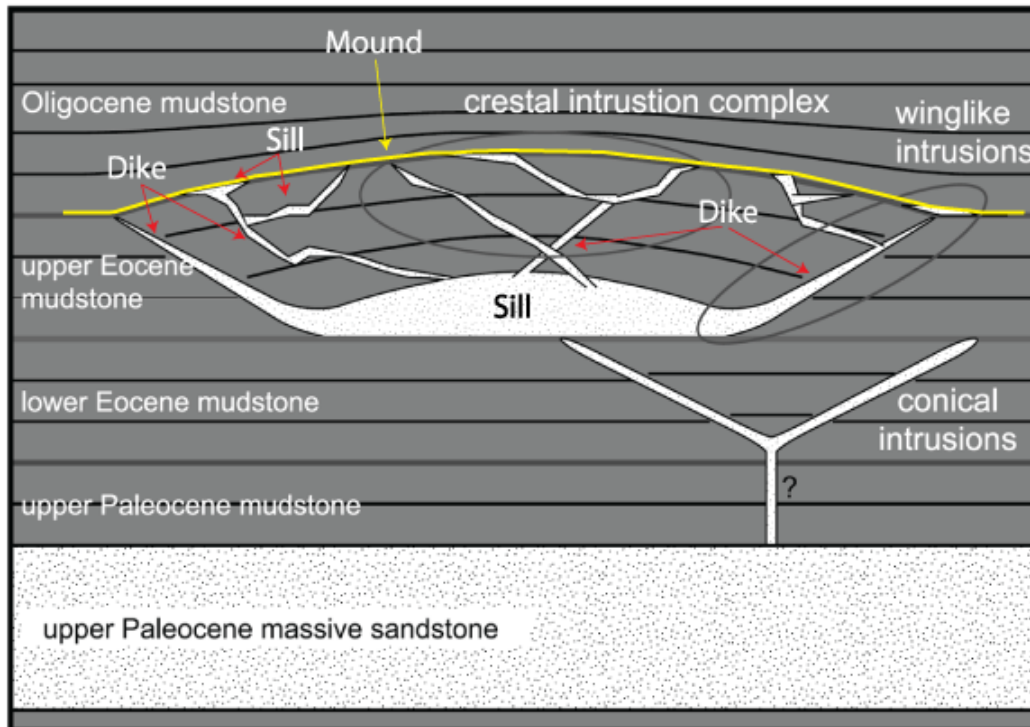


**Figure 3-8:** Schematic overview of different sand injectite geometries that are commonly observed in Paleogene (Paleocene, Eocene and Oligocene) strata in the North Sea (modified from Huuse et al., 2007).

The winglike structures are often well imaged on 2D seismic data, and are recognized as v- and w- brights (Macleod et al., 1999; Duranti et al., 2002). The high acoustic impedance contrast is often a result of carbonate cement within the sand injectite.

Dikes and sills are the most frequently observed sand injectite geometries (Lonergan et al., 2000). Delaney et al. (1986) suggest that dikes develop as a fracture that opens normal to the least compressive stress direction. In a basin that is not impacted by tectonic stress, the largest stress component will be the lithostatic stress (Figure 3-9), occurring as a result of the weight of the overlying sediments. A dike will develop in this kind of environment if the pore fluid pressure exceeds the horizontal stress together with the tensile strength of the host sediment, which tends to be oriented sub-parallel to gently-dipping beds (Delaney et al., 1986; Price and Cosgrove, 1990; Lonergan et al., 2000). Dikes tend to propagate upwards until the pore pressure exceeds the lithostatic stress (the fluid pore pressure are able to carry the weight of the overburden), and the intrusion continues as a sill (Lonergan et al., 2000). Since formation of sills require larger fluid pore pressures than the formation of dikes, dikes are more frequently

observed among the deeper intrusions. Sills occur more frequently at shallower depths (Lonergan et al., 2000). Figure 3-9 provides an overview and summary of where the different geometries occur in a tectonically passive environment, based on depth and pressure.

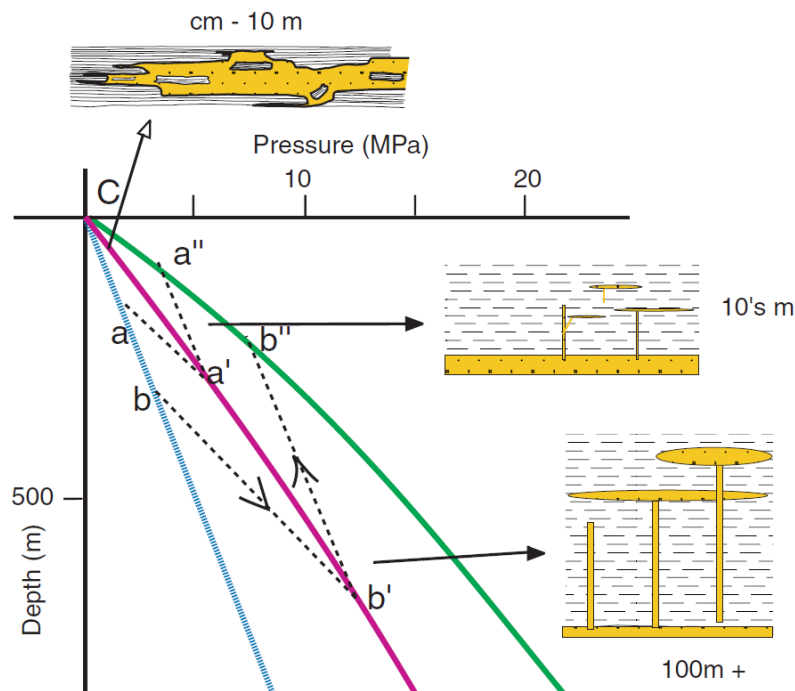


**Figure 3-9:** The figure displays the link between hydrostatic pressure and sand remobilization, in a basin where the largest stress is vertical. Two different scenarios are presented (a and b). The sand body of case a) is sealed at relatively shallow depth (point a), and consequently the pore fluid pressure transcends the horizontal pressure and causes seal failure at a shallow depth (point a'). The seal failure results in a dike, and transforms into a sill when the pore fluid pressure exceeds the lithostatic pressure (vertical pressure) (point a''). The sand body of case b) is sealed at a deeper level compared to a) (point b). The seal is breached at point b', and a dike starts to form. Because the breach of the seal happens at a deeper level compared to in case a), the differential pressure is larger, which implies that the fluid velocities will be higher and therefore capable of carrying more sand. When the pore fluid pressure exceeds the lithostatic pressure, the dike transforms into a sill (slightly modified from Lonergan et al., 2000).



## **4. Data and methods**

### **4.1 Basinal setting of remobilized sands worldwide**

This chapter describes the methodology of the literature study that is presented in chapter 5.

The literature was collected through a research using [oria.no](#) and [scholar.google.no](#). It is important to emphasize that there are observed sand injectites at more locations than what appears in this study, but the collected data represents a significant selection. The collected data include some papers describing certain sand remobilization provinces, as well as papers that include data from several locations.

The data was sorted according to the basin setting at the time of sand remobilization. Here, the basinal setting is defined as the location in the basin where the sand intrusions occur. A similar study was conducted by Jolly and Lonergan (2002). They categorized sand intrusions based on the depositional environment where the sand intrusions occur, and suggested different trigger mechanisms. The investigations in this thesis are broader than that of Jolly and Lonergan (2002), as it also includes what trigger mechanisms that are likely to be present in the specific tectonic settings where sand remobilization occur.

The sand intrusions and extrudites were categorized into three different groups according to their tectonic habitat: 1) convergent and transform margins, 2) inverted passive margins, 3) other settings. Convergent and transform margins involve basins characterized by compressional regime at the time of sand remobilization. Inverted passive margins include basins that were tectonically quiet at the time of injection. The group referred to as "other settings" includes remobilization of sand that reportedly occurred in tectonic settings where only one or a few examples were identified. The group called "other" will not be included in chapter 5, as most of those intrusions are small scale and the sand remobilization does not appear to be directly related to the tectonic setting of the basin. One example of sand intrusions that occur directly related to rifting was described by Ribeiro and Terrinha (2007). This location was excluded since there was found only one paper describing sand intrusions on this type of tectonic setting.

The different locations were summarized in Table 5-1. The table includes: 1) location, 2) basin name, 3) specific area, 4) inclined parent body, 5) time of remobilization, 6) basin setting at the time of remobilization, 7) location of remobilized sands in the basin, and 8) references to the different locations where sand remobilization occurs. In total, 27 different locations were

investigated. A complete version of the table presented in chapter 5.3 can be found in Appendix B.

#### **4.1.1 Limitations**

- Some of the areas where sand intrusions and extrudites are observed, are described thoroughly by several authors (e.g. the Panoche and Tumey Hills in California). In contrast, other sand intrusion networks are only briefly described in more general articles about sand intrusions (e.g. the Taranaki basin in New Zealand). Hence different uncertainties are associated to the analysis of the separate locations.
- A master project is assigned with a certain amount of time, and hence the time used on each location was limited. It could have been valuable to learn more about each geological setting, to get a better understanding of the formation of sand intrusions. With more time, more locations could have been included in the study.



### 4.1.2 Workflow

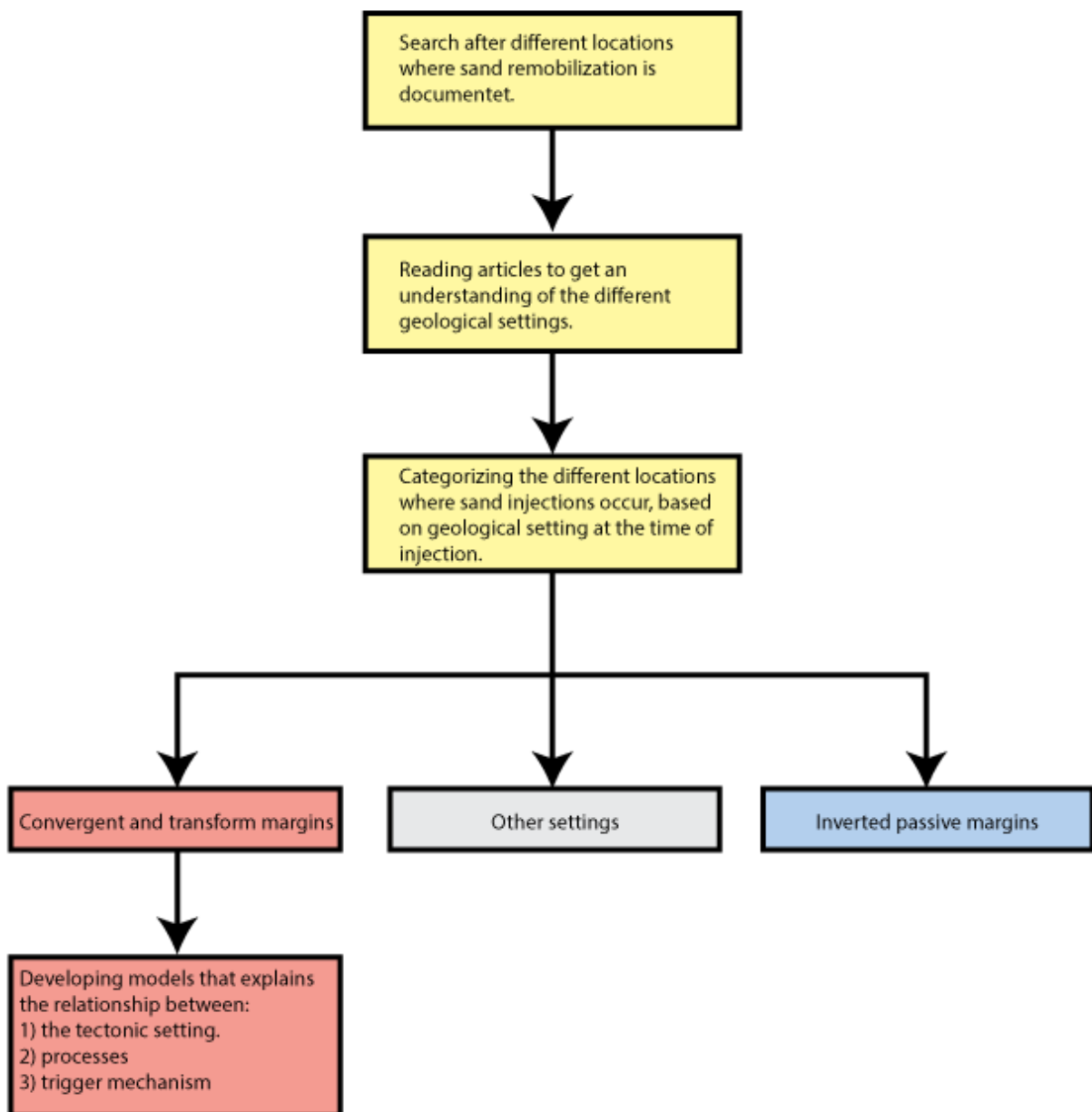


**Figure 4-1:** Displays the workflow chart of the literature study. The continuation of the workflow describing inverted passive margins are found in chapter 4.4.

## 4.2 Northern North Sea seismic data



**Figure 4-2:** The figure shows the extent of the regional seismic broadband data (3D-data), marked with the red line.

This study was based on a regional seismic dataset of the northern North Sea. The Northern Viking Graben (NVG) regional seismic Broadband data (3D-data) was provided by CGG. The dataset is a mega merge, covering most parts of quadrant 30, 31, 34, 35, and limited parts of 29, 33 and 36 (Figure 4-2).

The inlines are oriented N-S and the crosslines are oriented E-W. The seismic was collected with an interval of 12,5 m, but because of the large size of the dataset, it was cropped to make it easier to work with in the software. The crossline spacing was increased to 37,5m, and the inline spacing was increased to 56,25m after cropping. The depth was cropped at 5000 milliseconds.

The red reflectors represent positive values (peaks) and the blue reflectors represent negative values, which show that the data have normal polarity. The dataset is zero-phase processed.

### 4.2.1 Seismic interpretation and workflow

The data was interpreted in the Petrel Software, version 2015, developed by Schlumberger. The interpretation is backed by well data and figures from already published studies.

#### *Wells*

Most of the wells used for seismic interpretation in this study, was transferred from the Petrel project of former master student Lisa Marie Røynestad, but a few wells were also imported from NPD's database "Diskos". Well tops were retrieved from the NPD FactPages. However, several of the welltops that were imported into the project were inconsistent with each other, or with the literature.

**Table 4-1:** Overview of wells used as guidelines in seismic interpretation. The second column present wells used directly in seismic interpretation, and the third column present wells that have been used to correlate the literature with the seismic.

Wells	Guidelines in seismic interpretation	Used as guidelines when correlating the CSS-sequences from the literature with the seismic data
30/6-5	X	
30/6-11	X	
30/6-19	X	
30/11-1	X	
30/11-2	X	
30/11-4	X	
31/2-6	X	
31/2-7	X	
31/2-11	X	
31/5-3	X	
33/9-16	X	
34/7-1		X
34/7-4	X	X
35/8-2	X	X
35/8-3	X	
35/9-6 S	X	
35/10-1	X	
35/11-3 S		X

### *Interpretation of the CSS sequences*

The interpretation of the 10 CSS sequences was based on Faleide et al. (2002), and wells (Table 4-1).

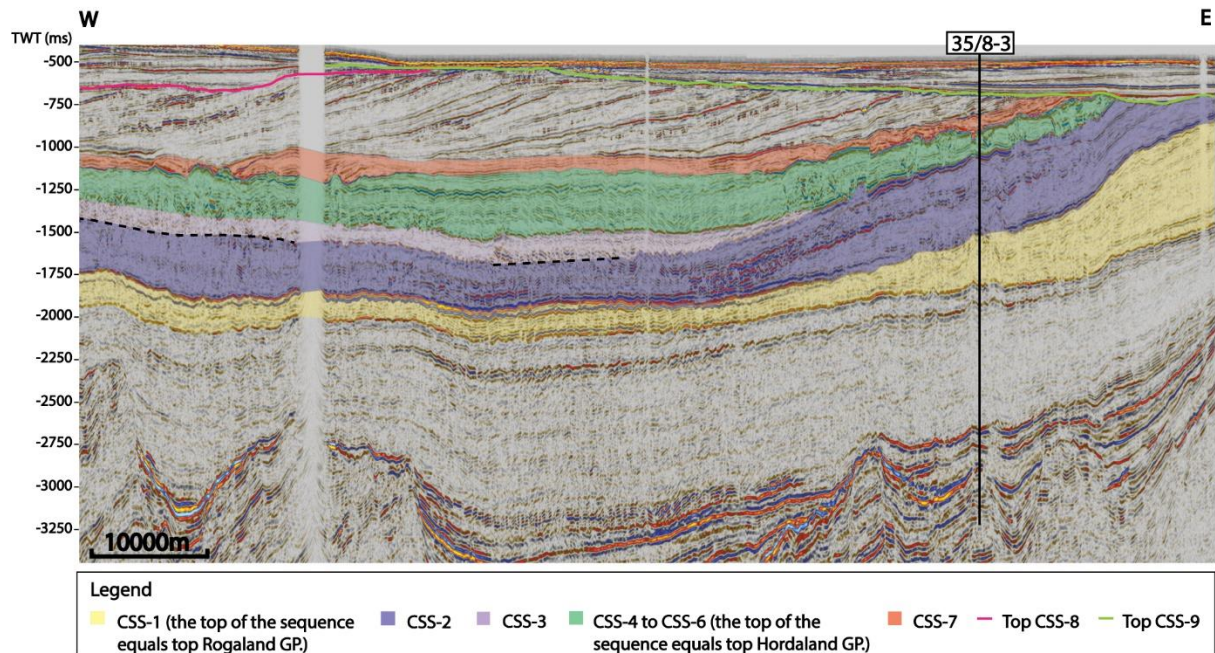


**Figure 4-3:** The seismic cross-section displays an overview of the interpreted seismic sequences.

The Hordaland Group is the main interval that was studied in this thesis. Disturbed reflectors are recognized in areas throughout the entire Hordaland Group. Disturbed reflectors or chaotic reflectors, are here used to describe areas where it is impossible to track the same seismic reflector through an area. Whereas continuous reflectors are in this thesis defined as undisturbed reflectors, which are possible to track through an area. The Hordaland Group consists of claystone interbedded with sandstone beds (Clausen et al., 1999), and has a high occurrence of sand intrusions. The Hordaland Group is bound by top CSS-1 and top CSS-6 (Figure 4-3).

*Top CSS-0* is a continuous reflector covering the entire study area. The interpreted reflector is characterized by a continuous, medium to strong reflector, and was therefore easy to track. Top CSS-0 was interpreted throughout the entire area, and the interpretation was mainly carried out using the seeded 3D-autotracking tool.

*CSS-1* represents the sediments of Late Palaeocene to earliest Eocene age (60,5 – 56 Ma) (Thyberg et al., 2000). Top CSS-1 corresponds to the top of the Rogaland Group, which is interpretable throughout the entire study area. The top Rogaland Group is represented by a relatively continuous reflector, not eminently disturbed by remobilization, which made it easy

to track. The interpreted horizon is recognized by a strong to medium amplitude, and the reflector is continuous. Top Rogaland was interpreted throughout the entire area, and the interpretation was carried out by seeded 3D-autotracking, supplemented with manual interpretation.

*CSS-2* belongs to the Hordaland Group, and represent the transition from Eocene to Oligocene strata (35,4 Ma). The top of the sequence is associated with a hiatus, mainly observed on the flanks of the basin (Thyberg et al., 2000; Faleide et al., 2002). The reflector that represents top *CSS-2* is relatively continuous, but is locally disturbed. The amplitude strength is medium to low. The reflector was challenging to track, and was therefore interpreted using the manual interpretation tool. Top *CSS-2* was only interpreted in certain areas.

*CSS-3* represent the lower part of the Oligocene succession, and is a progradational sequence, onlapping onto top *CSS-2* along the basin flanks (Faleide et al., 2002). Top *CSS-3* is interpreted to be located at a low amplitude reflector, which is locally notably disturbed. The top of the sequence marks the base of the overlying heavily polygonally faulted interval. The reflector representing top *CSS-3* is characterized as continuous to discontinuous, and recognized by a low to medium amplitude. It was challenging to track the reflector, and it was therefore interpreted using the manual interpretation tool. Top *CSS-3* was only interpreted in certain areas. It is believed that the seismic reflector in some areas are interpreted on the A-CT boundary.

*CSS-4* represents the uppermost sequence of the Oligocene succession (Eidvin and Riis, 1992; Faleide et al., 2002). The sequence is very thin in the northern North Sea, and is difficult to separate from the rest of the Miocene succession. The reflector is discontinuous with a medium to low amplitude strength. The top of the sequence was therefor only interpreted in some areas, where the horizon could be tracked.

*CSS-5/6* were hard to identify as separate sequences in the study area, and was therefore interpreted as one sequence based on the interpretation from Faleide et al. (2002). The two sequences together with *CSS7*, constitute the Miocene succession (Jordt et al., 1995; Michelsen et al., 1995). Top *CSS 6* correlates with the top of the Hordaland Group, which represents the Mid Miocene Unconformity. The unconformity was formed during a significant hiatus, allowing erosion and other post-depositional features to re-work the top Hordaland surface. Distinct channels were recognized in map view of the surface. Mounds are abundant on the top Hordaland surface, and they were investigated further in this thesis.

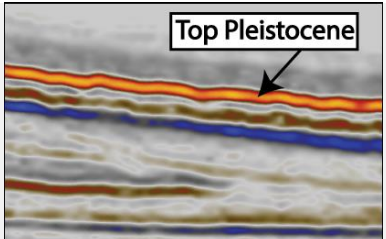
Although the top of the Hordaland Group is represented by a strong to medium and continuous reflector, the interpretation of the unconformity was challenging in certain areas, especially areas exposed to sand remobilization. The seeded 3D-autotracker was not always able to follow the correct reflector properly, due to truncated and onlapping reflectors. Accordingly, the top Hordaland Group was mainly interpreted manually.

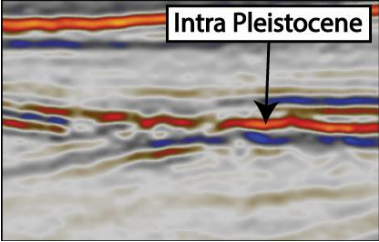
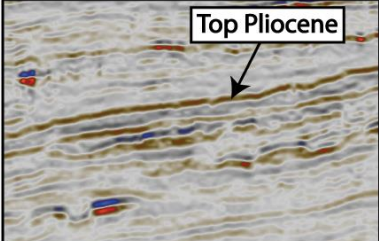
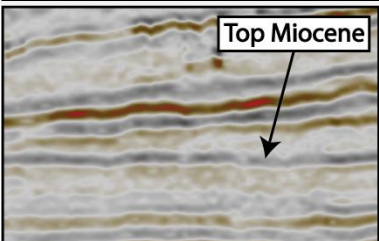
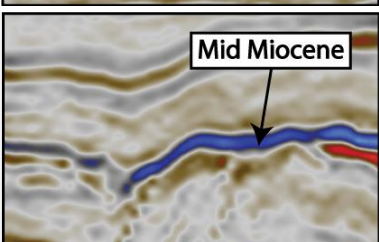
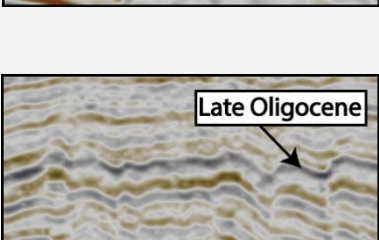
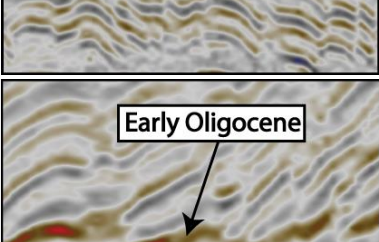
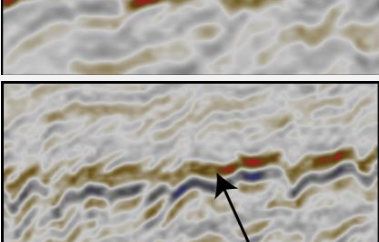
*CSS-7* represent the Utsira Formation and the lowermost part of the Nordland Group. It marks the top of the Miocene sequence, and onlaps onto top Hordaland Group. The reflector varies from continuous to discontinuous, and is recognized by medium to low amplitude. The surface was interpreted in most of the study area, and it was possible to interpret parts of the study area using the 3D-autotracker. The remaining parts of the surface was interpreted using the manual interpretation tool.

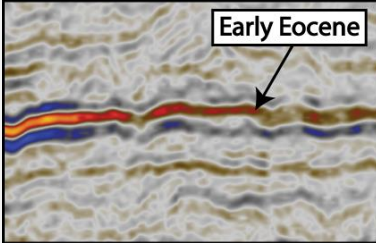
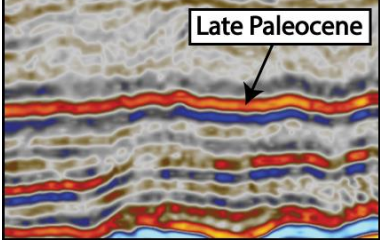
*CSS-8 and CSS-9* represent the Upper Nordland Group, and consists of Plio- and Pleistocene strata. Top *CSS-8* and top *CSS-9* were interpreted along a continuous to discontinuous reflector, characterized by a low to medium amplitude strength. The seeded 3D-autotracker, was used to interpret the two horizons, supplemented with the manual interpretation tool in areas where the reflector was discontinuous. Top *CSS-8* and top *CSS-9* was only interpreted in some areas of the study area.

*CSS-10* is the uppermost sequence of the Cenozoic succession, and consist of Pleistocene strata. Top *CSS-10* corresponds to the seabed, and is recognized by a continuous reflector with a strong amplitude. Due to its continuity, the 3D- autotracking tool was used to interpret the horizon throughout the study area.

**Table 4-2:** Overview of the interpreted horizons.

Seismic horizon	CSS sequence	Seismic phase	Description of reflector	Seismic signature
Top Pleistocene (Seabed)	Top <i>CSS-10</i>	Peak	Strong	

<b>Intra Pleistocene (Intra Nordland GP.)</b>	Top CSS-9	Peak	Strong to low	
<b>Top Pliocene (Intra Nordland GP.)</b>	Top CSS-8	Trough	Medium to low	
<b>Top Miocene (Intra Nordland GP.)</b>	Top CSS-7	Trough	Medium to low amplitude, and relatively continuous.	
<b>Mid Miocene (Top Hordaland GP.)</b>	Top CSS-5/6	Trough	Strong to medium amplitude and relatively continuous reflector, disturbed by injectites creating messy reflectors.	
<b>Late Oligocene (Intra Hordaland GP.)</b>	Top CSS-4	Trough	Relatively continuous to discontinuous.	
<b>Early Oligocene (Intra Hordaland GP.)</b>	Top CSS-3	Peak	Relatively continuous to discontinuous.	
<b>Top Eocene (Intra Hordaland GP.)</b>	Top CSS-2	Peak	Relatively continuous to discontinuous.	

<b>Early Eocene (Top Rogaland Group)</b>	Top CSS-1	Peak	Strong amplitude and continuous reflector.	
<b>Late Paleocene (Intra Rogaland GP.)</b>	Top CSS-0	Peak	Strong to medium amplitude, and relative continuous.	

#### 4.2.2 Surface maps

Surface maps (elevation maps were generated based on the seismic interpretations of top Rogaland Group and top Hordaland Group. The top Rogaland surface was mainly generated to make a thickness map of the Hordaland Group. The thickness map did not reveal more information of significant relevance to the study than what the surface map of top Hordaland Group showed. Therefore, the thickness map was excluded from chapter 6.

The vertical exaggeration of the surface map of the top Hordaland Group was set to 7,5. Vertical exaggeration enhances mounded features observed on the surface. The vertical spacing between the contour lines was set to 100ms.

#### 4.2.3 Seismic attributes

An RMS amplitude surface map was generated through CSS-3. A variance cube was also generated. None of these two seismic attributes revealed more information than the surface map (elevation maps) of top Hordaland Group, and consequently they were not used in this thesis.

#### 4.2.4 Uncertainties

- There is a lack of seismic data close to installations (e.g. Oseberg), which lead to some challenges in terms of seismic interpretation (Figure 4-4).
- Dim zones occur due to the merge of different seismic surveys (Figure 4-4).
- CSS-5 to CSS-7 occur as very thin sequences in the northern North Sea, sometimes also below seismic resolution.
- Manual interpretation generates a certain grade of uncertainty, as the seismic interpretation is influenced by the experience, geologic specialization and knowledge of the interpreter.



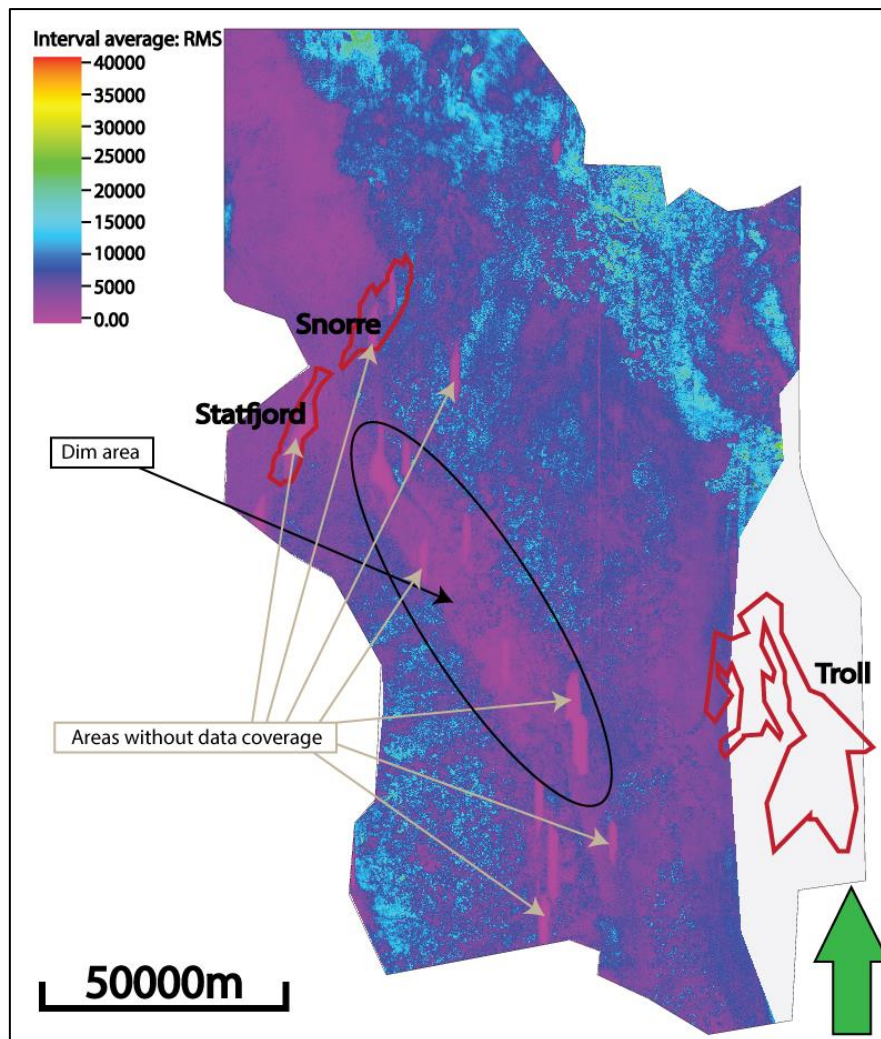


**Figure 4-4:** RMS amplitude map of the top Hordaland Group surface. It gives an overview of the distribution of holes in the seismic caused by the installations in addition to the dim zones which occur as result of the merge of different seismic surveys.

### 4.3 Well analyses

To get an overview of the sand distribution in the given interval of the study area, a mapping of the sand content in mounded features combined with disturbed reflectors were conducted. The motivation was to investigate the amount of sand relative to uplift in the mounds, and how the sand was distributed. To map the sand distribution, well analyses were conducted. More wells were imported to the Petrel project from the Petrel project of PhD student Fabian Tillmans and former master student Theodor Lien.

34 wells were included in the study, equally divided between wells penetrating mounds and wells penetrating areas characterized by unmounded areas and continuous reflectors. The identification of sand was based on information from logs retrieved from npd's webpage.

The information from the wells was organized in a table (Appendix C). The factors included in the table are: 1) well-ID, 2) year drilled, 3) presence of sand in the interval of interest, 4) description of the Hordaland Group, 5) total thickness of sand (meter) in the interval of interest, 6) comments.

Depth conversion in Petrel was carried out to measure the depth from top Hordaland to the base of the studied interval (top CSS-3). The depth conversion was based on velocity data from the closest well.

To get an overview of the lithology in mounds compared to the lithology in unmounded areas, the results from the well analysis were plotted in two different ways: 1) the total sand thickness in the interval of interest in each well, 2) the distribution of sand in mounded areas compared to the distribution of sand in unmounded areas. In plot 2) the y-axis shows the total amount of sand in percent, and the x-axis are divided into seven intervals based on sand thickness: 0m, <2m, 2-18m, 19-34m, 35-50m, 51-66m, >67m. Next, the amount of sand from every well were assigned to the belonging interval, and the total amount of sand in each interval was calculated. Finally, the percentage of the total amount of sand in all wells were calculated for each interval.

The amount of uplift versus sand content in the studied interval (top CSS-3 to top CSS-6) were also investigated. Figure 4-5 shows how the two components were measured. Uncertainties linked to measuring the uplift of the mounds is associated to what angle the well penetrates the mound. The well string is vertical, and hence they might not penetrate the well perpendicular to the mounds surface (Figure 4-5). This could lead to error in the measurements.

In the western part of the study area, the mounds are not as well defined as in east. Because the chaotic reflectors extend deeper than the base of CSS-4, the lower boundary of the studied interval is not recognizable. Consequently, only wells penetrating the eastern mounds were included in the last well analysis.

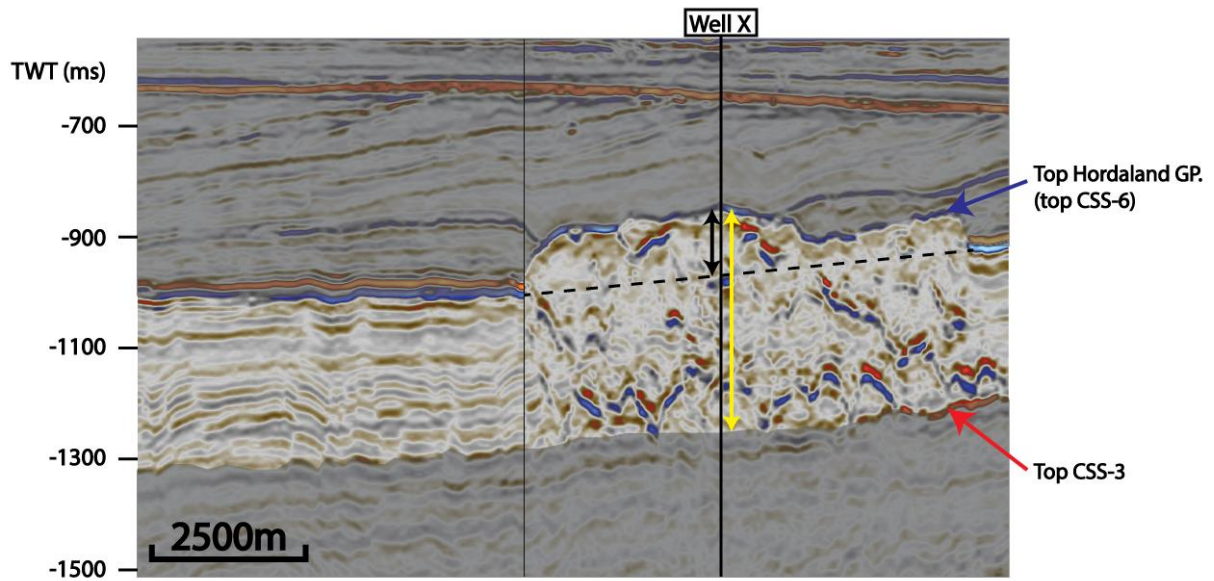


**Figure 4-5:** Seismic cross section that shows how the total sand thickness was measured (yellow arrow), and how the uplift was measured (black arrow). The wells are vertical, and hence might not be perpendicular to the mounds surface. This will lead to an error in the measurements.

#### 4.4. Workflow for inverted passive margins

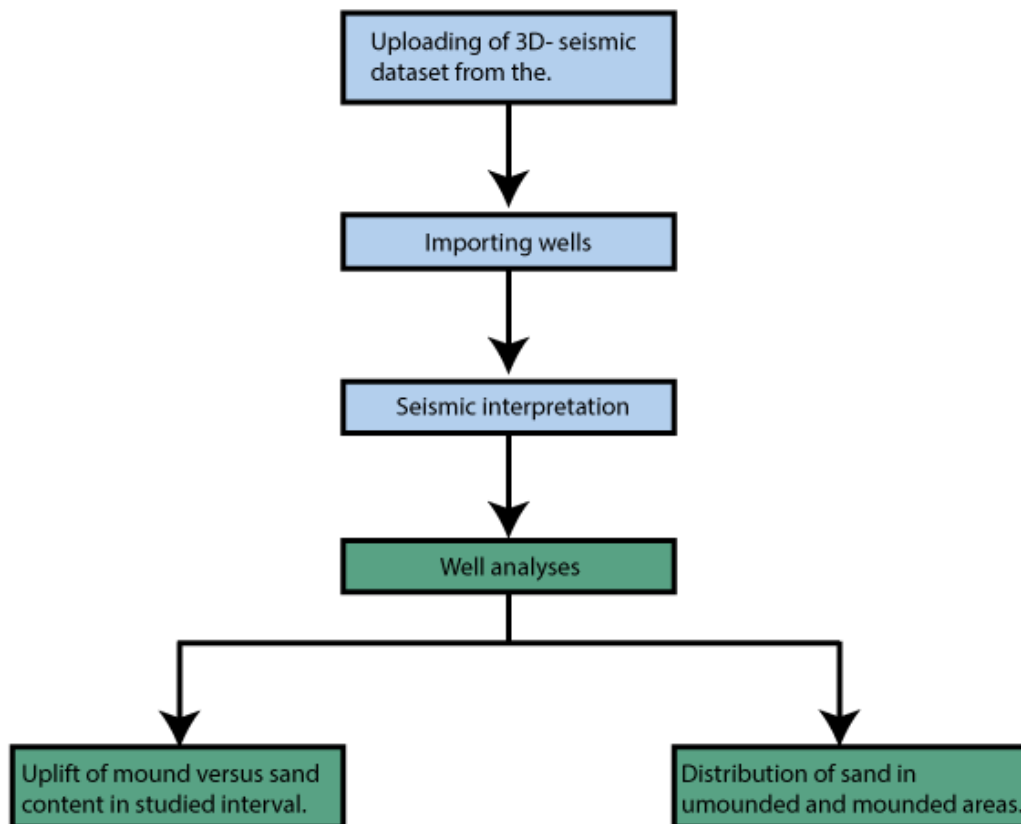


**Figure 4-6:** Displays the workflow chart for inverted passive margins.



## 5. Basinal setting of remobilized sands worldwide

Sand injectites are present in many sedimentary basins worldwide but are also absent in a number of basins. Their presence is often restricted to certain parts of basins or to specific time intervals. Several basins worldwide were studied to determine if sediment remobilization occurs at certain basinal settings, and to identify the most likely trigger mechanisms. The aim of the study is to investigate:

- 1) If there is a relationship between trigger mechanisms and the tectonic setting of the basin.
- 2) If occurrences of sand injectites differ among basins with different tectonic settings.

A significant number of locations where large scale sand intrusions are observed, were included in the study (Figure 5-1). Based on the examinations of these locations, two main basin settings were identified: 1) basins close to plate boundaries characterized by convergent or strike-slip tectonics, 2) inverted passive margins.

This chapter starts with descriptions of individual large scale sand intrusion provinces. The characteristics of the different locations are summarized in Table 5-1.



**Figure 5-1:** The green dots mark locations of sand intrusion included in this study. The red dots mark locations of injectites that is excluded from this study. Modified from Braccini et al. (2006).

## 5.1 Basins at convergent and strike-slip margins

### *Panoche hills and Tumey hills, California*

The Panoche hills intrusion province shows the best exposed parent-intrusion network in the world, extending over a stratigraphic distance of more than 1200m (Cartwright, 2010). Together with Tumey hills, Panoche hills represent a large coldseep system, which lasted for almost 2 m.y. (Minisini and Schwartz, 2007). The intrusion province is located on the western margin of the San Joaquin basin, previously a part of the Great Valley forearc system in California (Schwartz et al., 2003; Minisini and Schwartz, 2007; Cartwright, 2010).

The host units consist of the Late Cretaceous to Paleocene-aged Panoche and Moreno Formations (Cartwright, 2010; Vétel and Cartwright, 2010). The Panoche Formation is a deep marine fan deposit, which is in direct contact with the Jurassic – Cretaceous Franciscan subduction complex (Figure 5-2) in the west (Schwartz et al., 2003). Palladino et al. (2016) for the first time recognized sand intrusions along thrust faults within the Panoche Giant Intrusion complex.

According to Schwartz et al. (2003); Cartwright (2010); Vétel and Cartwright (2010), the remobilization happened in two phases: one during the Danian (Lower Paleocene) and one in Eocene. Sills developed in the lower part of the injection province, and mainly dikes in the more shallow parts of the network (Vigorito et al., 2008).

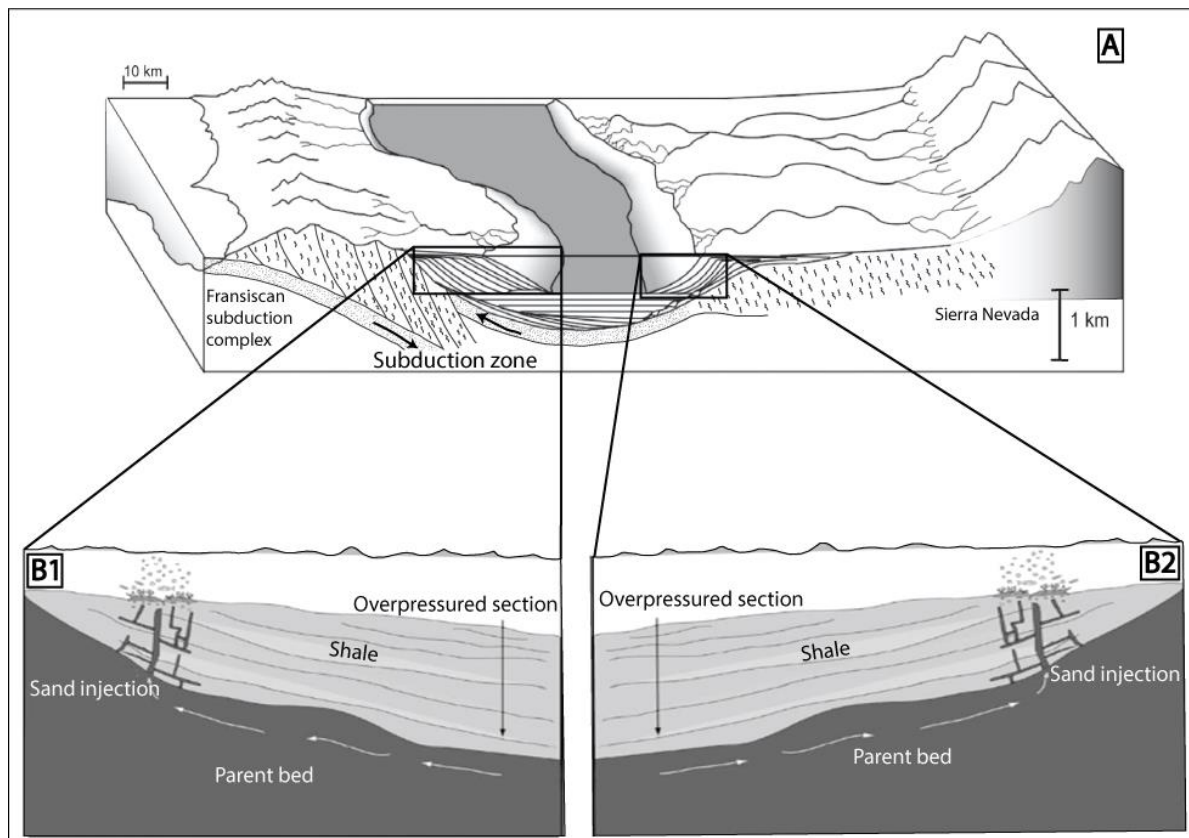


**Figure 5-2:** Basin setting in Panoche and Tumey Hills during injection. Figure A) shows an overview of the Franciscan subduction complex. Figure B1) and B2) shows a zoom-in view of the setting where sand is remobilized. Modified from McGuire (1988); Schwartz et al. (2003); Mitchell et al. (2010).

### *Dana Point, South West California*

The sediment remobilization at Dana Point in California, is recognized as extrudites, extruded in a deep-water setting. The injection occurred when the area was dominated by transform tectonics, linked to the San Andreas fault (Bouroullec et al., 2010).

Bouroullec et al. (2010) suggest that the sediment remobilization process was initiated subsequently above a structural high located below the sand injectites, controlling the fluid migration from the deeper strata and increased the pore pressure in the sandy Monterey formation (Figure 5-3).

The sand injectites occur in the muddy Monterey Formation and the extrudites occur at the base of the sandy Capistrano Formation (Bouroullec et al., 2010). The remobilized sand is most likely sourced from the sandy lowermost part of the Monterey Formation (Bouroullec et al., 2010).

Based on the observation that the muddy Monterey Formation is dated to upper Miocene, and the Capistrano Formation is dated to Pliocene, one can assume that the sediment remobilization

occurred during upper Miocene. According to Bouroullec et al. (2010), the remobilization happened as multiphase injection.

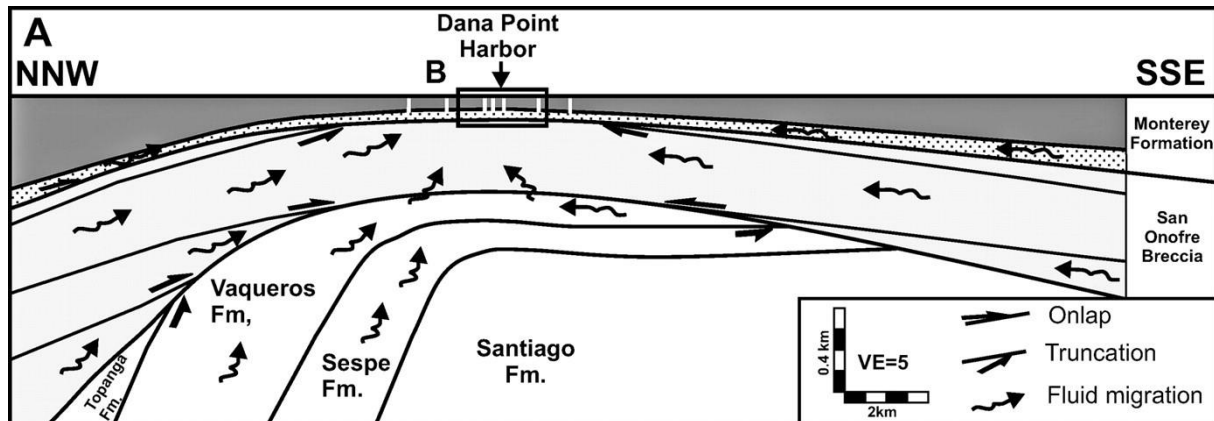


**Figure 5-3:** Structural setting of Dana Point at the time of injection (slightly modified from Bouroullec et al. (2010)). Figure 5-4 illustrates the regional tectonic setting of the area at the time of sand injection.

### *Santa Cruz, California*

The Yellow Bank Creek Complex is located northwest of Santa Cruz in the Santa Cruz Basin, which is a sub-basin of the La Honda Basin, affected by the San Andreas fault system. During Late Cenozoic, the Franciscan subduction complex rapidly changed from convergent regime to transform regime, controlled by the San Andreas fault zone (Atwater and Molnar; Dickinson and Seely, 1979). Sherry et al. (2012) suggest that the sediment remobilization was triggered by increased pore fluid pressure, together with seismic shaking, related to the San Andreas fault zone.

The sediment remobilization happened during Upper Miocene, and resulted in dikes and sills, including single bodies, clustered intrusions and some eruptions onto the Miocene seafloor (Boehm and Moore, 2002; Thompson et al., 2007). The intrusions originate from the Upper Miocene Santa Margarita sandstone, and intrude upwards into the Upper Miocene Santa Cruz Mudstone (Thompson et al., 2007).



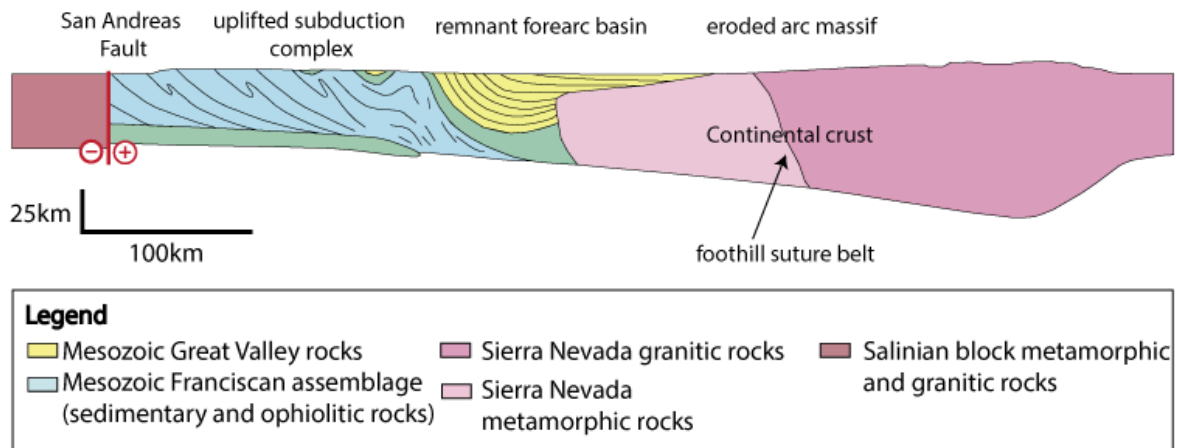


**Figure 5-4:** Tectonic setting of Santa Cruz during Miocene (slightly modified from Bloet et al. (2017)).

### *Quebec, Canada*

In Quebec, sand injectites are documented in the lower parts of the Early Ordovician Tourelle Formation, also known as Cap Ste-Ann section (Hiscott, 1979). The geometry of the remobilized sand is dominated by sills, but dikes are also well developed. The sand intrusions are interpreted to be sourced from a slightly inclined sandy channel-fill sequence. During Early Ordovician (deposition of the Tourelle Formation), the formation of the Taconian orogeny was initiated, and hence the area was affected by a compressional regime (Figure 5-5).

Hiscott (1979) suggests two alternative trigger mechanisms for subsurface sediment remobilization. One alternative is that the sediment remobilization was triggered by lateral pressure transfer, in addition to slumping that caused loading and liquefaction of deeper strata. The parent sand is located southwest of the study area, but it is unclear what type of deposit the liquefied sand originates from. The other suggestion is linked to development of the Taconian Orogeny. Hiscott (1979) suggests that the sand injection might have been triggered by earthquakes, and that the earthquakes potentially was the trigger mechanism that caused the slumping.

The timing of the sand injection was not given by Hiscott (1979), but since the intrusions are hosted by the Early Ordovician Tourelle Formation, it can be assumed that the injection happened in Mid to Late Ordovician.

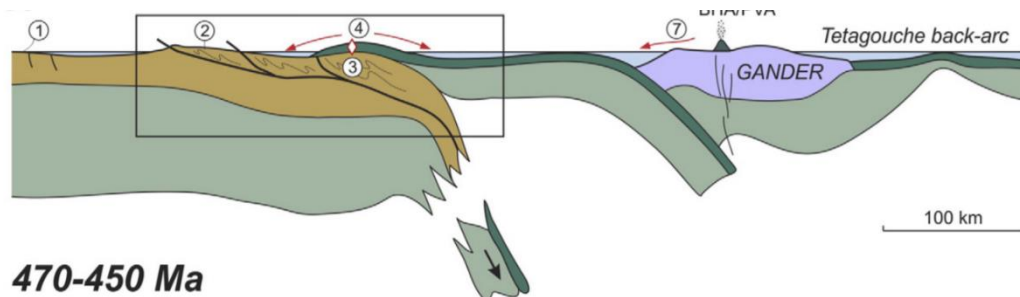


**Figure 5-5:** Tectonic setting of Quebec from Mid Ordovician to Silurian (the Taconian Orogeny). 1) Erosional unconformity and normal faulting. 2) Stacking of nappes, 3) taconian metamorphism, 4) debris derived from the ophiolite, 5) syn-obduction sedimentation, 6) magmatism, 7) debris derived from the arc (slightly modified from Tremblay and Pinet (2016)).

### *Southern Chile*

Sand injectites in the Magallanes basin of southern Chile were described by Winslow (1983) and Hubbard et al. (2007). Hubbard et al. (2007) described injections hosted by the Cerro Toro Formation of Cretaceous age. Unlike most of the other locations included in this literature study, the remobilized material is very poorly sorted and contain grain sizes from mud to cobbles. The sand intrusions were interpreted to be sourced from the margins of submarine channel deposits.

Winslow (1983) also describe intrusions hosted by Late Cretaceous volcanoclastic strata (Mastrichtian), and argue that the trigger is linked to compression linked to thrusting in the accretionary prism. The highest occurrence of dikes appears at the toe of the largest thrust faults, intruding into the hanging wall (Figure 5-6).

Both Winslow (1983) and Hubbard et al. (2007) propose that the distribution of injectites is structurally controlled, based on the mapping of the orientation of the injectites in their study area.

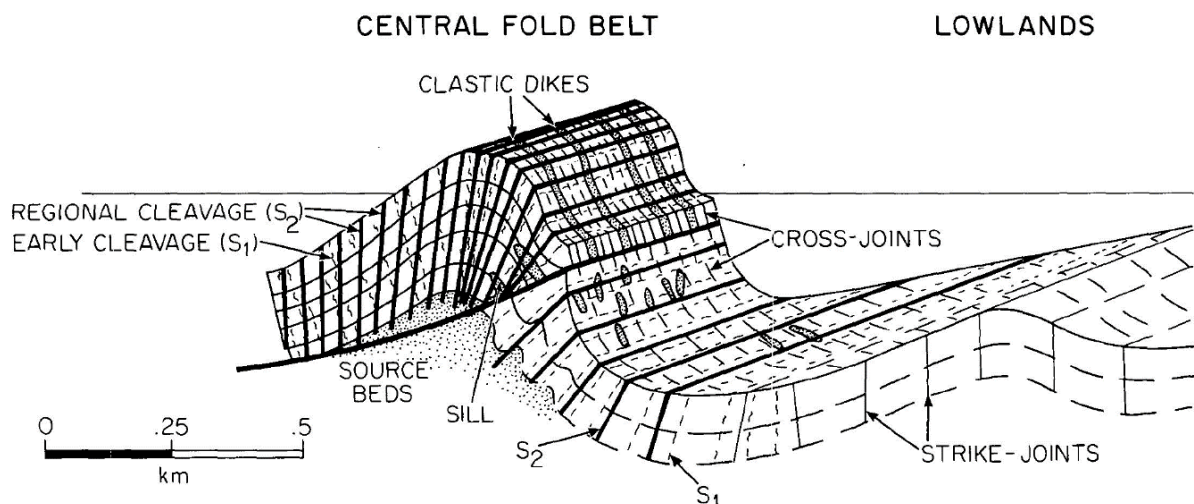


**Figure 5-6:** Schematic sketch of the relationship between the source and host rock of the sand intrusion. Note how the sand migrate into the joints (Figure 3 in Winslow (1983)).

### *Cauca Valley, Western Colombia*

The Cauca Valley is located in the Colombian Andes. During Plio-Pleistocene, the area was dominated by a compressive tectonic regime. The regime reflected a complex plate tectonic configuration, between the Nazca, Caribbean and South American plate, and the Panama- Costa Rica microplate (Pennington, 1981; Taboada et al., 2000).

Sand injectites are documented within the Plio-Pleistocene Zarzal formation, deposited in a lacustrine environment (Neuwerth et al., 2006). The remobilization occurred mainly by liquefaction of sand, and are observed as structureless intrusions injected into the surrounding rock. Fluidization also occurred as intrusions along fractures and bedding planes (Neuwerth et al., 2006). There is no evidence indicating that the sediment remobilization is triggered by sediment gravity flows. Consequently, seismicity was proposed as the most likely trigger mechanism by Neuwerth et al. (2006).

### *Israel*

Clastic dikes are described on the western margin of the Dead Sea Basin, and are hosted by the Late Pleistocene lacustrine Lisan Formation (Porat et al., 2007; Marco et al., 2014). During Pleistocene, the area was located in a fold and thrust system, and hence controlled by a convergent regime (Figure 5-7; Porat et al., 2007; Alsop and Marco, 2011). Consequently, the sand injection probably occurred after the deposition of the Lisan Formation (Late Pleistocene) and before the formation of the current landscape (Porat et al., 2007). Porat et al. (2007) suggested that the sand remobilization was triggered by seismic shaking linked to the earthquakes occurring along the Dead Sea fault zone, causing fluid pressure build-up.

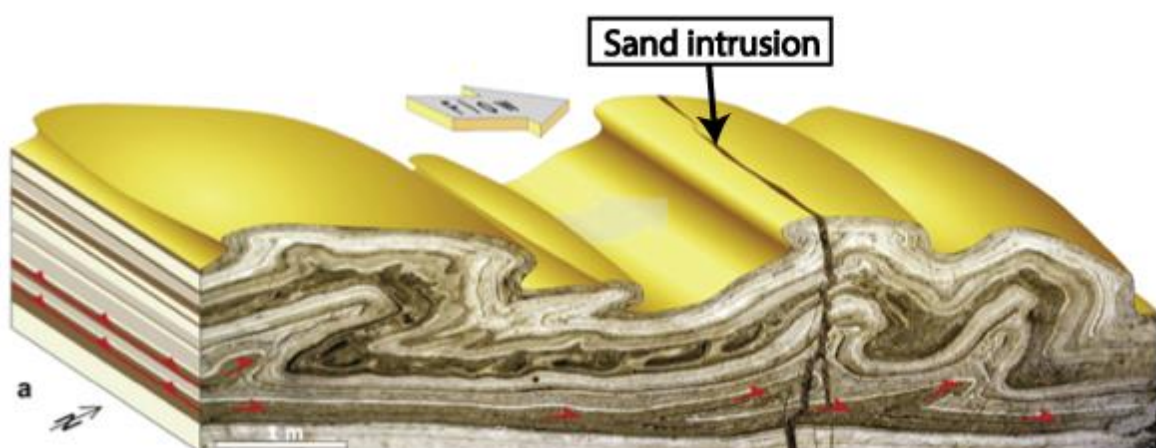


**Figure 5-7:** The model shows the relationship between the thrust folds and the injected dike (slightly modified from Alsop and Marco (2011)).

*Eastern Mediterranean*

In the eastern Mediterranean, on the continental margin outside the coast of Israel, clastic large-scale injectites are observed along the Afiq Submarine canyon in the Levant basin, hosted by Pliocene strata, i.e. the Yafo Formation/Yafo Sand Member (Frey-Martinez et al., 2007). According to Frey-Martinez et al. (2007) the remobilization happened during Zanclean (Pliocene) and Gelasian (Pleistocene), as an alternating process varying between injection episodes and deposition of deep-water sedimentation (Figure 5-8).

The continental margin outside the coast of Israel, is characterized by active tectonics, composed by a complex plate configuration (Frey-Martinez et al., 2007). The Pliocene epoch was dominated by deep-water sedimentation, in addition to clinoforms that were building out, sourced from the Yafo Formation (carbonate member). The area of progradation was exposed to large-scale slumping and gravitational tectonics (Almagor, 1980, 1984; Garfunkel, 1984; Garfunkel and Almagor, 1985; Almagor, 1986; Garfunkel and Almagor, 1987; Frey Martinez et al., 2005).

The area is characterized by mounding, caused by the remobilization, and each mound is flanked by kilometre scale depressions (Frey-Martinez et al., 2007). Frey-Martinez et al. (2007) propose that the trigger mechanism is related to earthquakes linked to active margin-compression.

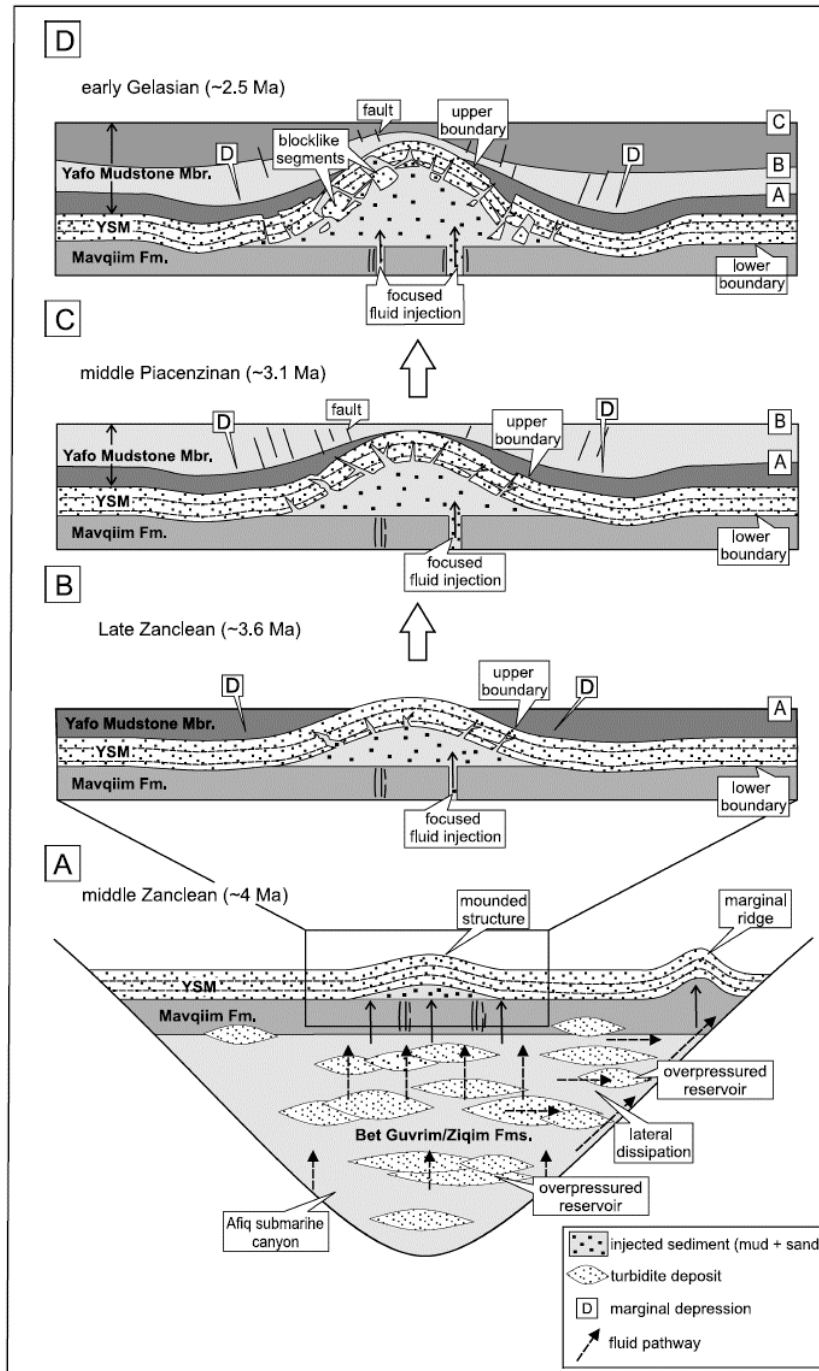


**Figure 5-8:** The figure is developed by Frey-Martinez et al. (2007), and show a model that explains the main events in the formation of the mounded features. YSM marks the Yafo Sand Member (Figure 16 in Frey-Martinez et al. (2007)).

### *The Apennines, Italy*

Sand injectites are documented within the Tortonian (Miocene) Marnoso-arenacca Formation, which consists of turbidites. The injection process occurred during Miocene, when the area was characterized by compressional regime (Huuse et al., 2010). The sand intrusions appear relatively shallow, suggesting a relationship between sediment sliding and sediment remobilization along faults (Gamberi, 2010). Gamberi (2010) believe that the trigger

mechanism is associated to loading, in addition to vertical and lateral fluid migration causing overpressure in shallow sand bodies, resulting in sediment remobilization.

### ***Japan***

Injectites are described by e.g. Ito et al. (2016) in a Pliocene trench-slope basin on the southern Boso Peninsula, at the basin floor of the trench, related to the tectonically active basin (Ito et al., 2016). The sand injections are hosted by the uppermost part of the Shiramazu Formation (Ito et al., 2016).

Boehm and Moore (2002); Duranti (2007); Jonk et al. (2007a); Thompson et al. (2007); Hurst et al. (2011); Sherry et al. (2012), Ito et al. (2016) propose that the sediment remobilization was initiated by seismicity and rapid loading (slides, slumping and storm waves). The seismicity was considered as the main trigger mechanism (Ito et al., 2016).

### ***Southeast Schmidt Peninsula, Sakhalin, Russia***

Sand injectites are documented on the southeastern coast of Schmidt Peninsula, Sakhalin, Russia (Macdonald and Flecker, 2007). During Miocene, the area was characterized by a retroarc geological setting, dominated by a dextral strike-slip system. The intrusions are present as sills, dikes and sheets, hosted by the Mid Miocene Pil'sk Suite, in addition to a small amount of dikes occurring in the underlying Tysk Suit. The largest occurrence of sand injectites is located in the high-strain zones (Macdonald and Flecker, 2007)

Macdonald and Flecker (2007) proposed an unexposed Paleogene suit or an offshore, deeper water sandstone unit within Miocene to be the parent beds. The age of the remobilization episode is also unclear. They conclude that the injection must have happened post Pil'sk and pre- or syn-deformational of the overlying Mayamraf Suit, in other words during Late Miocene.

Based on geological setting and timing, Sakhalin is compared to Santa Cruz in California (Figure 5-4). What separates the two is the scale and the geometry (Macdonald and Flecker, 2007).

### ***Midland Valley, Scotland***

The sand injection complex in Midland Valley, Scotland, is described as one single dike, creating a network combined with smaller dikes and sills branching out from the main intrusion. The injectite complex is hosted by the Dinantian-age (Early Carboniferous) oil-shale group of Scotland (Greensmith, 1957; Jonk et al., 2007b). Based on the mineral composition, sand-rich units above and below the dike represent good parent unit candidates (Jonk et al., 2007b).

Injectites occur at the western limb of an anticline that is plunging towards the northeast. The dikes are trending E-W, and cut through the tilted strata (Figure 5-9).

There are two theories describing how the remobilization process happened:

- Carruthers et al. (1912) proposed that the intrusions resulted from downward infilling of joints, which developed whilst the Dinantian-aged oil-shale group was deposited.
- Greensmith (1957) proposed that the sediment remobilization happened during Early Cretaceous, by upwards injection, triggered by seismic activity.

Jonk et al. (2007b) concluded that based on their study, it is impossible to achieve an unequivocal answer, but either way the injection happened during Early Cretaceous (Jonk et al., 2005b; Jonk et al., 2007b). At that time, the Midland Valley was characterized by numerous tectonically and volcanically active basins (Jonk et al., 2007b).

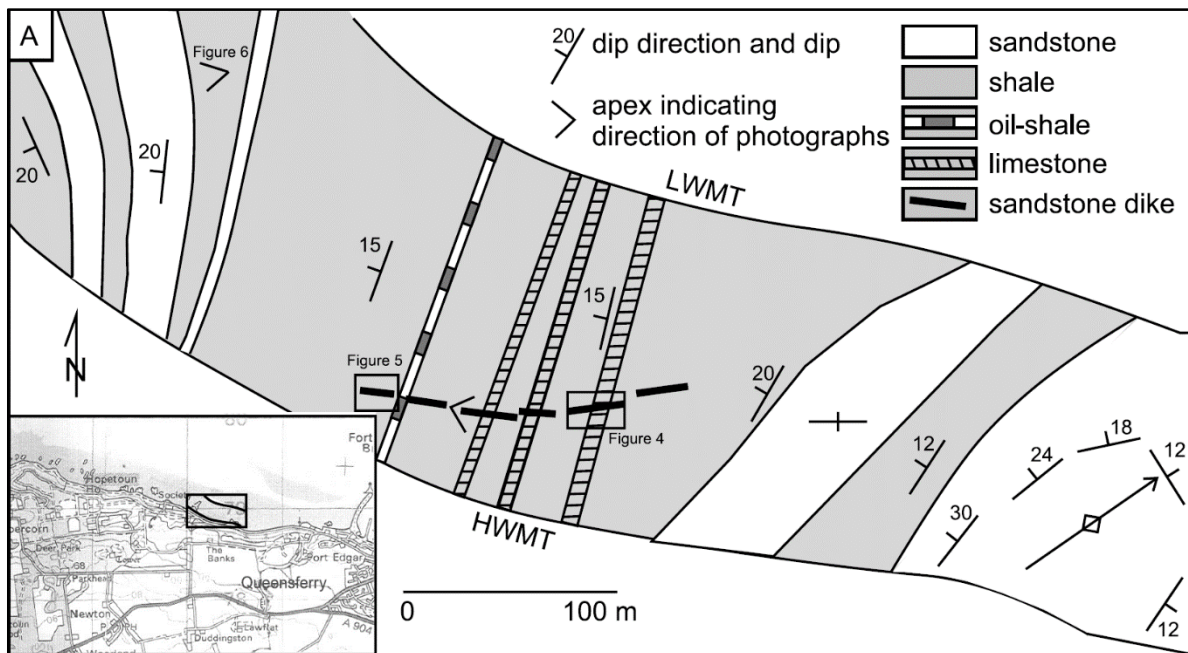


**Figure 5-9:** The figure displays the location of the injectites (mapview), in relationship to the dip of the host strata. HWMT marks the high water mean tide, and LWMT marks the low water mean tide (Figure 3a in Jonk et al. (2007b)).

### *West Texas*

The sand injectites in the Marathon basin, West Texas are relatively small-scale and show a variety of geometries, dominated by clastic dikes and sills (Diggs, 2007). The host of the sand injectites is a submarine-fan complex, called the Carboniferous Tesnus Formation, which were deposited in a tectonically active, migrating foredeep (Figure 5-10; Diggs, 2007). The Tesnus Formation accumulated due to the collision between Gondwana and Laurentia, and the compressional regime probably triggered the sediment remobilization (Diggs, 2007). The

remobilization happened during the Carboniferous (Diggs, 2007). The injectites show no system linked to the paleoslope, primary bedding and later structural trends, which indicates that the injection occurred at shallow depths, likely in relation to the accretionary prism (Diggs, 2007).

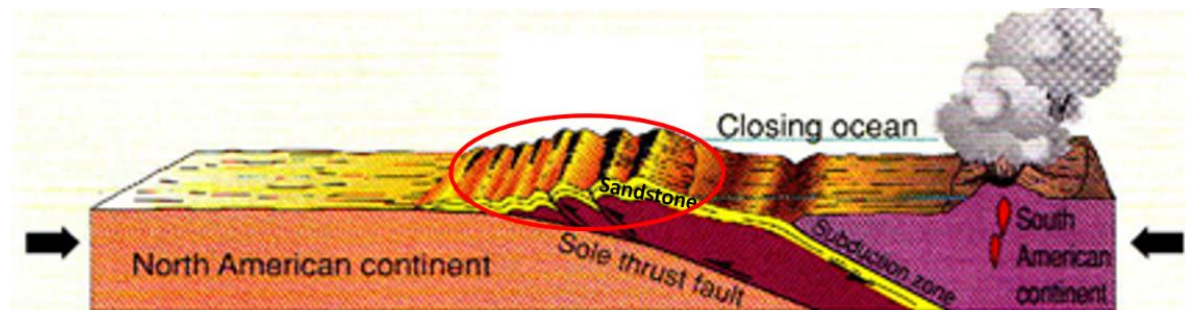


**Figure 5-10:** The figure displays the tectonic setting of the Marathon basin at the time of injection. The red circle marks the area where the sediment remobilization occurs (slightly modified from a picture from an exhibition at Big Bend visitor center).

### *Tabarka, Tunisia*

The injections the Tabarka, Northern Tunisia, is documented within the Oligo-Miocene Numidian Flysch Formation, and have a regional extent within the Maghrebien Flysch Basin (Thomas, 2011). The Maghrebien Flysch Basin was a foreland basin, in the western part of the Mediterranean Basin, which represented remains of the neo-Tethys ocean during Late Oligocene time (Thomas, 2011).

The intrusions are connected to the steep upper slope channel complexes, and are injected laterally into inter-channel slope deposits (Thomas, 2011). The injection process most likely happened during deposition or early burial of the Numidian Flysch Formation, hence during Oligocene to Miocene time (Thomas, 2011).

Thomas (2011) suggest that the injection was triggered by rapid deposition, and he use the injectites in Vocontian Basin (France) as an analogue. Figure 5-11 shows the basin setting during Late Oligocene. The observed sand injectites is located on the opposite side of the basin, relative to the subduction zone, which is different from other locations linked to convergent tectonics, e.g. Panoche Hills (where the sediment remobilization happened as a result of the compression caused by the colliding plates).



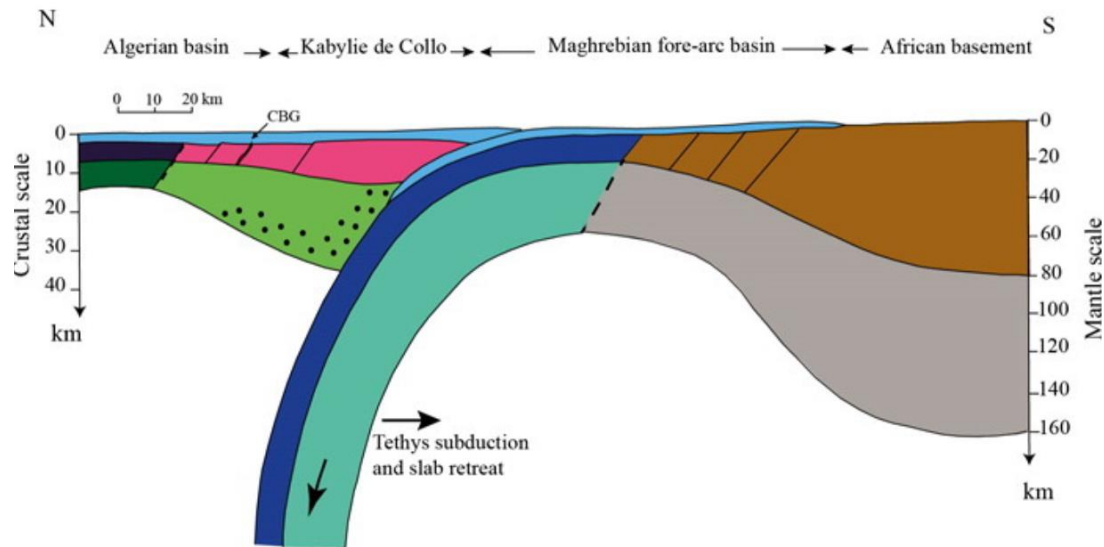


**Figure 5-11:** Tectonic setting of the Maghrebian Flysch Basin, during Late Oligocene (slightly modified from Abbassene et al. (2016)).

### *Utah, The United States*

On the Colorado Plateau in the United States, sand injection pipes (not the same as dikes) occur in Jurassic aeolian deposits in the Navajo Sandstone, Entrada Formation, Carmel Formation and Page Sandstone, which extends from Moab to Lake Powell (Chan et al., 2007).

Aeolian examples differ from deepwater settings, with respect to environmental controls and lithologies, but the basic concepts are the same (Chan et al., 2007). At the Colorado Plateau, water-saturated sabkha in addition to a relatively high water table, comprise the main factors that made the remobilization possible (Chan et al., 2007).

Chan et al. (2007) concluded that the trigger mechanism is problematic to understand, but they argued that it is not linked to dune progradation. Instead it is more likely that several trigger mechanisms were active during the deposition of the aeolian sandstones. Earthquakes and volcanism related to subduction during the Jurassic were considered as probable trigger mechanisms because of the proximity to the subduction zone (Chan et al., 2007).

### *Wyoming, The United States*

Sand injectites are found in the Cretaceous Mowry Formation, within the eastern Bighorn Basin in Wyoming (Beyer, 2015). The parent sand is proved to be the overlying Cretaceous Frontier Formation, more precisely the Peay Sandstone Group, sourced from the Cordilleran thrust belt as it was migrating towards east (Beyer, 2015). The sand injectites occur as sills and dikes at the nose and western flank of the fold.

Beyer (2015) suggested that the sediment remobilization was triggered by the Laramide compression, prior to or in the beginning of the formation of the Sheep Mountain Anticline, which is located within the Cordillera foreland. Already existing cracks might have acted as migration paths (Beyer, 2015). The downward injection probably occurred as a result of a highly stratified horizontal stress within the Frontier Formation, as a consequence of the depositional pattern, burial and lithification history of the area (Beyer, 2015)

## 5.2 Basins at inverted passive margins (flank and toe of slope)

### *South Africa*

Truswell (1972), Cobain et al. (2015) and Cobain et al. (2017) describes sand injectites in basin-floor lobes in the Karoo basin in South Africa. The injectites are observed as sills and dikes within the Permian Ecca Group. Injectites in the Karoo basin were sourced from the base of lobes at the basin floor, and from slope channels (Figure 5-12; Cobain et al., 2017). Cobain et al. (2017) suggested that lateral pressure transfer was the main trigger mechanism. None of the mentioned authors describe the timing of the remobilization, but since the host rock is of Permian age, the injection must have happened later.

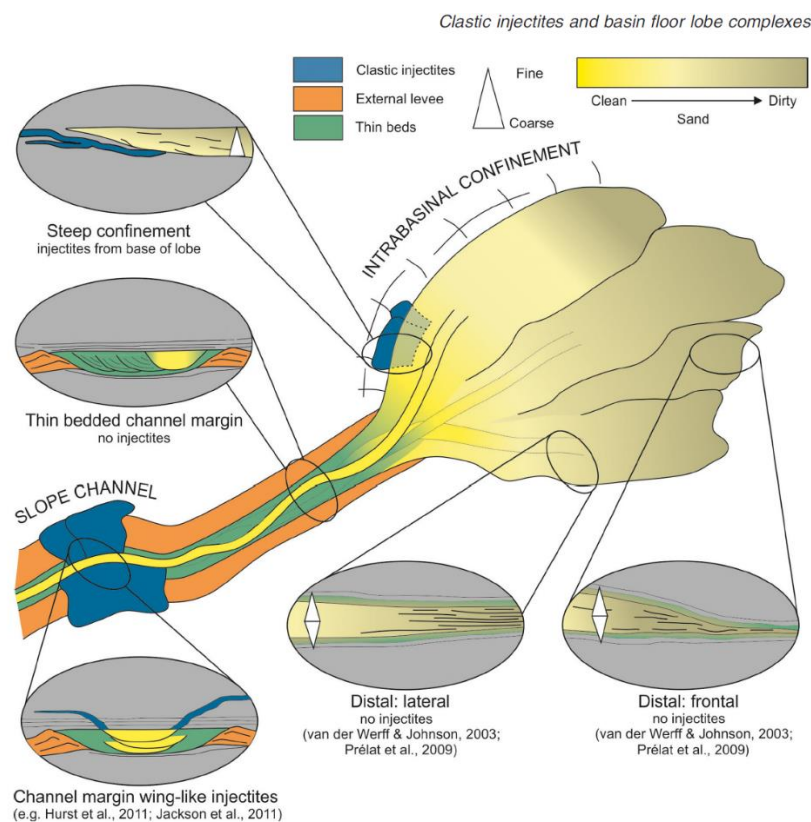


**Figure 5-12:** The sketch shows how the sand injectites are distributed related to the slope and basin floor fan (Figure 8.1 in Cobain et al. (2017)).

***Australia***

Injectites are described in the Dampier sub-basin on the northwestern shelf of Australia. The injectites were sourced from the Angel Formation, a sand rich deep-water fan system (Dharmayanti et al., 2006). Injectites in the Dampier sub-basin are only briefly described in the literature.

***Angola***

The injectites in the Lower Congo Basin are documented in Upper Miocene sediments, and they were sourced from the Upper Miocene fan deposits (Monnier et al., 2014). They are characterized as large-scale injectites, and their geometries are described as conical and saucer-shaped, similar to the observations in the North Sea. The injectites were directed upwards and commenced at the updip fringe of a submarine lobe (Monnier et al., 2014).

The timing of the remobilization is dated to the Miocene – Pliocene transition, but it only lasted for a short amount of time (Monnier et al., 2014). Because of its short duration, Monnier et al. (2014) propose that the sediment remobilization most likely was caused by a single event, and possibly due to salt diapiric movements. The salt migration caused flank uplift, and presumably fault displacement. Another likely trigger mechanism, contributing in the process of overpressure build-up, is lateral pressure transfer (water flow), enhanced by the inclined margins of the lobe. Monnier et al. (2014) suggest that lateral transfer probably occurred as a result of hydrocarbon migration. In the study area, filling of the Miocene reservoirs took place in Late Miocene and Early Pleistocene, which correlates well with the timing of the sediment remobilization (Figure 5-13; Monnier et al., 2014).

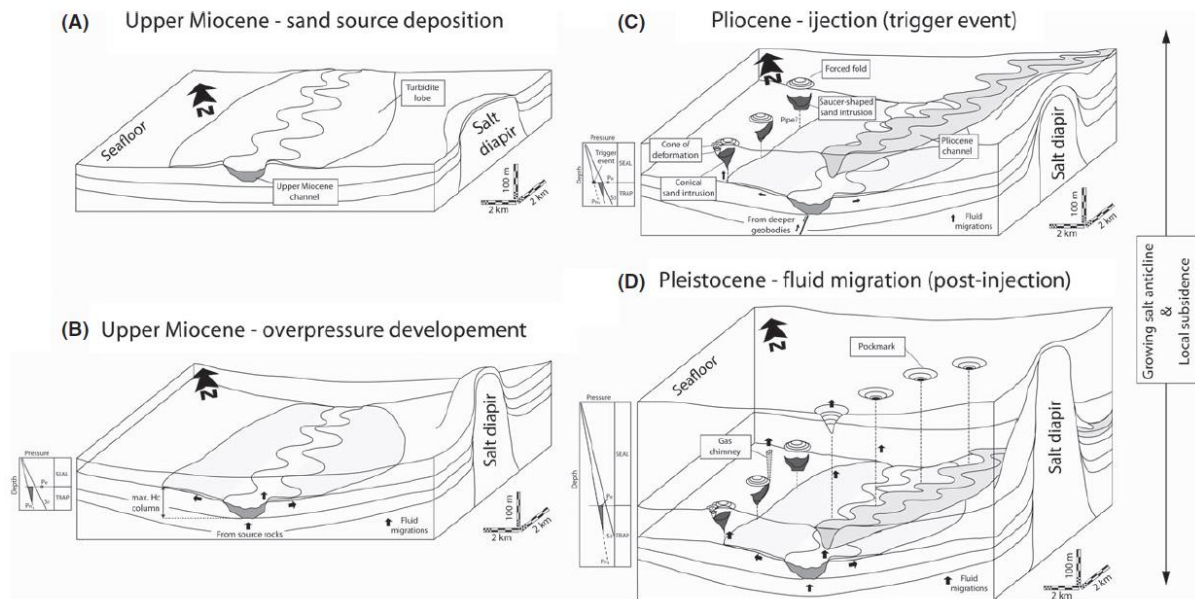


**Figure 5-13:** The figure describes how Monnier et al. (2014) suggest that sand intrusions were triggered. A) Describes a sand rich submarine channel complex. B) Hydrocarbon migration along the sandy fringes of the channel lobes. The migration of salt caused uplift of the flanks, and overpressure in the sandy aquifer developed as a result of buoyancy affecting the hydrocarbon column in addition to lateral pressure transfer. C) Sand intrusions were formed due to an opening of a fracture caused by movement in the salt. D) Fluids may have moved through the sand intrusions and to the seabed, observed as pockmarks (Figure 12 in Monnier et al. (2014).

### China

The Bohai Bay basin was developed by extensional and transtensional tectonics (Allen et al., 1997; Allen et al., 1998; Qi and Yang, 2010). Occurrences of sand intrusions are described at the toe of slope in a lacustrine Cenozoic sub-basin, called the Jiyang Depression, which is located in the eastern part of the Bohai Bay Basin. The Jiyang Depression is enclosed by three uplifted highs: one in the southeast, one in west, and one in the northwest (Zhang et al., 2016).

The accumulated sediments in the Jiyang Depression consist of Paleogene, Neogene and Quaternary strata. The Paleogene strata are further divided into three Formations (Jiang et al., 2011). The sand injectites occur in the lower part of the Eocene Shahejie Formation, which is the oldest interval of Paleogene (Allen et al., 1998; Zhang et al., 2016). The Shahejie is characterized by an extraordinary high sedimentation rate, and consequently, several fan-deltas and braid-deltas developed along the border for the lake (Zhang et al., 2016). Zhang et al. (2016) suggested that the high sediment influx generated slides and slumps which might have triggered sediment remobilization (Figure 5-14).

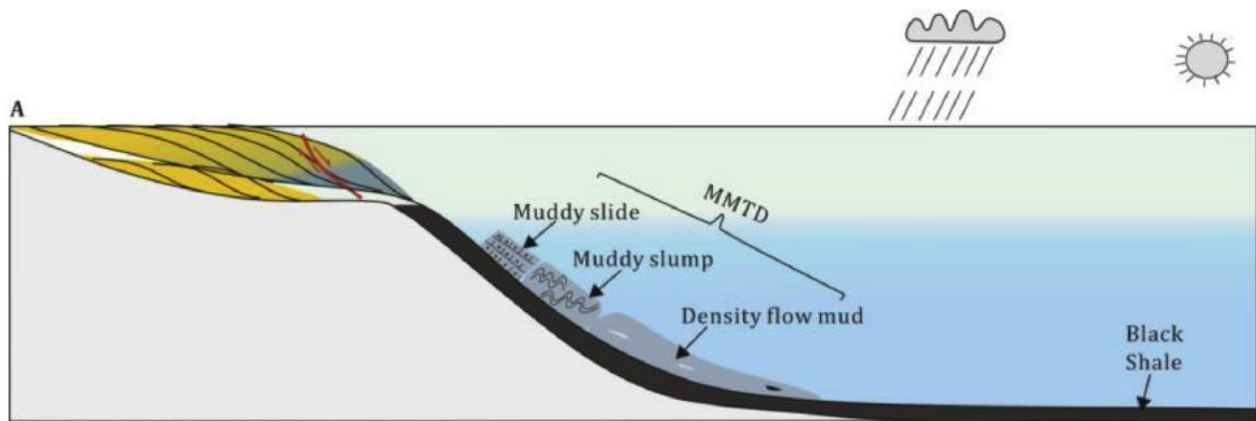


**Figure 5-14:** Basinal setting of the Bohai Bay Basin during sand remobilization (Slightly modified from Zhang et al. (2016).

### *The North Sea (UK)*

During Early Cenozoic, the Faeroe-Shetland basin was exposed to a major uplift-event. This event provided significant clastic sediment input to the basin during the Palaeocene (Hall and Bishop, 2002). Large submarine fans also developed during early Mid Eocene (Mitchell et al., 1993). After this period, mainly muddy sediments were deposited on top of the clastic sediments during Eocene and Oligocene (Shoulders et al., 2007). The sediment remobilization commenced in Mid Miocene and lasted until Late Miocene. The injection episode coincides with an uplift episode of the basin flanks (Davies et al., 2004).

Sand injectites in the Faeroe-Shetland show a conical large-scale geometry (Cartwright et al., 2008), and appear in host rocks dated from Eocene to Miocene (Shoulders et al., 2007). They occur at the toe of slope, the flank and the slope in the basin (Shoulders et al., 2007). Shoulders and Cartwright (2004) have found strong evidence indicating the sand injectites are sourced from sand-rich Mid Eocene submarine fans. However, it is likely that such a large intrusion province originated from several parent units, and Shoulders et al. (2007) therefore suggested that Palaeocene sands also contributed as parent units.

### *Southeastern France*

During Cretaceous, the Vocontian Basin was located at a palaeo-inverted passive margin (Figure 5-15; Ziegler, 1990). Sand injectites in the Vocontian Basin mainly occur in the channel banks, laterally sourced from sandy channels (Parize and Friès, 2003), and represent an architectural element of a complex turbiditic system (Parize and Friès, 2003; Parize et al., 2007). In other words, the sand injectites occur at the slope and toe of slope. The sand injections are hosted by Aptian to Albian (Cretaceous) marly formations, and the remobilization happened the same epoch (Parize et al., 2007). Both dikes and sills are present, but the dikes originate

from the sills. Based on field observations Parize and Friès (2003) suggested that the sand intrusions propagated both upwards and downwards.

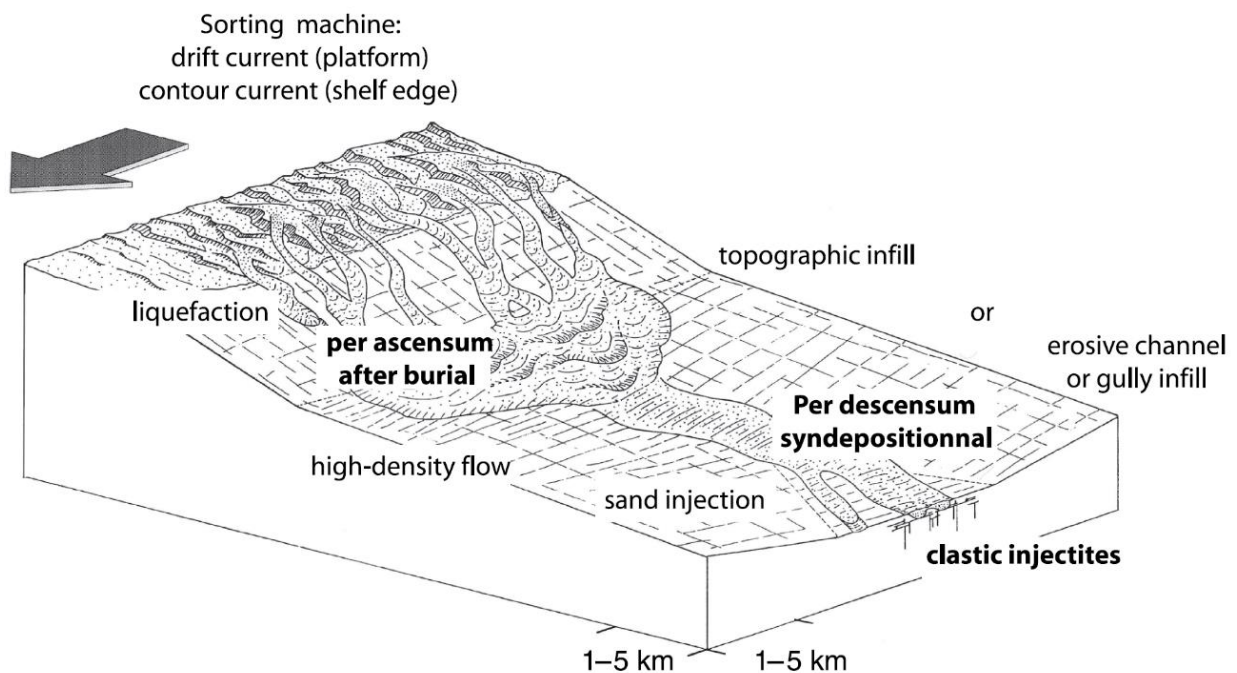


**Figure 5-15:** Model developed by Parize et al. (2007), describing the basinal setting, sand supply to the basin, and where in the basin the clastic injectites occur (Figure 4 in Parize et al. (2007)).

### ***India***

In the Bay of Bengal, sand injectites are documented in the Krishna-Godavari Basin. The modern day configuration is a good analogue to what it looked like in the Pliocene when the remobilization occurred (Shanmugam et al., 2009). Sand injectites are observed on the slope and at the toe of slope (Shanmugam et al., 2009). According to Shanmugam et al. (2009), seismicity is a likely trigger mechanism, both when it comes to mass transport and sand injections. Mass transport deposits characterize the basin margin, and Shanmugam et al. (2009) have also proposed that the mass transport processes triggered sand remobilization.

### ***County Clare, Ireland***

The western Irish Namurian basin contains both sand injectites and sand volcanoes (extrudites), located at the slope and the toe of slope (Gill and Kuenen, 1957; Jonk et al., 2007a). Gill and Kuenen (1957) observed a clear link between sand volcanoes and slumping; all the largest sand volcanoes (above 10 feet in diameter) were apparently connected to fractures originating from shear-plane systems associated to deep-channel slumps. They did not observe clear evidences of compression and accumulation of sediments at the toe of slope, and consequently they discussed if the sand remobilization was caused by slumping and sliding, triggered by an

earthquake, or if the sand injection and extrusion was triggered by the earthquake itself. An alternative explanation of the lack of piling-up features at the toe of slope could be that the sediment piles have been removed by sweeping and erosion (Gill and Kuenen, 1957).

Jonk et al. (2007a) do not write anything about the timing of the remobilization. The slumping and the sand remobilization are assumed to have occurred simultaneously, and since Gill and Kuenen (1957) mentioned that the slumps are of Carboniferous age, the sand remobilization are assumed have occurred during Carboniferous.

### ***Rosroe Peninsula, Western Ireland***

Archer (1984) describes sand injectites, observed as sheets, in the Early Ordovician Rosroe Formation, which was deposited as a deep-marine fan. Sand intrusions were, according to Lonergan et al. (2000), formed at very shallow depths, and were most likely triggered by depositional events, e.g. mass transport processes.

The sand intrusions occurring at Rosroe Peninsula, Ireland, are apparently only briefly described in the literature.

### ***Outer Moray Firth, The North Sea (UK)***

The Outer Moray Firth belongs to the North Sea, UK sector, and hence it is positioned at an inverted passive margin (Cartwright, 2010). In this area sediment remobilization occurred during Eocene (Duranti and Hurst, 2004). Sand injectites represent good reservoirs also in this part of the North Sea, e.g. Chestnut and Alba reservoirs (Huuse et al., 2005)

Conical and winglike sand intrusions are frequently observed at Outer Moray Firth, like the rest for the North Sea Basin, and most of the Upper Paleocene and Eocene sandstones are connected to remobilization (Huuse et al., 2005). The area is characterized by polygonal faulting, and it is a possibility that the sand has intruded along the polygonal faults (Lonergan et al., 2000). Like in the rest of the North Sea, possible trigger mechanisms have been suggested to be related to sliding and slumping, but Huuse et al. (2005) also suggested earthquakes as a possible trigger mechanism.

## **5.3. Occurrence of remobilized sand linked to basinal setting: summary**

Table 5-1 shows a summary and overview of the locations where sand injection occurs, described in section 5.1 and 5.2.

**Table 5-1:** Overview of the distribution of sand injection provinces worldwide, and which basin setting they belong to. A complete version of the table is attached in Appendix B.

Location	Basin	Specific area	Inclined parent body	Time of remobilization	Basin setting at time of remobilization	Location of remobilized sands	References
<b>South Africa</b>	Karoo basin				Inverted passive margin	Toe of slope (Proximal in the basin floor lobes, linked to pinchouts)	(Cobain et al., 2015; Cobain et al., 2017)
<b>Angola</b>	Lower Congo Basin		Yes	Miocene - Pliocene transition	Inverted passive margin (flank uplift generated by salt diapirism)	Toe of slope (Updip fringe of submarine lobe)	(Monnier et al., 2014; Oluboyo et al., 2014)
<b>Australia</b>	Dampier Sub-basin				Inverted passive margin		(Dharmayanti et al., 2006)
<b>California</b>	San Joaquin Basin	Panoche and Tumey Hills	Yes	Lower Palaeocene and Eocene	Convergent (Compressional) margin	Above crest of sloping permeable sediments	(Schwartz et al., 2003; Minisini and Schwartz, 2007; Vigorito et al., 2008; Cartwright, 2010; Vétel and Cartwright, 2010; Palladino et al., 2016)
<b>Southwestern California</b>		Dana Point	Yes	Miocene	Transform (Compressional) margin		(Bouroullec et al., 2010)
<b>California</b>	Santa Cruz Basin	Santa Cruz	Yes	Miocene	Transform (Compressional) margin	Basin margin	(Boehm and Moore, 2002; Thompson et al., 2007; Sherry et al., 2012)



<b>Canada</b>		Quebec	Yes		Convergent (compressional) margin	Slope	(Hiscott, 1979; Tremblay and Pinet, 2016)
<b>Southern Chile</b>	Magellanes basin		Yes		Retroarc foreland basin (Convergent margin)		(Winslow, 1983; Hubbard et al., 2007)
<b>China</b>	Bohai Bay Basin				Inverted Passive margin	Basin Slope Transition	(Zhang et al., 2016)
<b>Western Colombia</b>		Cauca Valley		Plio-Pleistocene	Convergent (compressional) margin		(Neuwerth et al., 2006)
<b>The North Sea (UK)</b>	The Faroe-Shetland Basin			Mid – Late Miocene	Inverted passive margin	Flank, Slope, toe of slope	(Mitchell et al., 1993; Hall and Bishop, 2002; Davies et al., 2004; Shoulders and Cartwright, 2004; Shoulders et al., 2007; Cartwright, 2010)
<b>South–East France</b>	Vocontian Basin			Cretaceous (Aptian to Mid Albian)	Inverted passive margin	Slope, toe of slope (channel banks)	(Parize and Friès, 2003; Parize et al., 2007)
<b>India</b>	Krishna-Godwari basin	Bay of Bengal		Pliocene	Inverted passive margin	Slope and toe of slope	(Shanmugam et al., 2009)
<b>Ireland</b>	Western Irish Namurian basin	County Clare		Carboniferous	Inverted passive margin	Slope and toe of slope	(Gill and Kuenen, 1957; Jonk et al., 2007a)
<b>Western Ireland</b>		Rosroe Peninsula			Inverted passive margin	Toe of slope	(Archer, 1984; Lonergan et al., 2000)
<b>Israel</b>	Dead Sea Basin			Pleistocene-Holocene	Convergent (compressional) margin		(Porat et al., 2007; Alsop and Marco, 2011)
<b>Eastern Mediterranean</b>	Levant basin	Outside the coast of Israel	No	Pliocene and Pleistocene	Convergent (compressional) margin		(Frey-Martinez et al., 2007)

<b>Italy</b>		Apennines	Yes	Late Miocene	Convergent (compressional) margin		(Gamberi, 2010; Huuse et al., 2010)
<b>Japan</b>		Boso Peninsula		Pliocene or later	Convergent (compressional) margin	At the toe of the trench-slope basin	(Ito et al., 2016)
<b>The North Sea (Norway)</b>	The North Sea Basin			Palaeocene, Early Eocene, Oligocene, Miocene	Inverted passive margin	Flank and toe of slope	(Jenssen et al., 1993; Lonergan et al., 2000; Faleide et al., 2002; Jonk et al., 2005a; Cartwright, 2010; Christensen, 2015; Rundberg and Eidvin, 2016)
<b>Russia</b>		Southeast Schmidt Peninsula, Sakhalin	Yes	Miocene	Transform margin		(Macdonald and Flecker, 2007)
<b>The North Sea (UK)</b>	North Sea Basin	Outer Moray Firth		Eocene	Inverted passive margin		(Lonergan et al., 2000; Duranti and Hurst, 2004; Huuse et al., 2005; Cartwright, 2010)
<b>Scotland</b>		Midland Valley	Yes		Convergent (compressional) margin		(Jonk et al., 2005b; Jonk et al., 2007b; Underhill et al., 2008)
<b>West Texas</b>	Marathon Basin		Yes	Carboniferous	Convergent (compressional) margin	In accretionary prism	(Diggs, 2007)
<b>Tunisia</b>	Maghrebian Flysch Basin	Tabarka	Yes	Oligo-Miocene	Convergent (compressional) margin	Lateral injection originating in channel complex in upper slope environment	(Thomas, 2011)

<b>The U.S.</b>	The Colorado Plateau	Utah	Jurassic	Convergent (compressional) margin		(Chan et al., 2007)
<b>The U.S.</b>	Eastern Bighorn Basin	Wyoming	Cretaceous	Convergent (compressional) margin	The western flank and the nose of of the Sheep Mountain Anticline	(Beyer, 2015)



## 6. Observations from the northern North Sea

Chapter 5 demonstrated an overrepresentation of sand remobilization at inverted passive margins, and the North Sea basin shows the largest intrusion province in the world (Cartwright, 2010). The injectites are present in Cretaceous to Pleistocene strata, but are most frequently observed in Eocene to Oligocene strata (Figure 6-1; Jolly and Lonergan, 2002; Hurst and Cartwright, 2007). Furthermore, sand intrusions are absent in the Central Trough area (Figure 6-1; Huuse et al., 2010). The frequent occurrence of sand injectites in the North Sea implies that there must have been favorable conditions for initiation of sand remobilization.

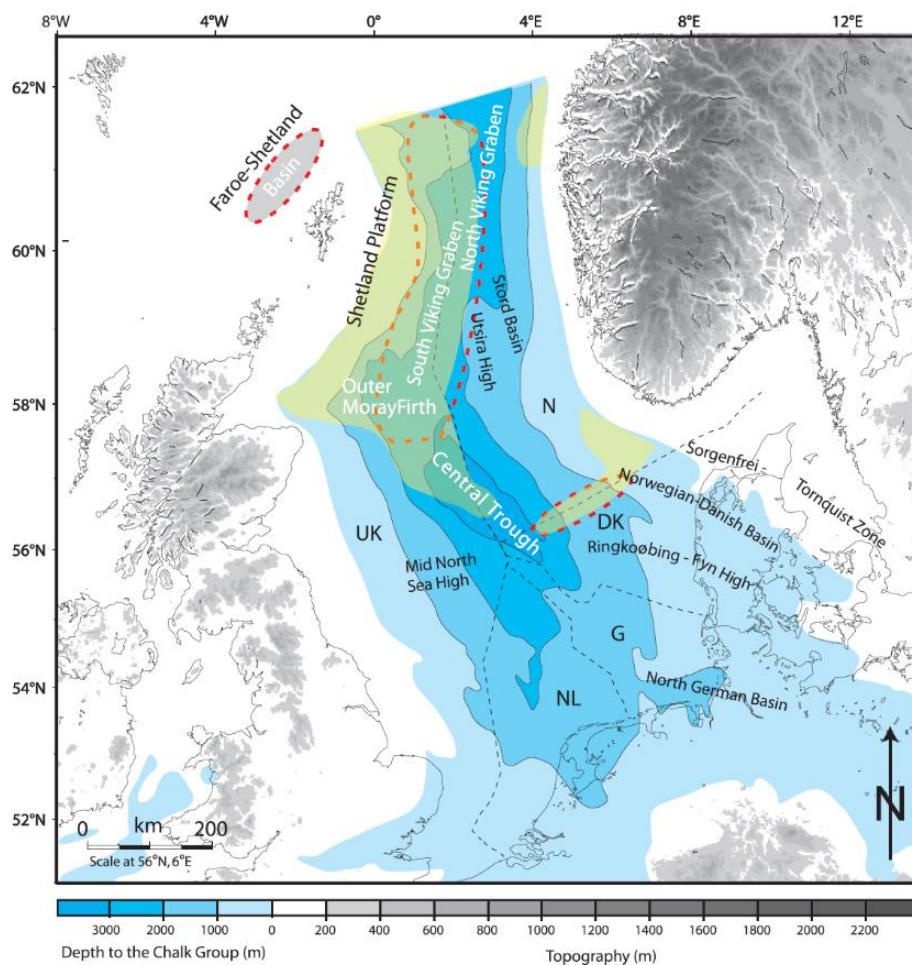


**Figure 6-1:** The map shows the distribution of large-scale sand injectites, in the Paleogene. The injectites are marked with the dashed red line, and the distribution of Paleocene sand is marked with semitransparent yellow (Slightly modified from Huuse et al. (2007)).

The aim of the investigations presented in the forthcoming chapter is to see if the observations coincide with the hypothesis developed in chapter 5. The hypothesis suggests that remobilization of sand occur more frequently in basins located at certain tectonic settings. The

northern North Sea basin represents an inverted passive margin. Here, the focus will be to search for evidence proving a link between trigger mechanisms and processes that occur frequently at inverted passive margins.

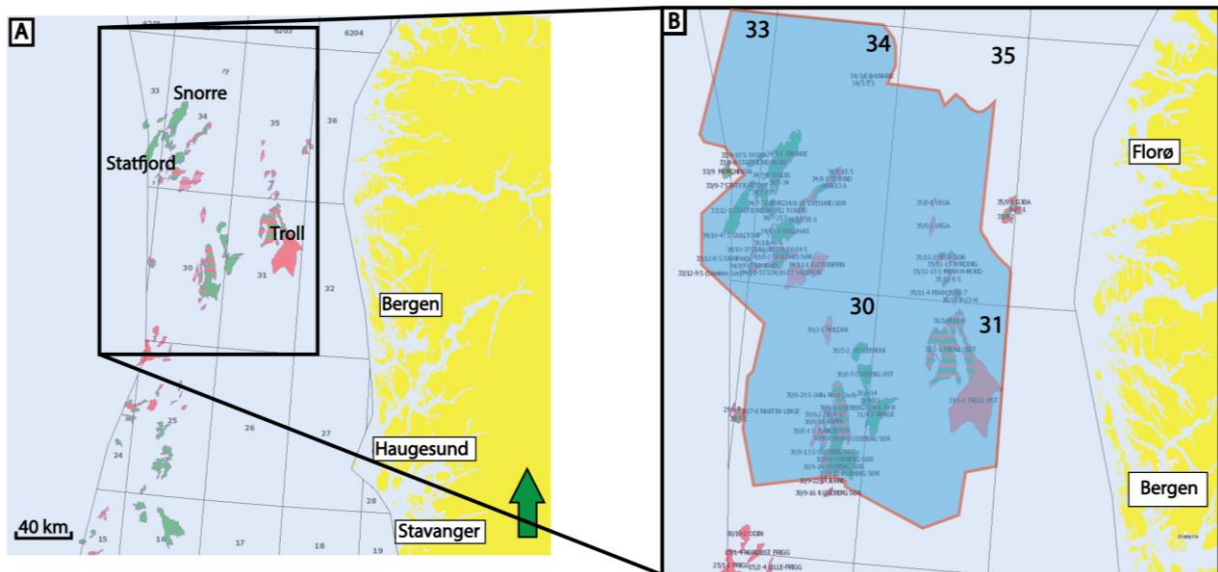


**Figure 6-2:** The map shows the extent of the study area. Slightly modified from NPD factpages (retrieved from their web page November 2017). A) Shows an overview picture of where the study area is located. B) shows a zoom-in of the location of the study area.

The location of the study area is displayed in Figure 6-2, and is divided into seven smaller areas (Figure 6-3). The subdivision of the study area is based on the variation in seismic characteristics from north to south (area 1, 2 and 3) and east to west (subarea A, B and C).

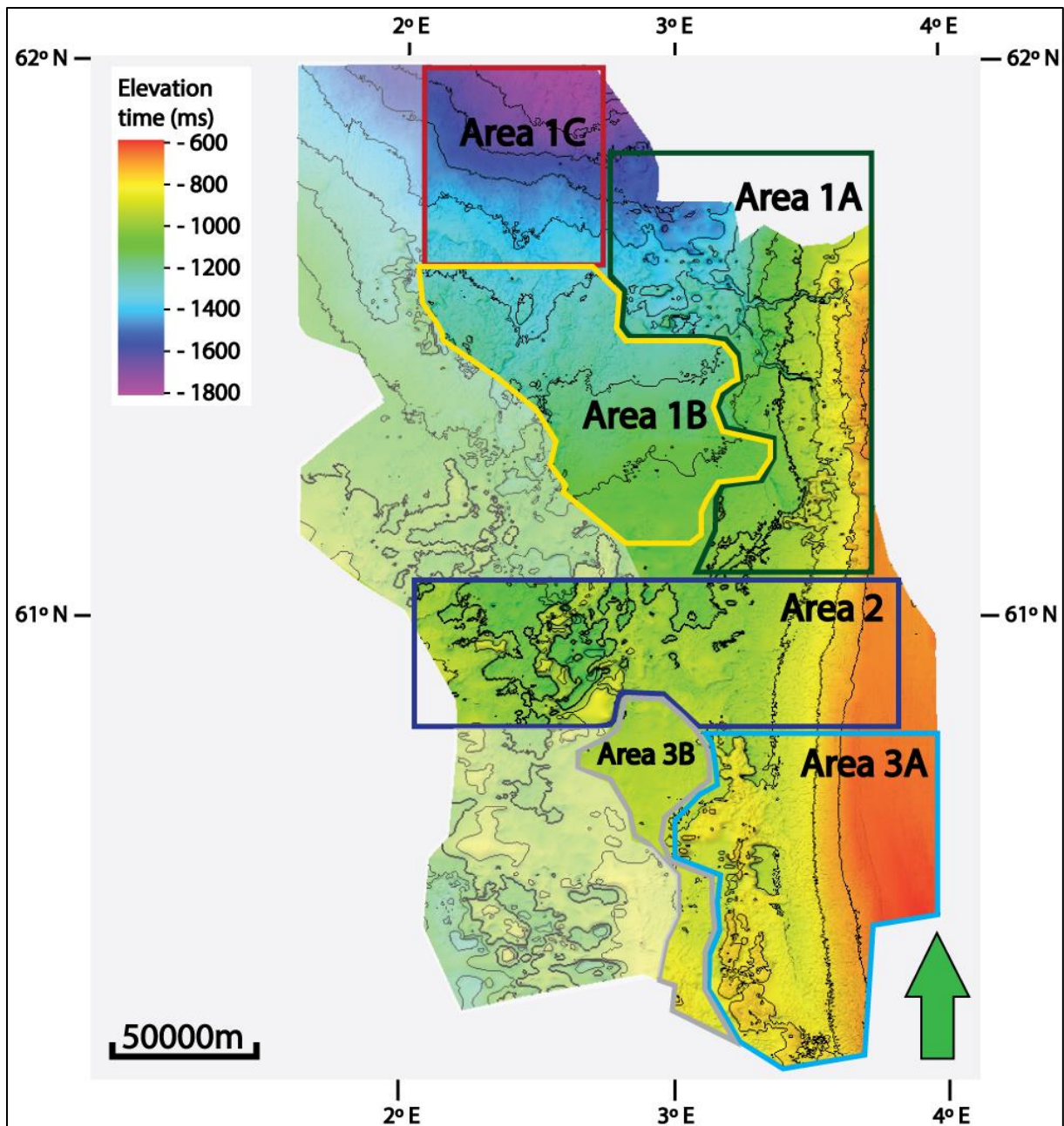


**Figure 6-3:** Elevation map of top Hordaland Group displaying an overview of the subdivision of the study area. The vertical exaggeration is set to 7,5 to make the mounds easier to recognize.

Disturbed reflectors together with thickening of the studied interval are frequently observed within the Hordaland Group. The thickening of the interval is observed in profile view, but also stands out in map view observed by a color change towards yellow, orange and red (Figure 6-4). From here and onwards the thickening of layers forming mounded features will be referred to as mounds.

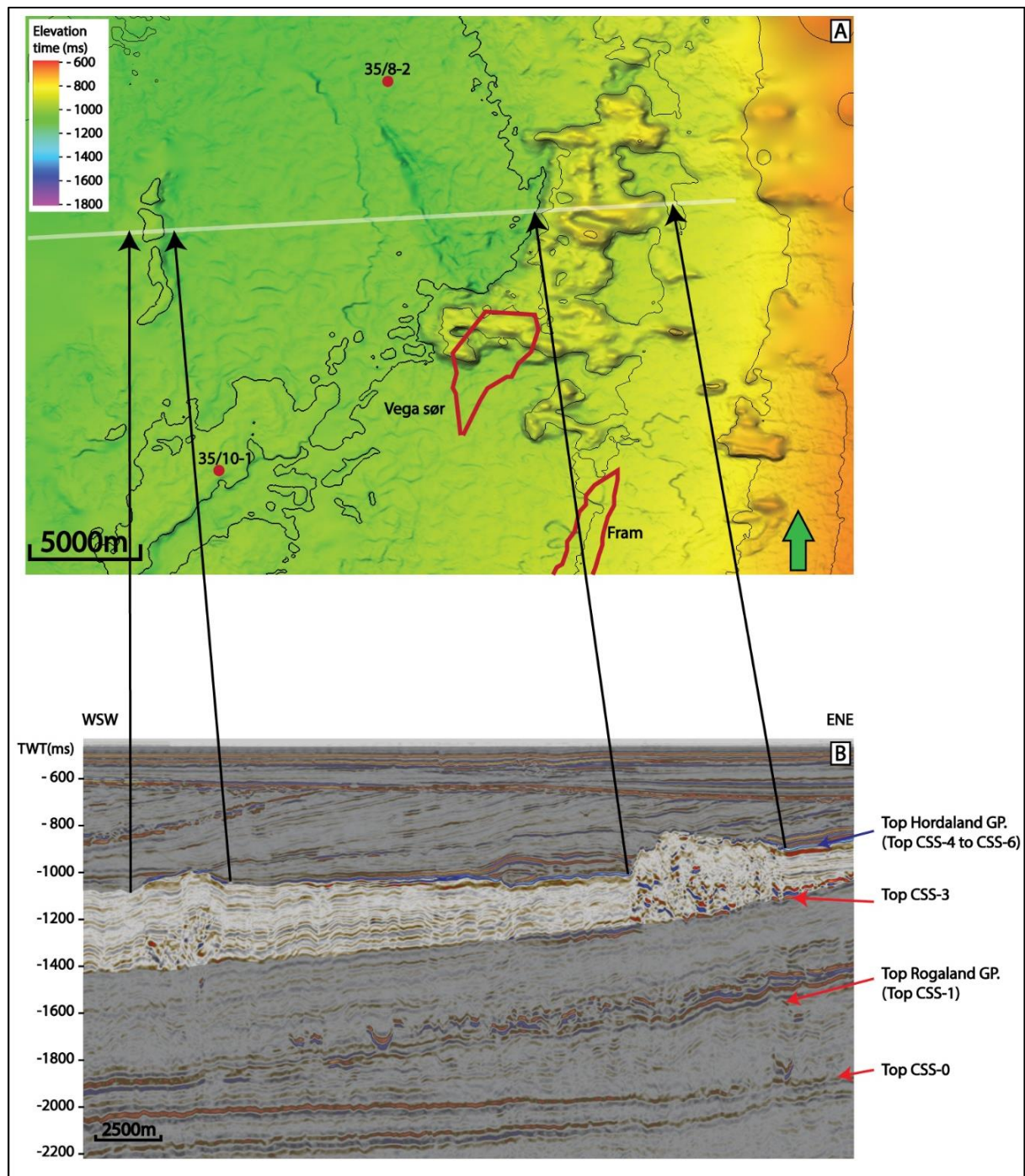


**Figure 6-4:** Figure A) shows an elevation map of top Hordaland Group. Figure B) displays a seismic cross section, cutting through the mounded features. The location and orientation of the seismic profile is displayed by the semitransparent white line in Figure A). The black arrows pointing from Figure B to Figure A, shows how the mounded features in profile view correlates to the elevated areas in map view. The two figures are located within area 1A.

### 6.1 Seismic observations in area 1A

Area 1A extends from the basin-flank transition to the upper flank (west to east) and from the northeastern to the central parts of the study area (Figure 6-3).



### 6.1.1 Shapes of mounds

In area 1A, mounds are observed frequently along the basin flank transition and at the flank. The large mounds appear to be arranged together in groups, forming clusters or ridges. Smaller mounds occur solely at the upper flank.

The northern part of the subarea shows mounds arranged in clusters, with overlying layers onlapping onto the mounds. This type of arrangement of the mounds is observed west of the basin-flank transition, close to where the gradient of the slope changes (Figure 6-5). Figure 6-6 shows a cross-section that cuts through the clustered mounds from WSW to NE. The seismic profile shows several connected mounds, in addition to two mounds that are disconnected to the others. Within the largest mound, chaotic and bright reflectors are observed towards the northeast. The reflectors are brighter and less chaotic in the southwestern part of the largest mound. Some of the brights observed on the edge of the west-southwestern part of the large mound, appear as almost vertical and extend from approximately top CSS-3 to top Hordaland Group (Figure 6-6). The smaller mounds, located west and east of the largest mound show bright and chaotic reflectors at the base of the studied interval, and continuous and dim reflectors in the upper part of the mound.

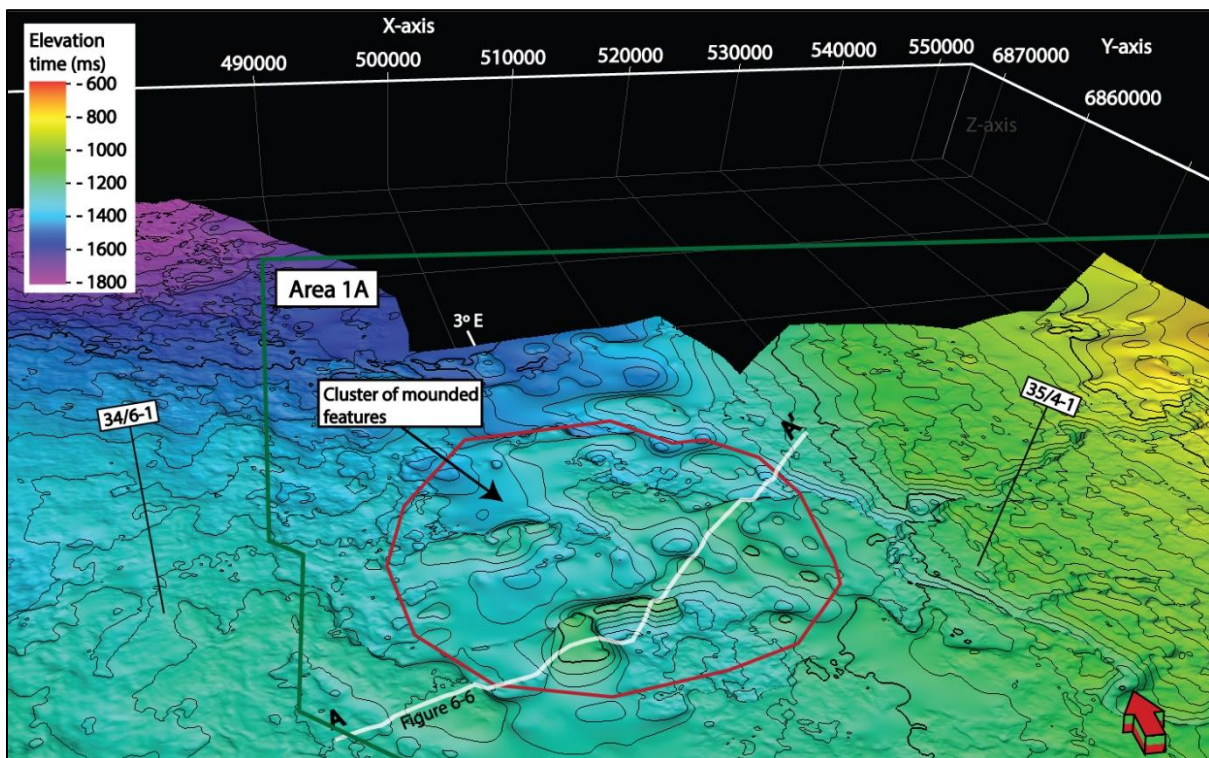


**Figure 6-5:** Elevation map of the northernmost part of area 1A (a part of top Hordaland Group). The dark green frame marks the extent of area 1A. The clustered mounds are observed within the red circle. The vertical exaggeration is set to 7,5 to make the mounds easier to recognize, and the contour lines show a spacing of 30ms.

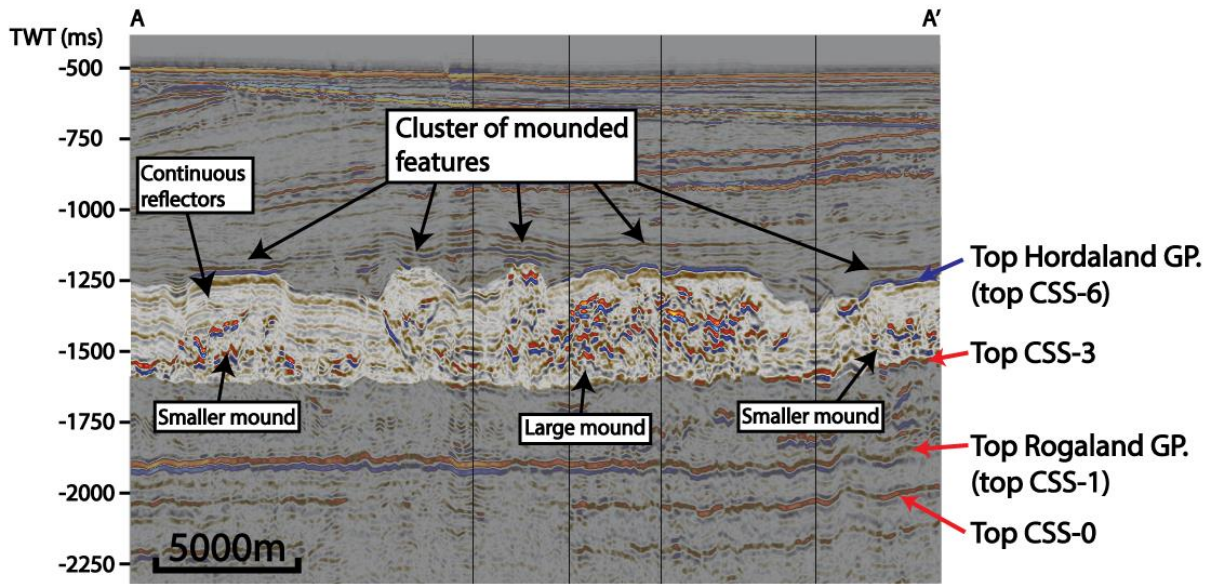


**Figure 6-6:** Seismic cross-section of a composite line that is cutting through the clustered mounds. The studied interval is marked by the highlighted area. The location and orientation of the seismic profile is displayed in Figure 6-5.

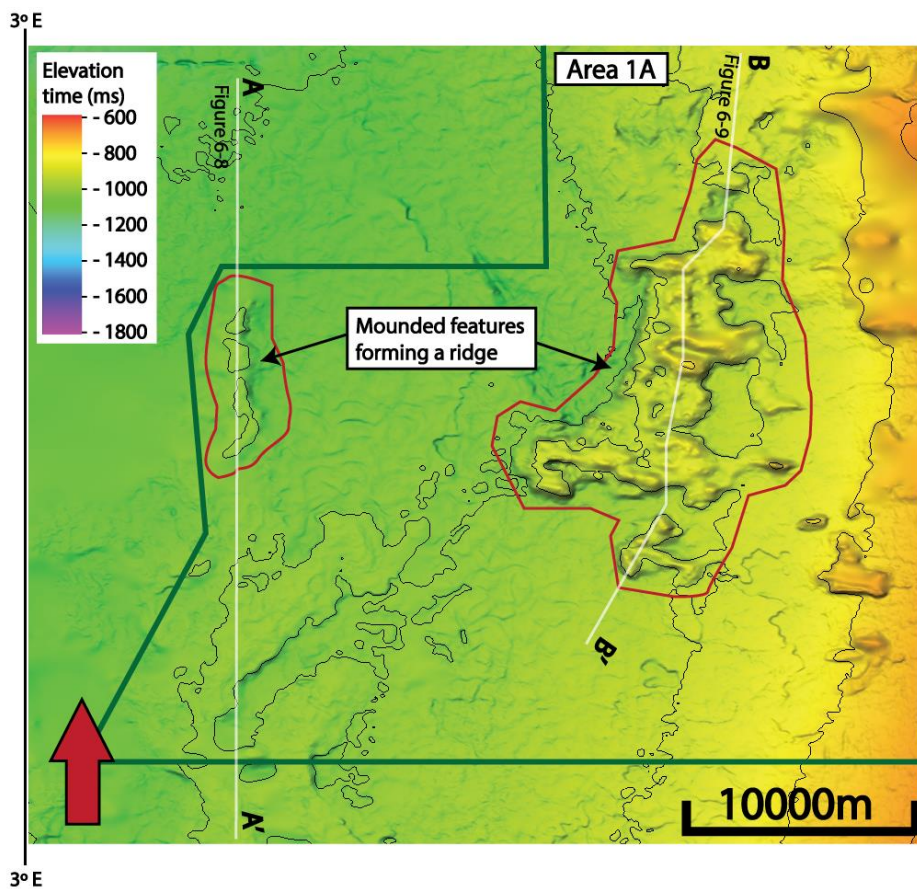


**Figure 6-7:** Elevation map of the southernmost part of area 1A (parts of top Hordaland Group). The dark green frame marks the extent of subarea 1A. The mounds arranged as ridges are observed within the red circles. The vertical exaggeration is set to 7,5 to make the mounds easier to recognize.

Further south within area 1A, the mounded features create ridges, parallel to the eastern margin (trending N-S). The ridges were first recognized in map view, as the ridges stand out due to the contour lines and changes in color, representing changes in elevation (Figure 6-7). Figure 6-8 and 6-9 show cross-sections cutting through the two ridges recognized in Area 1A. The smallest and shortest ridge show one elongated mound, oriented approximately N-S. Figure 6-8 is a seismic cross-section that cuts through the ridge-shaped mound, and show bright and chaotic reflectors only at the base of the studied interval. Some of the bright reflectors form W-shaped 2D-geometries. The upper part of the mound shows dim and more continuous reflectors.

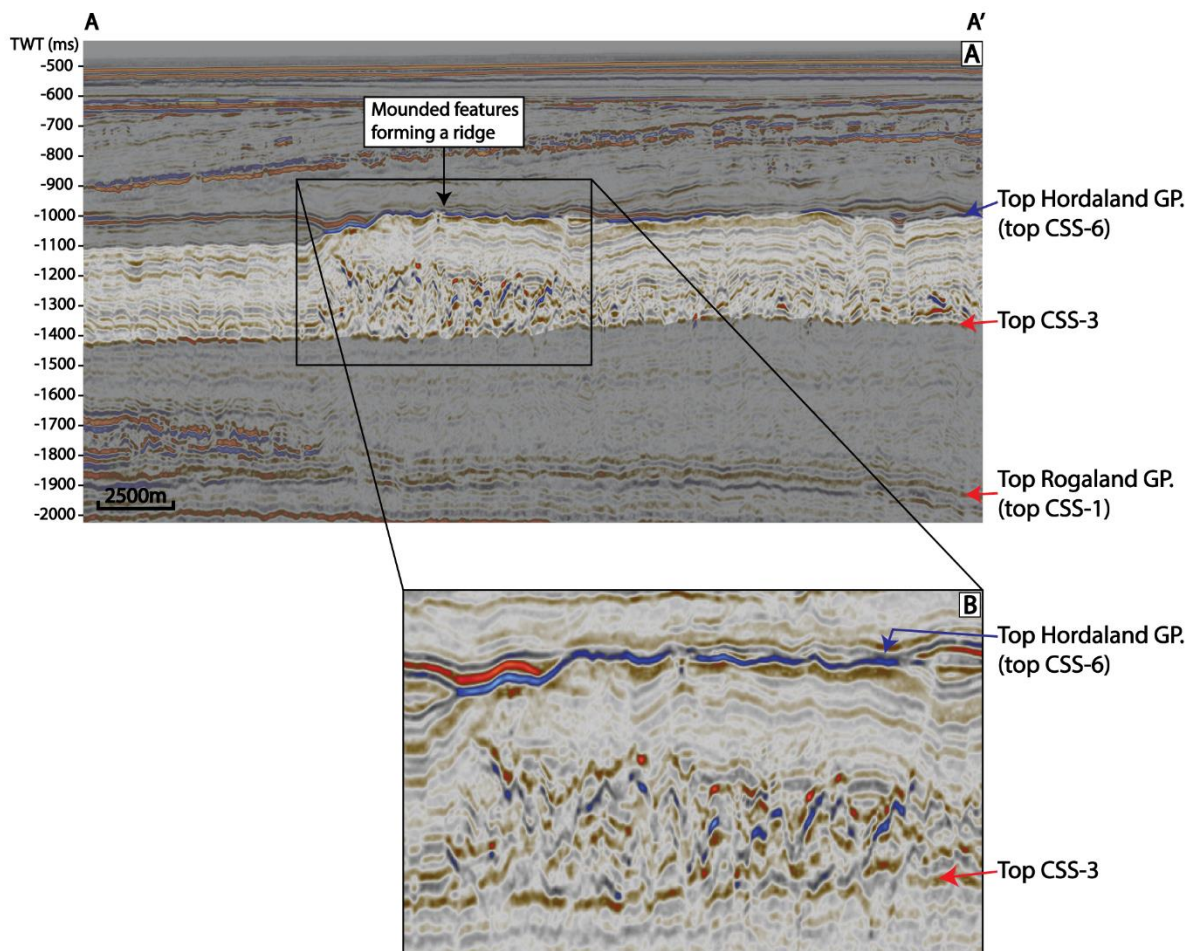


**Figure 6-8:** Figure A) displays a seismic cross-section that cuts through the smallest ridge, and also show the adjacent areas to the mound. Figure B) displays a zoom-in picture of the ridge-shaped mound. The studied interval is marked by the highlighted areas. The location and orientation of the figure is displayed in Figure 6-7.

The largest ridge-shaped mound consists of several connected, smaller mounds that together form a NNE-SSW trending ridge. The mounds that create the largest ridge-shape (Figure 6-9), consist of several connected and smaller mounds that together form a NNE-SSW trending ridge. The mounds consist of chaotic reflectors in most of the studied interval, but dim reflectors with preserved continuity are observed in the upper part of the mound. A very sharp boundary

between mounded and unmounded areas is recognized in the southern part of the large mound. Here the reflectors suddenly change from chaotic and bright to continuous, dimmer and parallel (Figure 6-9).

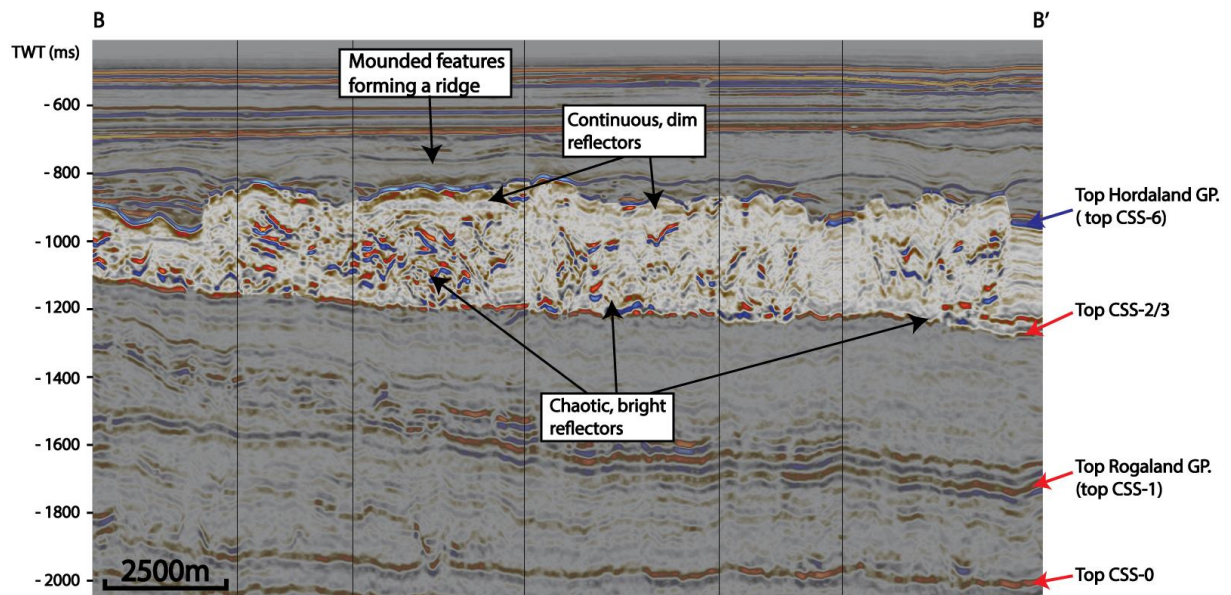


**Figure 6-9:** Seismic cross-section of a composite line that cuts through the largest ridge-shaped mounds. The studied interval is marked by the highlighted area. The location and orientation of the seismic profile is displayed in Figure 6-7.

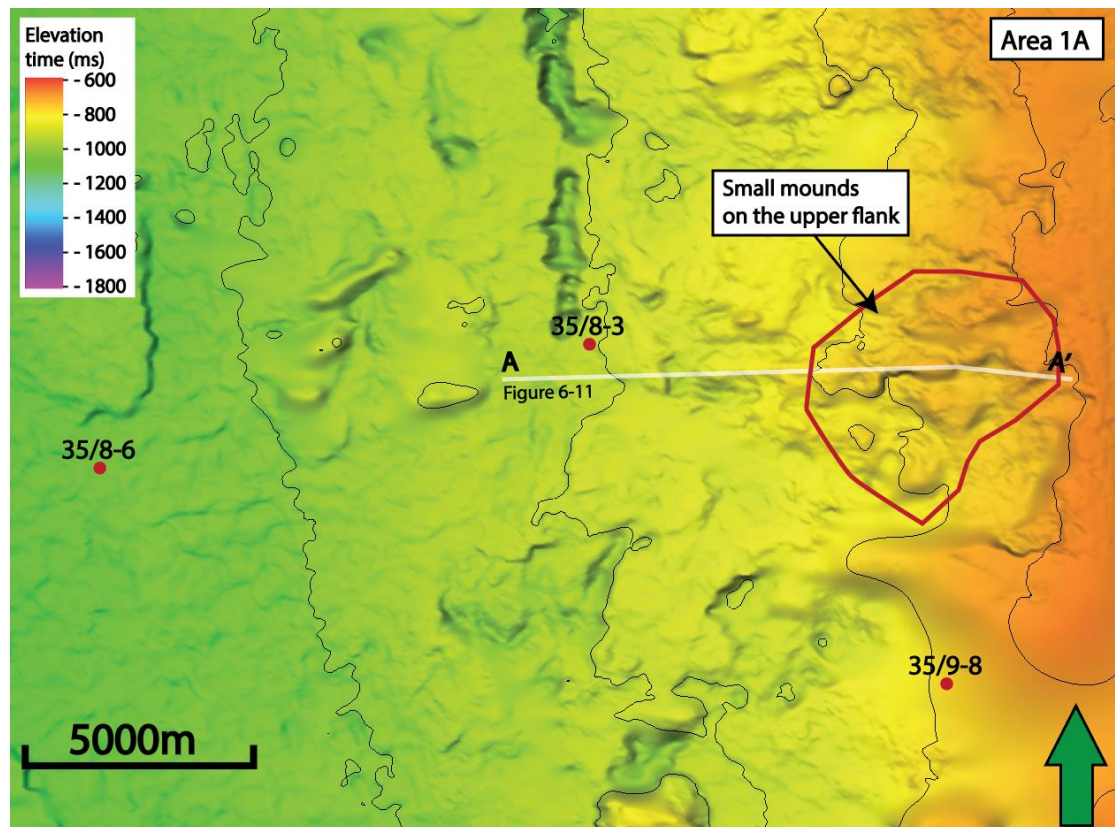


**Figure 6-10:** Elevation map of parts of the middle area of subarea 1A (parts of top Hordaland Group). Small mounds at the upper flank are observed within the red circle. The vertical exaggeration is set to 7,5 to make the mounds easier to recognize, and the contour lines show a spacing of 50ms.

Mounds are also observed on the flank in subarea 1A. The mounds on the upper flank are smaller and less elevated compared to the mounds closer to the basin, and occur both alone and in clusters. An example of several mounds occurring adjacent to each other on the upper flank is viewed in Figure 6-10. Figure 6-11 shows a seismic cross-section cutting through mounds on the upper flank. The seismic profile displays a lower grade of chaotic and bright reflectors compared to the mounds closer to the basin floor.

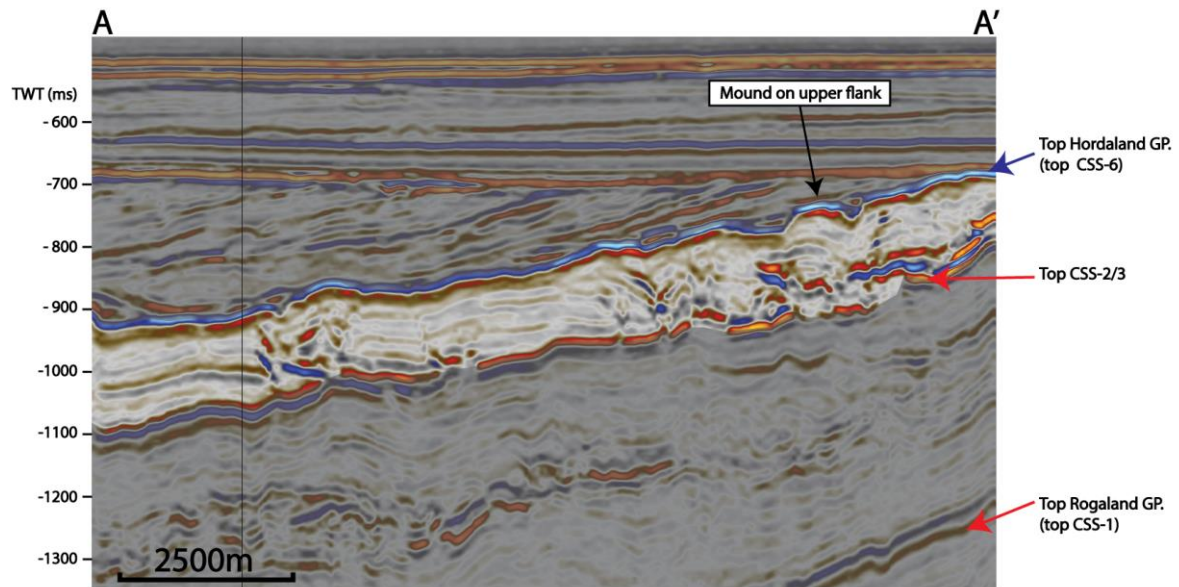


**Figure 6-11:** Seismic cross-section of a composite line that cuts through one of the mounds on the upper flank, located in the middle part (N-S direction) of area 1A. The studied interval is highlighted. The location and orientation of the seismic profile is displayed in Figure 6-10.

### 6.1.3 Distribution of mounds

Figure 6-12 shows an overview of how the mounds in subarea 1A are distributed. Three different mound arrangements are present in subarea 1A. The clustered mounds with largest lateral extent appear to be located in the north of subarea 1A, some downdip the of the basin-flank transition and some at the slope. The ridges occur in the southern part of the subarea, and finally the smaller mounds occur along the entire eastern margin. Overall, the clustered group of mounds extends further into the basin compared to the southern ridges in subarea 1A.

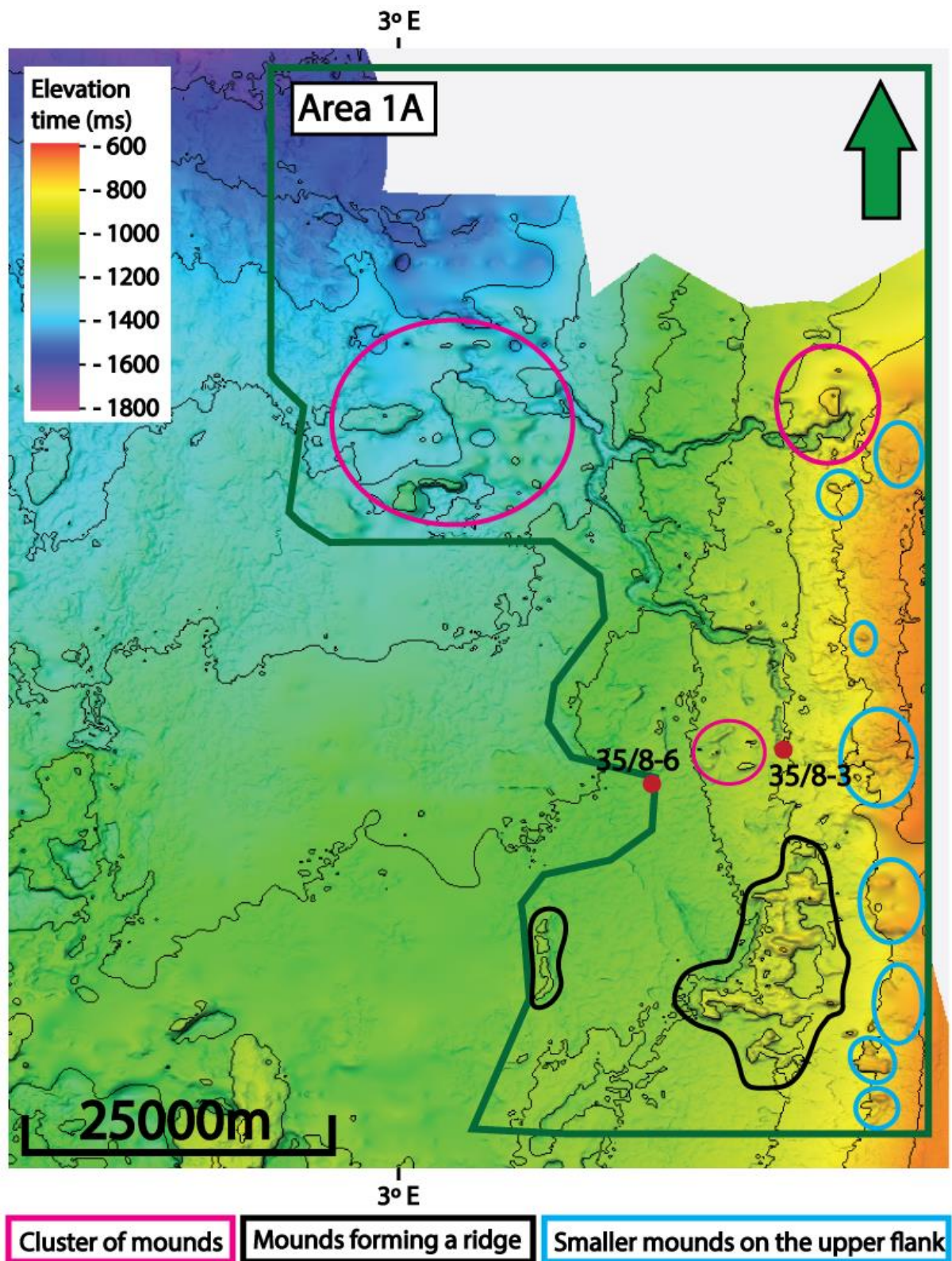


**Figure 6-12:** Elevation map of the top Hordaland Group, displaying the distribution of mounds in subarea 1A. The vertical exaggeration is set to 7,5 to make the mounds easier to recognize.

### 6.1.4 Seismic observations outside the mounds

Unmounded areas occur between the mounds. The unmounded areas are visible in map view (Figure 6-13), but become much clearer in profile view. In the areas outside of the mounds, two types of seismic characteristics occur (Figure 6-14 and 6-15). First, parallel, continuous and undisturbed reflectors are observed (Figure 6-14 and 6-15). The continuous reflectors tend to be dimmer than the chaotic reflectors. Secondly, parallel, continuous reflectors affected by polygonal faulting occur.

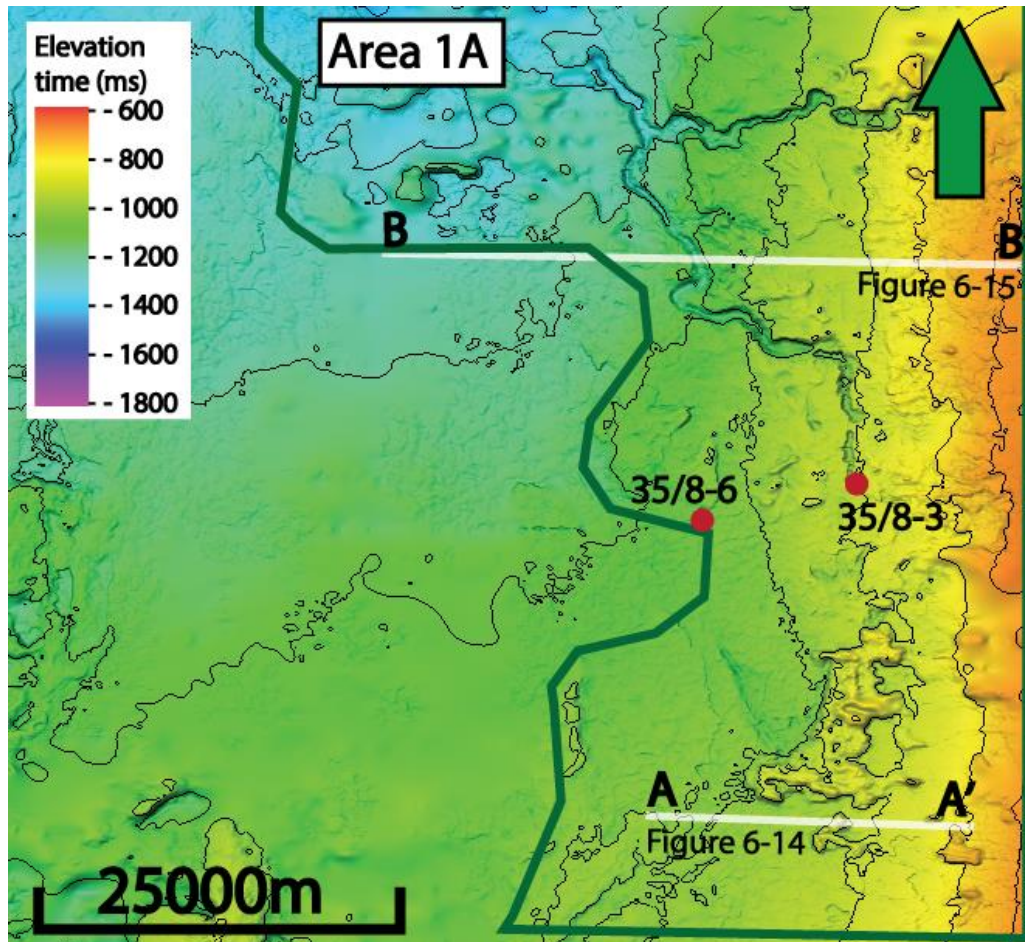


**Figure 6-13:** Elevation map of parts of top Hordaland, displaying location of Figure 6-14 and 6-15 (semi-transparent white lines). The vertical exaggeration is set to 7,5.

Figure 6-14 shows a seismic line located in the southern part of area 1A. The seismic line shows that the unmounded areas occur at the westernmost part of the area and at the eastern flank. The western part of the seismic cross-section displays relatively dim, continuous and inclined reflectors, affected by polygonal faults in the lower part of the studied interval. At the flank, the unmounded area is characterized by continuous, undisturbed, parallel reflectors throughout the entire studied interval. The lowermost reflectors are onlapping onto top CSS-2/3.



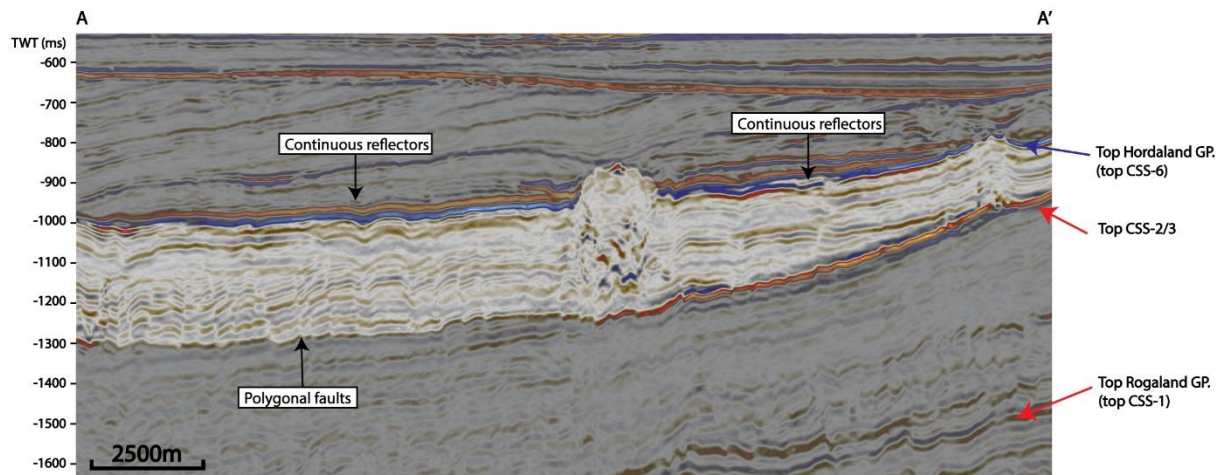


**Figure 6-14:** Seismic cross-section of an E-W oriented composite line that displays an unbounded area within subarea 1A. The studied interval is highlighted. The location and orientation of the seismic profile is displayed in Figure 6-13.

Figure 6-15 shows a seismic profile located further north than that shown in Figure 6-14. Here, the unbounded areas are also located in the westernmost part of the seismic line and on the flank. The unbounded area to the south in subarea 1A is characterized by continuous, inclined, undisturbed and parallel reflectors on the flank, and hence resembles the unbounded area north in subarea 1A. The two areas are different in that there is onlap onto the CSS-2/3 in the southernmost seismic profile, but not in the northern area. The unbounded area in the western part of the seismic profile is characterized by continuous and parallel reflectors at the top of the studied interval, whereas chaotic bright reflectors dominate the lowermost part of the interval (Figure 6-15).

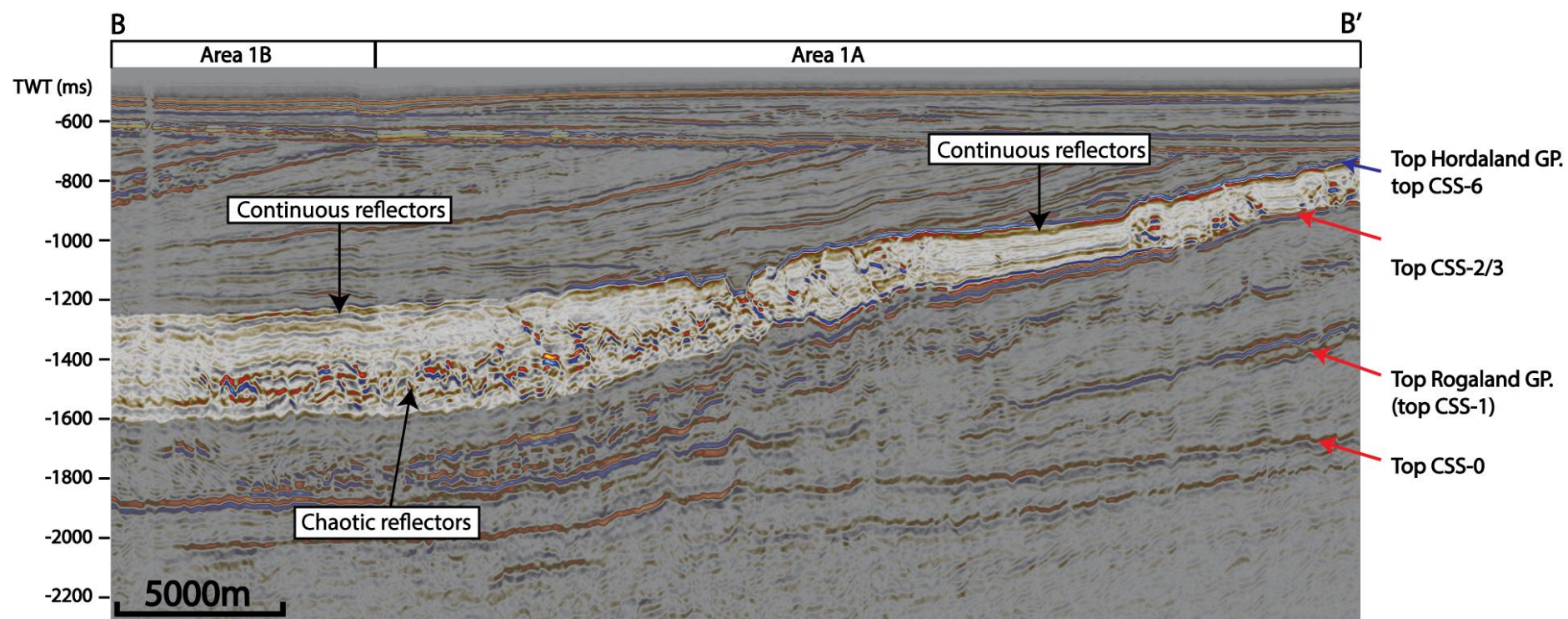


**Figure 6-15:** Seismic cross-section of an E-W oriented composite line displaying an unrounded area within subarea 1A. Note that the seismic line extends into subarea 1B in the western part of the seismic profile. The studied interval is highlighted. The location and orientation of the seismic profile is displayed in Figure 6-13.

## 6.2 Seismic observations in area 1B

Subarea 1B covers a large part of the basin center (Figure 6-16). It is characterized by lack of mounds and mostly continuous reflectors. Figure 6-17 shows a seismic cross-section from the northern part of area 1B (Figure 6-16). Here the studied interval thickens towards the east. In the west the seismic reflectors are characterized as continuous, and dim reflectors. The seismic reflectors in the east differs from those in west, and are characterized as continuous, parallel and medium strong reflectors. In the east, disturbed and bright reflectors are recognized in the lower part of the studied interval.

Figure 6-18 is located in the southern part of area 1B (Figure 6-16). Here, the studied interval is recognized by undisturbed, parallel, medium strong to dim reflectors. The studied interval is characterized by an overall uniform thickness (from west to east) and relatively flat reflectors that show evidence of polygonal faulting.

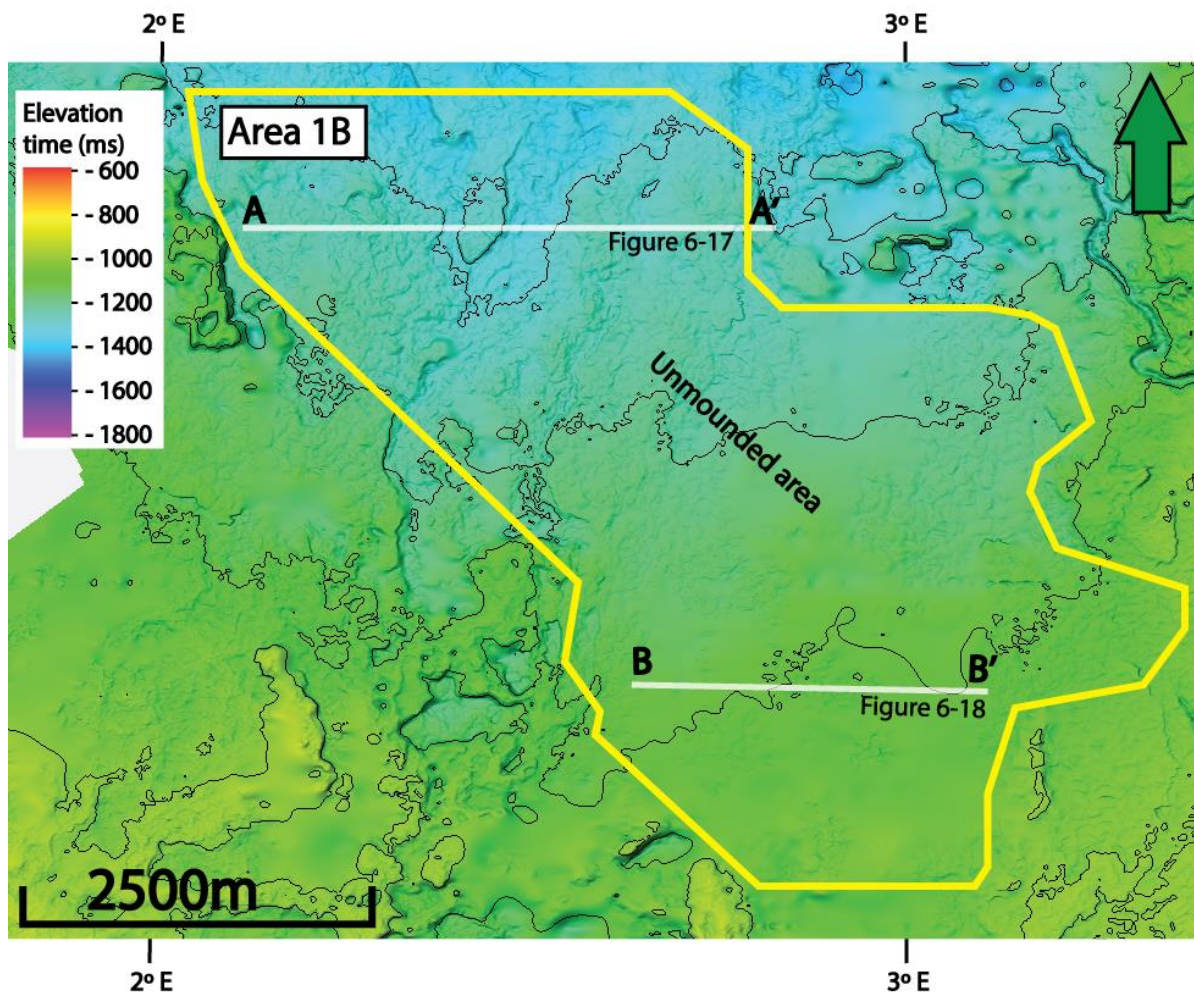


**Figure 6-16:** Elevation map of subarea 1B (parts of top Hordaland GP.), displaying the location of Figure 6-17 and 6-18 (semi-transparent white lines). The vertical exaggeration is set to 7,5.

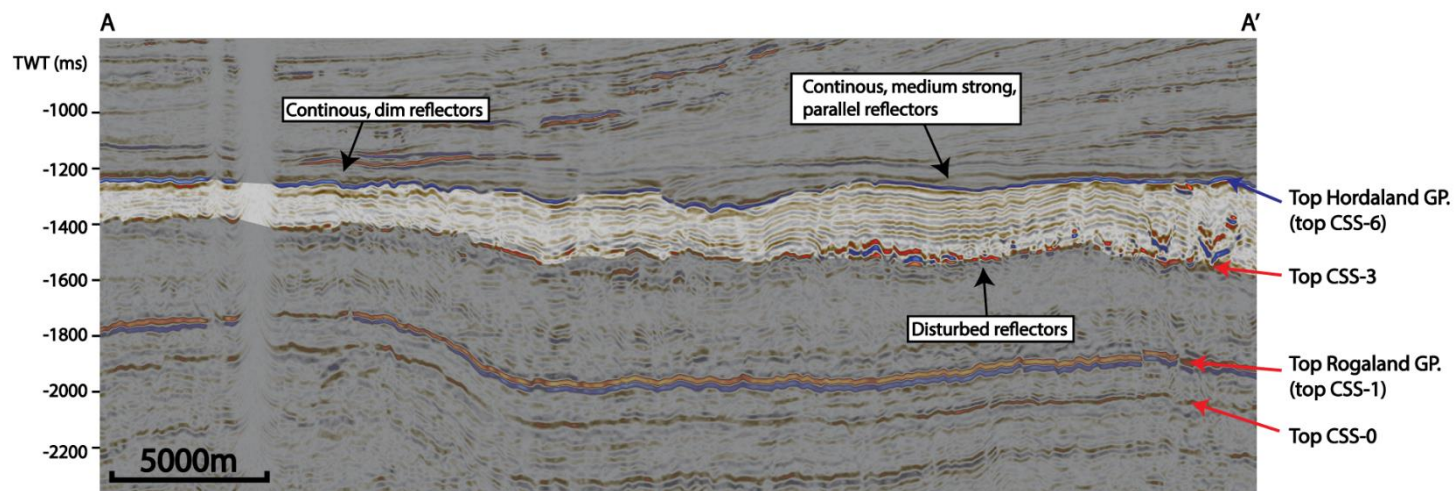


Figure 6-17: Seismic cross-section of a E-W oriented seismic profile located within the northern part of subarea 1B. The studied interval is highlighted.

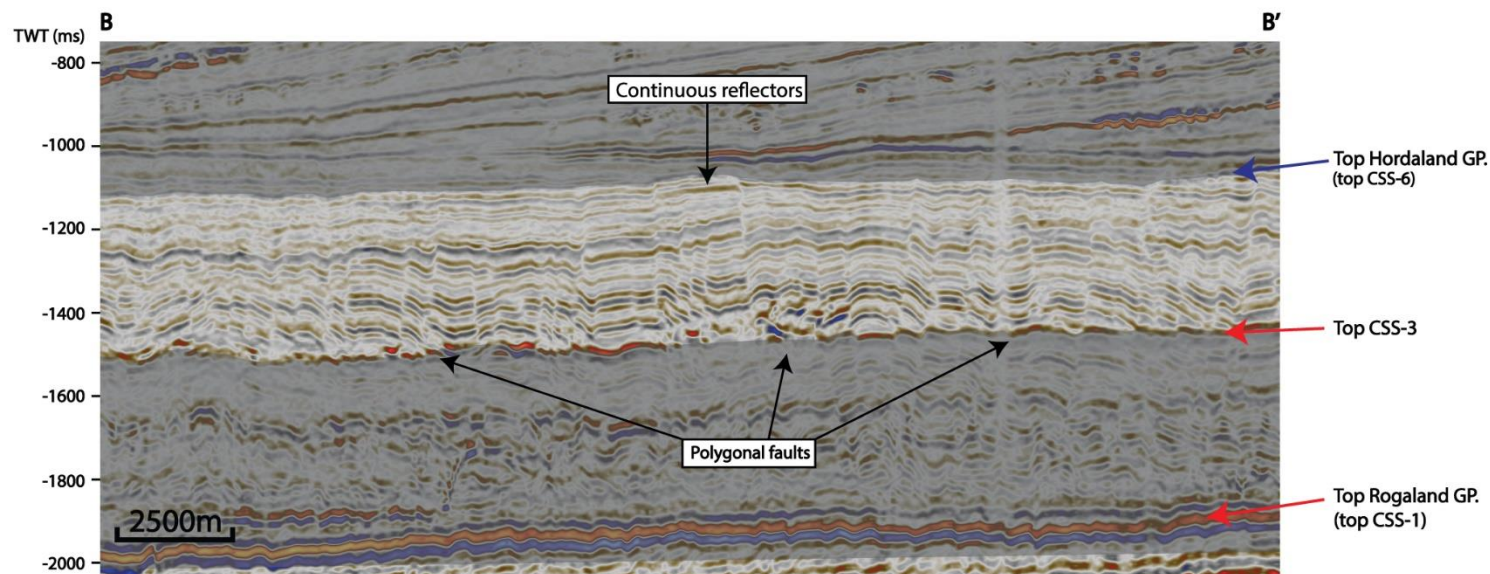
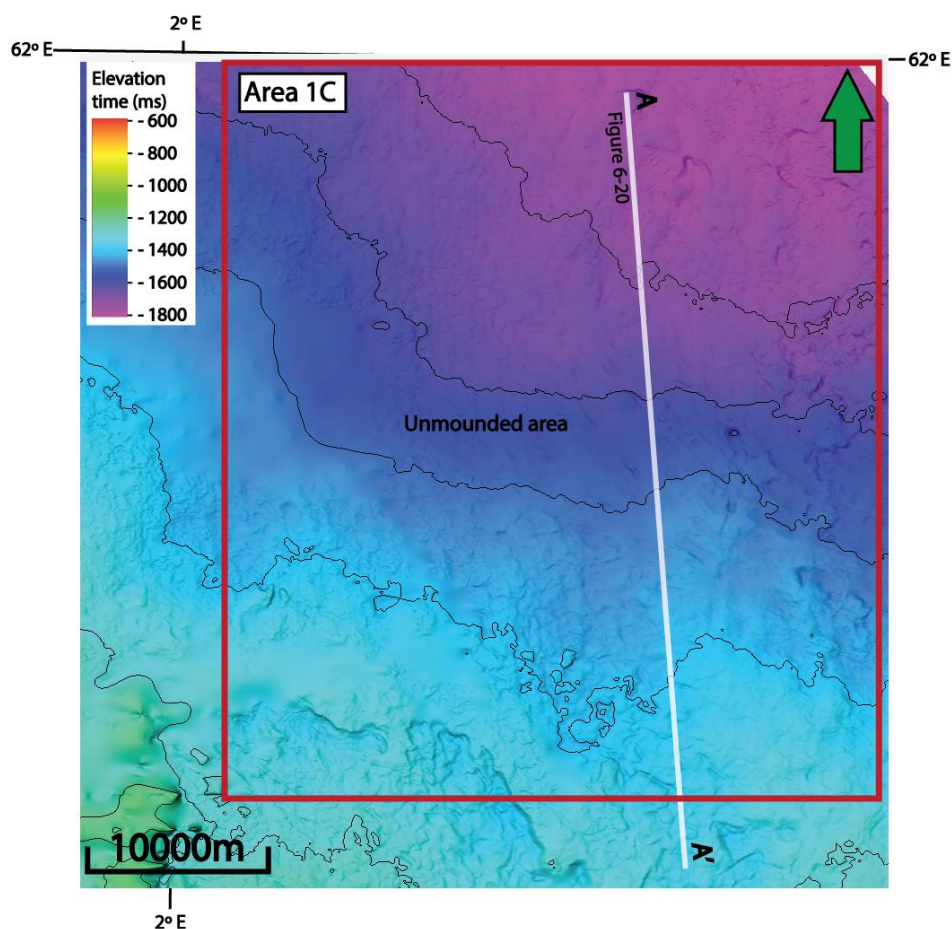


Figure 6-18: E-W oriented seismic cross-section located within the southern part of subarea 1B. The studied interval is highlighted.

### 6.3 Seismic observations in area 1C

Subarea 1C is located in the central, northernmost part of the study area. Here, no mounds are observed. The boundary between area 1B and 1C marks a transition from relatively horizontal layers, to northward dipping layers. The northwards dipping layers are recognized in map view by a change in colour from blue to purple. Figure 6-19 provide a detailed overview of the area. In the northernmost part of Figure 6-20, continuous, parallel and medium strong reflectors are observed. In the southernmost part of Figure 6-20, continuous, parallel, relatively dim reflectors are observed. Polygonal faults are observed close to the transition between area 1B and 1C. An overall thinning of the studied sequence is observed from south to north.



**Figure 6-19:** Elevation map of subarea 1C (a part of top Hordaland GP.), displaying the location of Figure 6-20 (semi-transparent white lines).

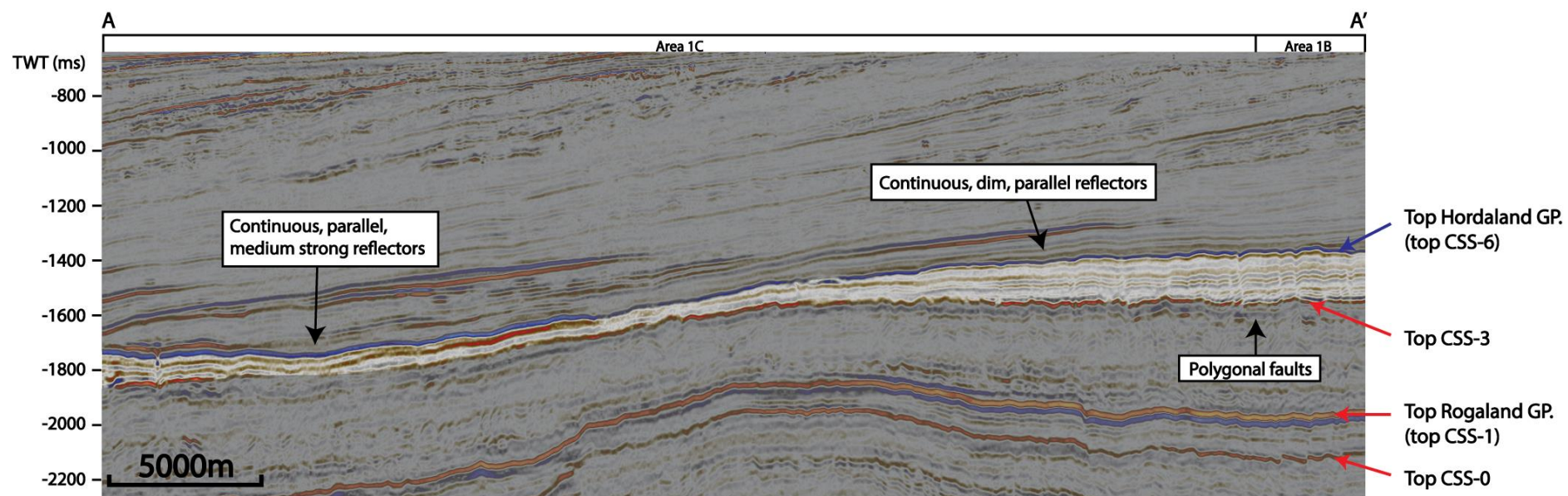


**Figure 6-20:** Cross-section oriented N-S in subarea 1C. The studied interval is highlighted, and a significant thinning of the sequence is observed from the south (A') to the north (A).

## 6.4 Seismic observations in area 2

Area 2 is located approximately in the middle of the study area (N-S direction), and covers the total E-W extent of the study area. Unlike the other subareas, area 2 shows mounds also within the central parts of the basin (Figure 6-21).

### 6.4.1 Shapes and distribution of mounds

Most parts of area 2 are characterized by large mounds, arranged in a cluster. Figure 6-22 shows a seismic profile cutting through the clustered mounds. The gaps between mounds are characterized by chaotic reflectors. Dim and chaotic reflectors are observed within the mounds. Brighter reflectors are observed in the western part of the section, but since the change in amplitude is observed from the seabed to the base of the profile. This is reason to believe that it is not a geological feature. The chaotic reflectors are present below top CSS-3, which is different from what is observed in the rest of the study area. An alternative explanation is that the chaotic reflectors observed deeper than top CSS-3 are caused by interference from top CSS-3. This fits well with the observation showing that the reflection strength within the mounds is less than what is seen in other areas (Figure 6-22).

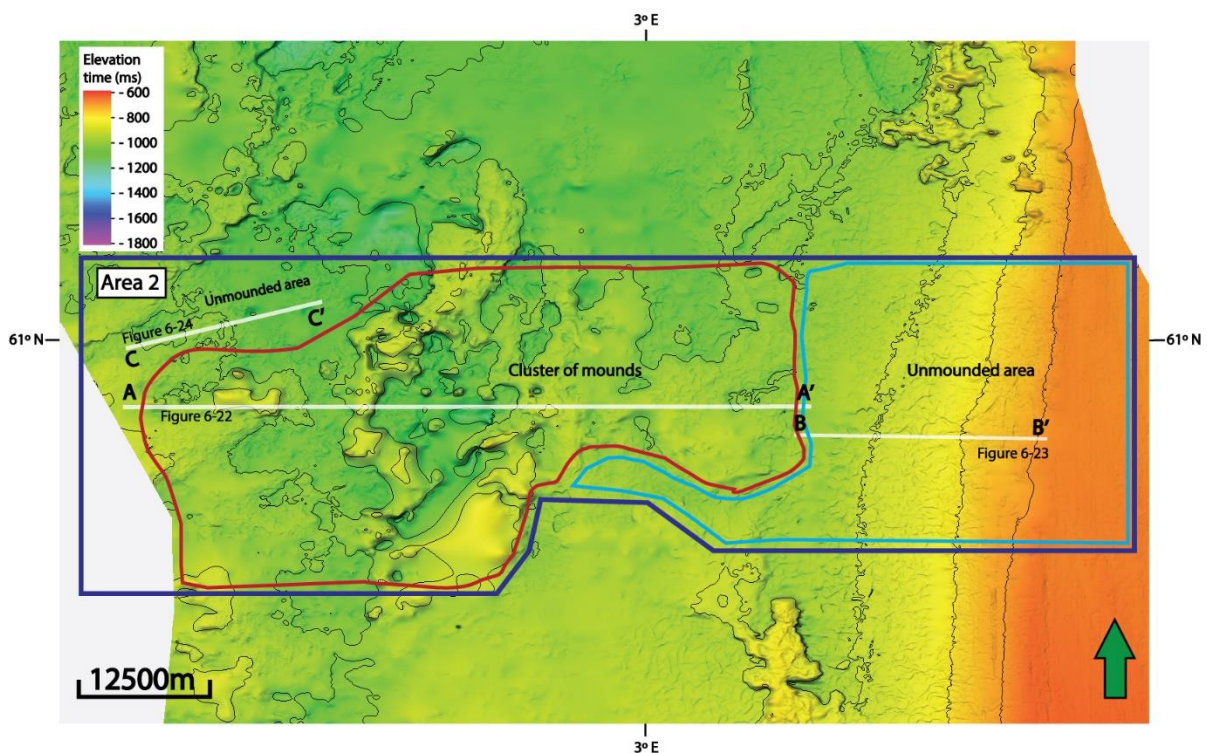


**Figure 6-21:** Elevation map of area 2 (a part of top Hordaland GP.), displaying the location of Figure 6-22, 6-23 and 6-24 (semi-transparent white lines). The red line surrounds the area characterized by clustered mounds, and the light blue line surrounds the area characterized by continuous reflectors.

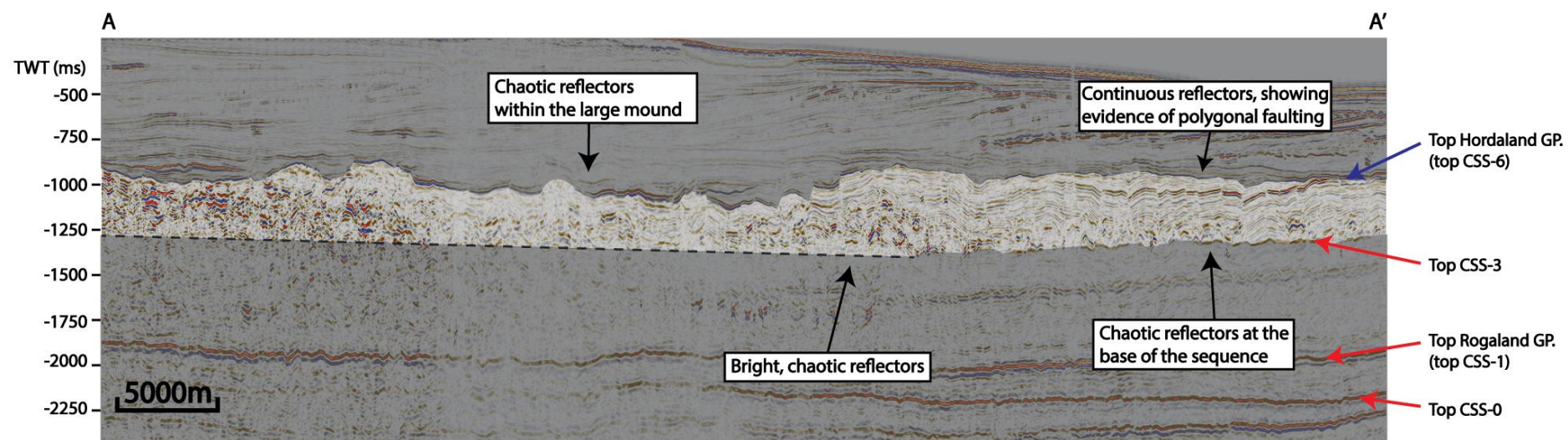


**Figure 6-22:** Seismic cross-section, oriented E-W cutting through the clustered mounds. The studied interval is highlighted. The dashed line represents an area where it was impossible to follow the reflector representing top CSS-3. Figure 6-21 displays the location of the seismic profile.



### 6.4.2 Unmounded areas

The eastern part of area 2 is unmounded (Figure 6-21). Figure 6-23 shows an E-W oriented seismic section across the eastern flank of the basin. Continuous, parallel, dim reflectors dominate the unmounded area. Polygonal faulting is also present, most frequently observed in the western part of the unmounded area, i.e. along the basin flank transition (Figure 6-23). The thickness of the studied sequence is increasing towards the basin. The studied sequence is unmounded in the northwestern part of area 2. Unlike the eastern unmounded area, this area is characterized by chaotic and dim reflectors (Figure 6-24). The chaotic reflectors are observed from the top of the Hordaland group to the top of the Rogaland Group, and consequently top CSS-3 was not recognized.

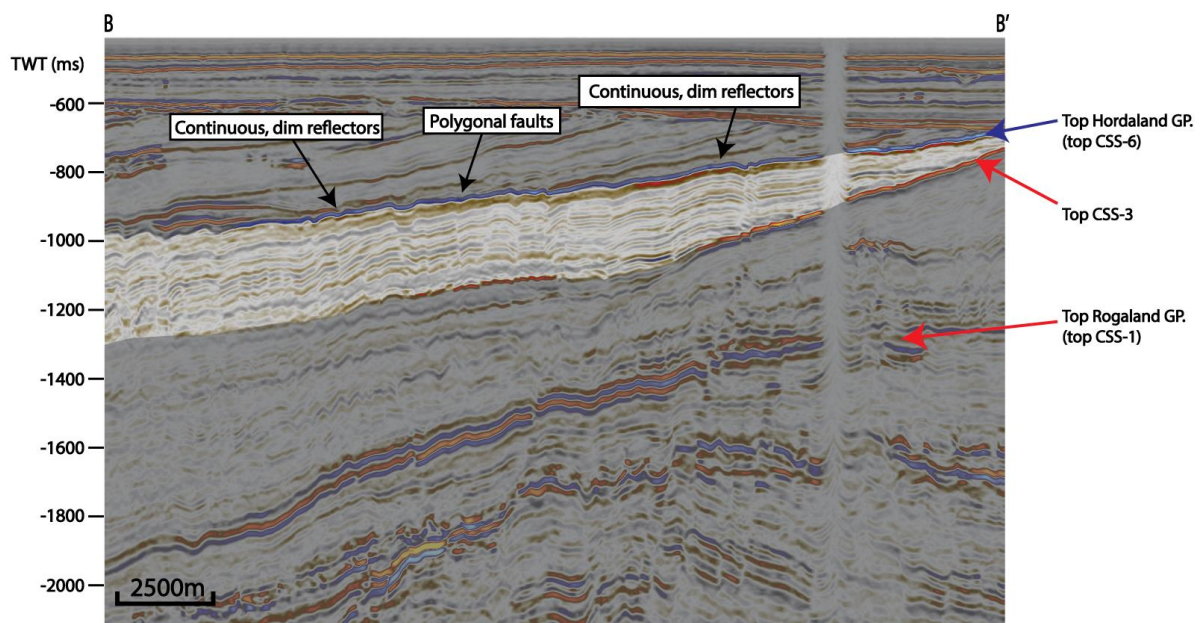


**Figure 6-23:** Seismic profile that cuts through the eastern part of area 2. The eastern area is dominated by continuous reflectors. The studied interval is highlighted.

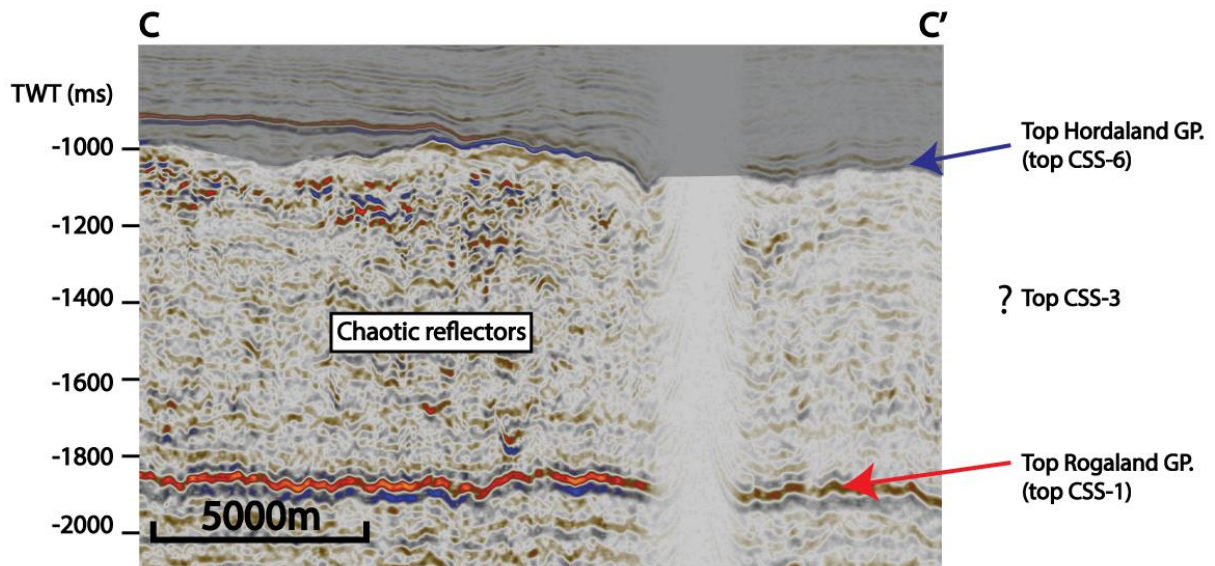


**Figure 6-24:** Seismic profile that cross-cuts the unmounded area in the northeastern part of area 2. The entire Hordaland Group is characterized by chaotic reflectors, and consequently top CSS-3 is not recognized.

### 6.5 Seismic observations in area 3A

Subarea 3A area is located in the southeastern part of the study area. In the western part of the subarea (closest to the basin floor), the area is characterized by mounds that form ridges. The ridges are oriented parallel to the eastern margin. An unmounded area is observed in the east (Figure 6-25).

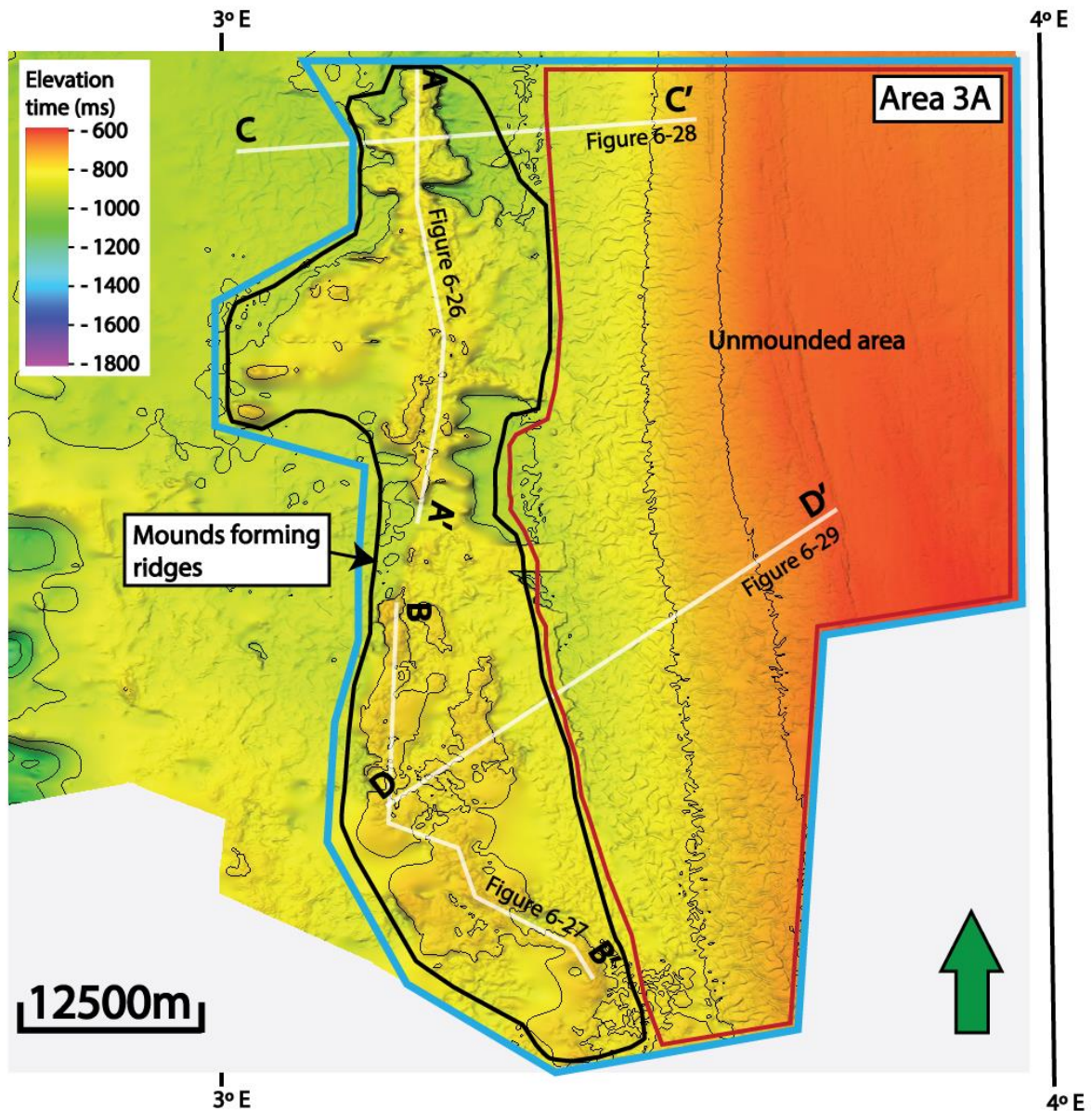


**Figure 6-25:** Elevation map of subarea 3A (cover parts of top Hordaland Group). The Figure displays the location of Figure 6-26, 6-27, 6-28 and 6-29. The red line surrounds the unmounded area, and the black line surrounds the area characterized by mounds forming ridges.

### 6.5.1 Shapes and distribution of mounds

Two N-S trending ridges are observed in subarea 3A, and the southernmost ridge appears to be a continuation of the northernmost ridge. The mounds are located along the basin flank transition, which is also the delineation of area 3A. Figure 6-26 shows a seismic profile across the central parts of the northernmost ridge. Overall, the figure shows very chaotic reflectors. The northernmost part of the figure displays dim and medium strong chaotic reflectors.

In the upper part of the studied interval areas of bright, parallel reflectors are observed. The southernmost part of Figure 6-26 shows medium strong, chaotic reflectors. A dim zone is observed in the uppermost part in the southern part of the studied interval.

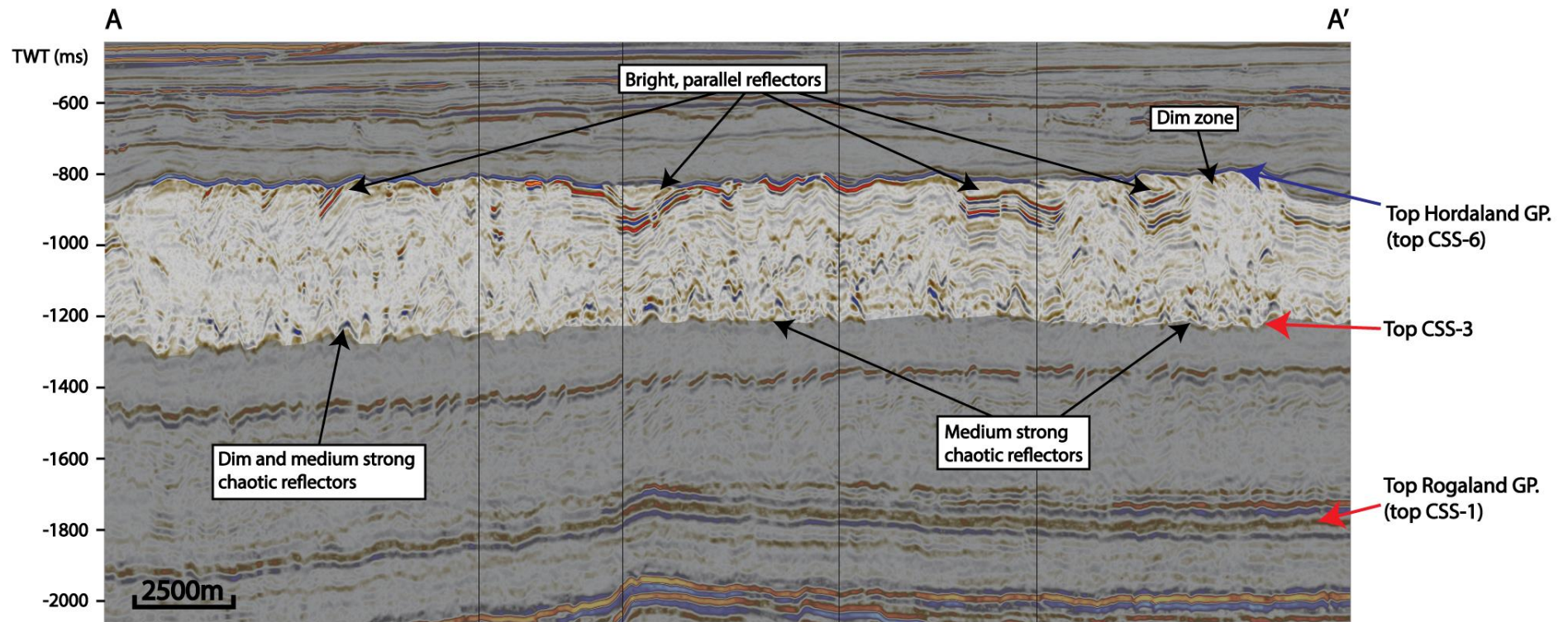


**Figure 6-26:** Seismic profile that cuts through the northernmost ridge in area 3A, trending N-S. Chaotic reflectors dominate the interval of interest. The interval of interest is highlighted. The location of the figure is displayed in Figure 6-25.

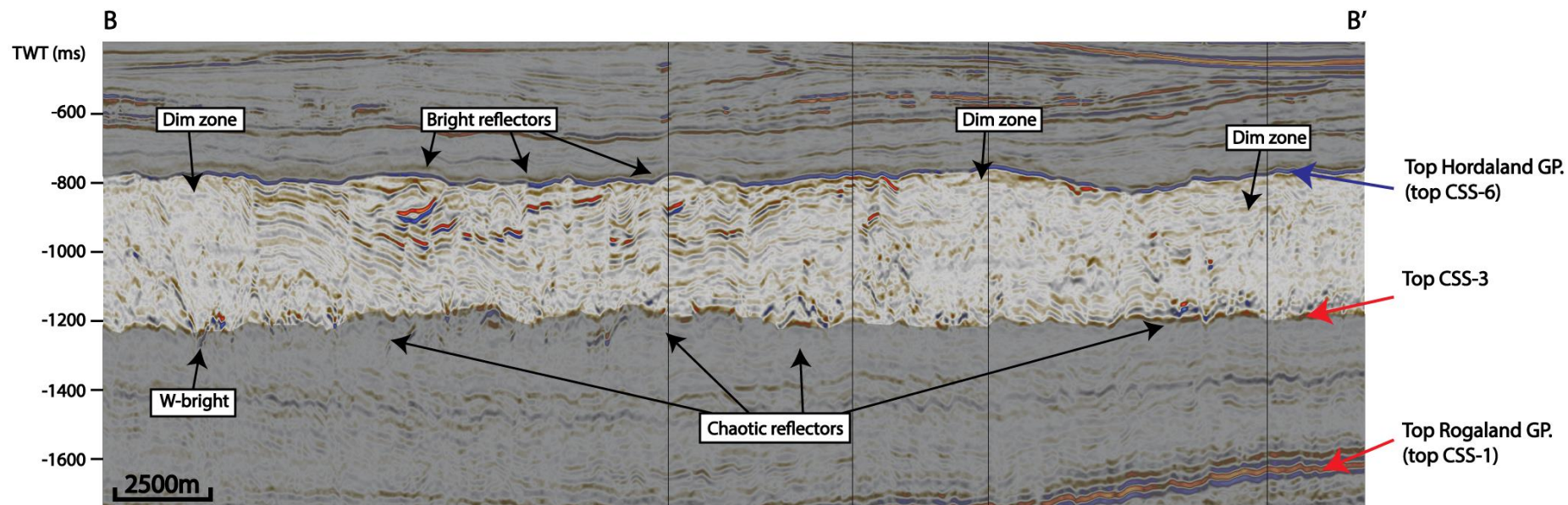


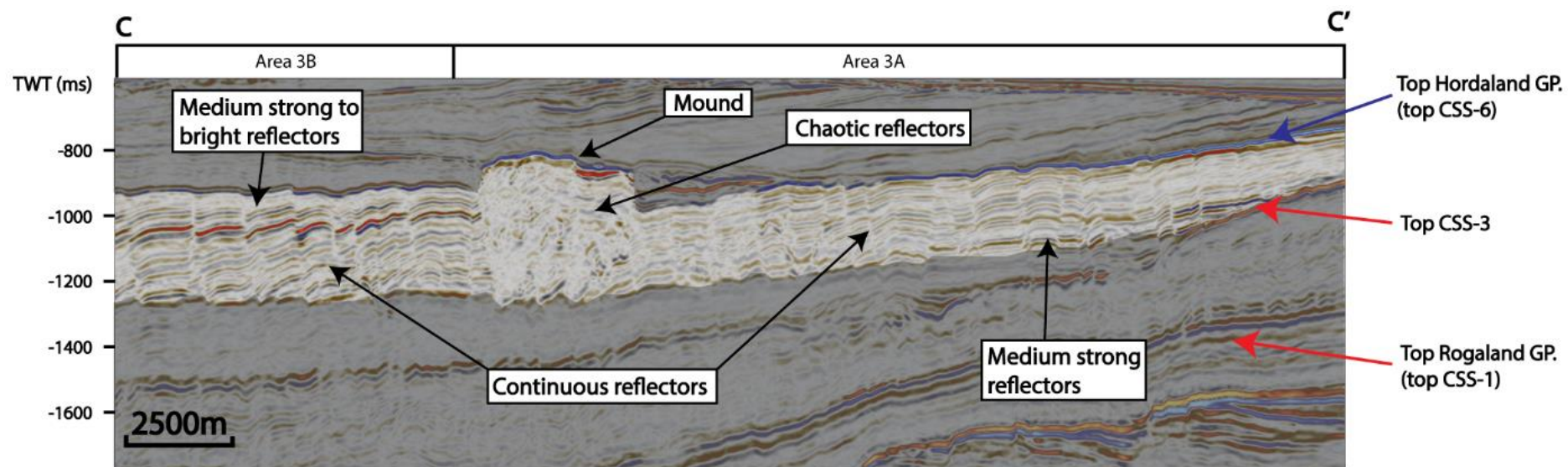
**Figure 6-27:** Seismic profile that cuts through the southernmost ridge in area 3A, trending N-S – SSE. Chaotic reflectors dominate the lowermost part of the studied interval, whereas the uppermost part also show parallel, relatively continuous reflectors. The interval of interest is highlighted. The location of the seismic profile is displayed in Figure 6-25.

### 6.5.2 Unmounded area

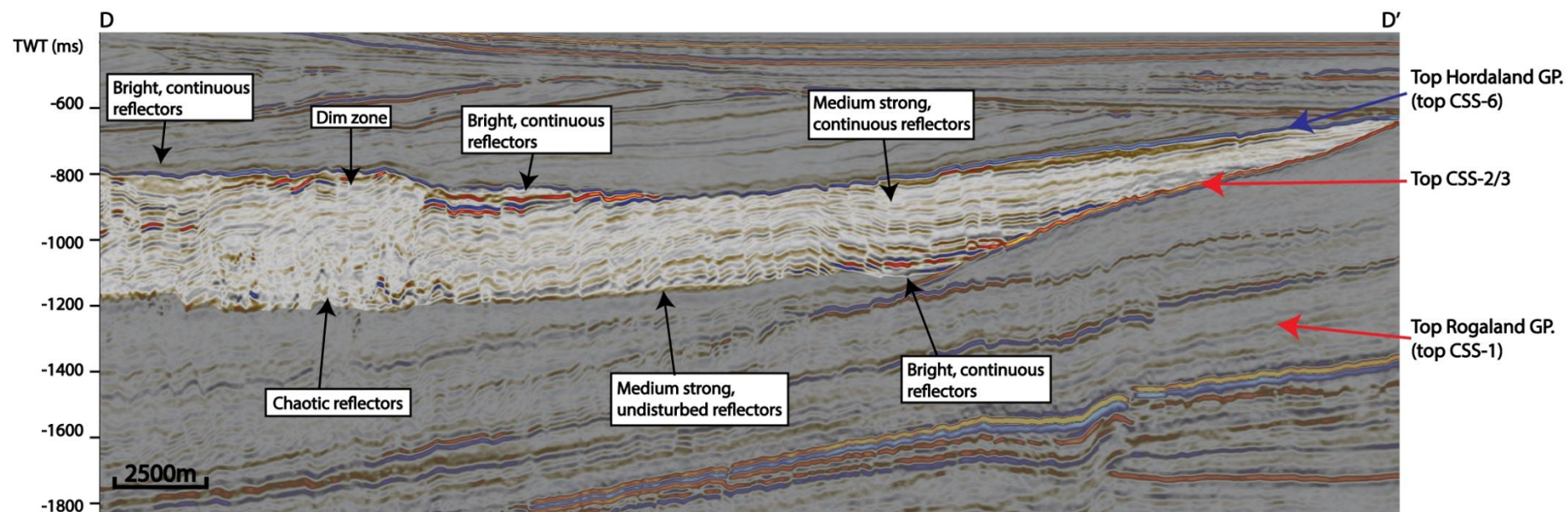
The unmounded area is located on the basin flank in the eastern part of subarea 3A (Figure 6-25). It is characterized by continuous reflectors and polygonal faulting (Figure 6-28 and 6-29).

Figure 6-28 shows a seismic profile from the northern part of the subarea, extending into area 3B in the west. Here, the studied interval is dominated by continuous reflectors, that show evidence of polygonal faulting. The mound observed in the middle of the seismic section represents a part of the ridge observed in mapview. East of the mound, inclined, continuous, medium strong and polygonally faulted reflectors are observed. Other observations show relatively flat, continuous, bright and polygonally faulted reflectors west of the mound. The sequence west of the mound shows a thicker sediment package compared to the sequence east of the mound.

Figure 6-29 is located in the southern part of area 3A. It shows a seismic profile that extends from the upper flank (C'), through the mounded area and to the basin (C). The eastern part of the seismic section shows continuous, parallel, slightly inclined and mainly medium strong reflectors. At the base of the studied sequence, bright reflectors occur at the point where the inclination of the slope increases. The base of the studied interval (top CSS-3) show a relatively smooth reflector in areas where the reflectors above and below show evidence of polygonal faulting. This indicates that the top CSS-3 has been interpreted along the A-CT boundary, and not at top CSS-3.



**Figure 6-28:** Seismic cross-section from the northern part of subarea 3A, extends into area 3B in the western part of the figure. The studied interval is characterized by continuous, parallel reflectors, disturbed by chaotic reflectors and a mound in the west of subarea 3A. The studied interval is highlighted. The location of the seismic section is displayed in Figure 6-25.



**Figure 6-29:** Seismic cross-section from the southern part of subarea 3A. The studied interval is characterized by continuous, parallel reflectors, disturbed by chaotic reflectors and a mound in southwest. On each side of the mound continuous reflectors are observed. The studied interval is highlighted. Figure 6-25 displays the location of the seismic section.



## 6.6 Seismic observations in area 3B

Subarea 3B represents the basin centre in the southern part of the study area (Figure 6-30). In comparison to subarea 1B, subarea 3B display a narrower basin with absence of mounds. Area 3B can be divided into a southern part and a northern part.

Figure 6-31 shows the northernmost part of area 3B, and extends into area 3A in the east and into the undescribed area in the west (Figure 6-30). The eastern part of the seismic section is recognized by bright to medium strong, continuous, relatively flat, polygonally faulted reflectors. The gap in the seismic is caused by the platform at the Brage field. The western part of the seismic section is characterized by dim, relatively flat and continuous reflectors. A low-angled mound is observed in the western part of the seismic section. The mound is characterized by chaotic bright reflectors. The chaotic reflectors continue below top CSS-3, similar to that observed in the western part of area 2.

Figure 6-32 shows the extent of the narrow basin, in addition to parts of the adjacent areas. Continuous, bright, relatively flat and polygonally faulted reflectors characterize the basin center. The thickness of the interval increases towards east. Close to the mound, the reflectors are slightly inclined and uplifted.

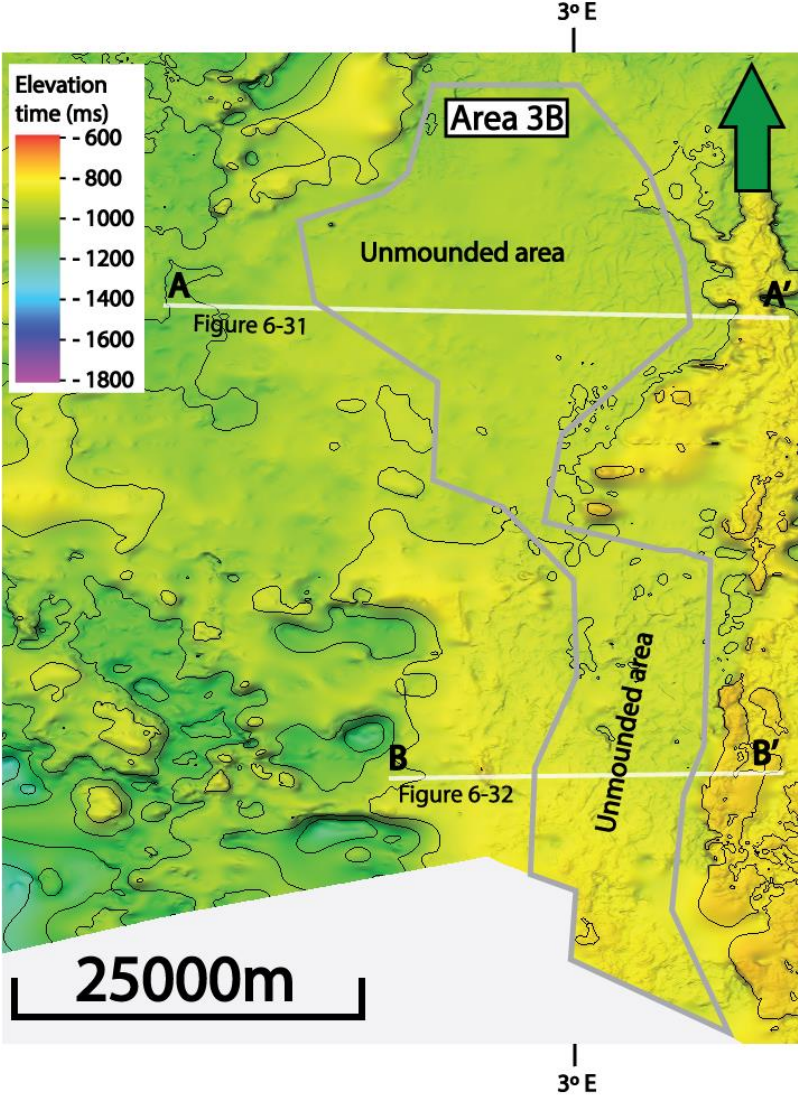
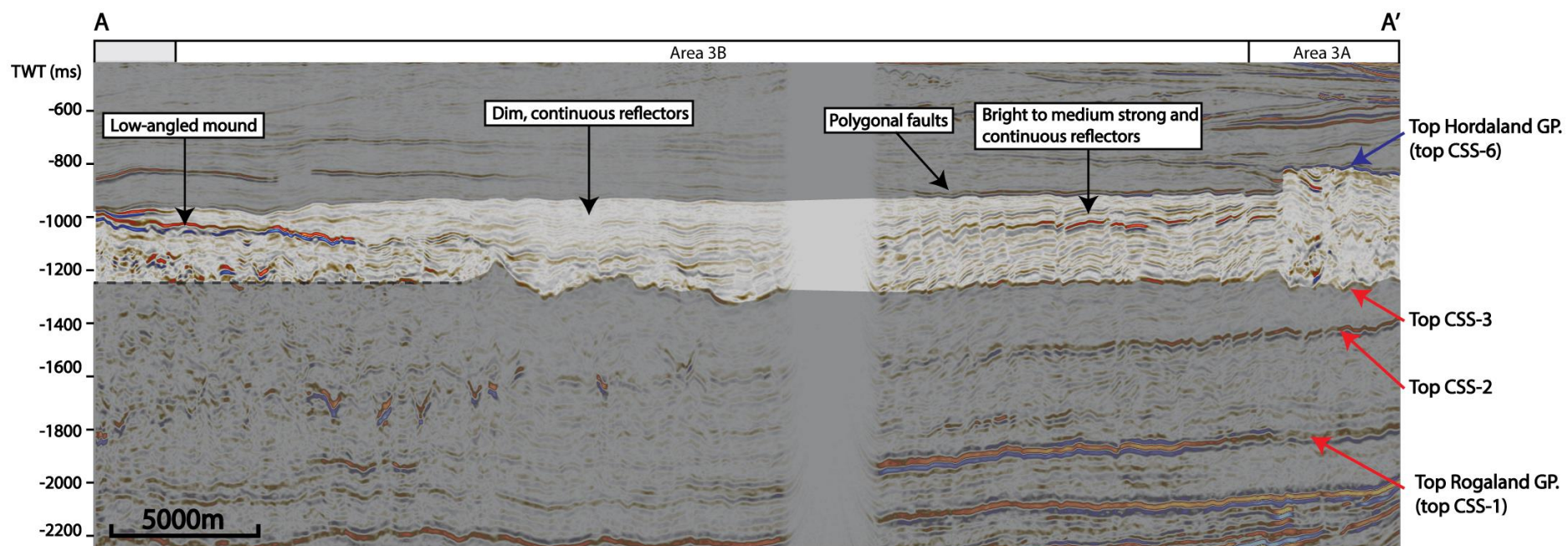
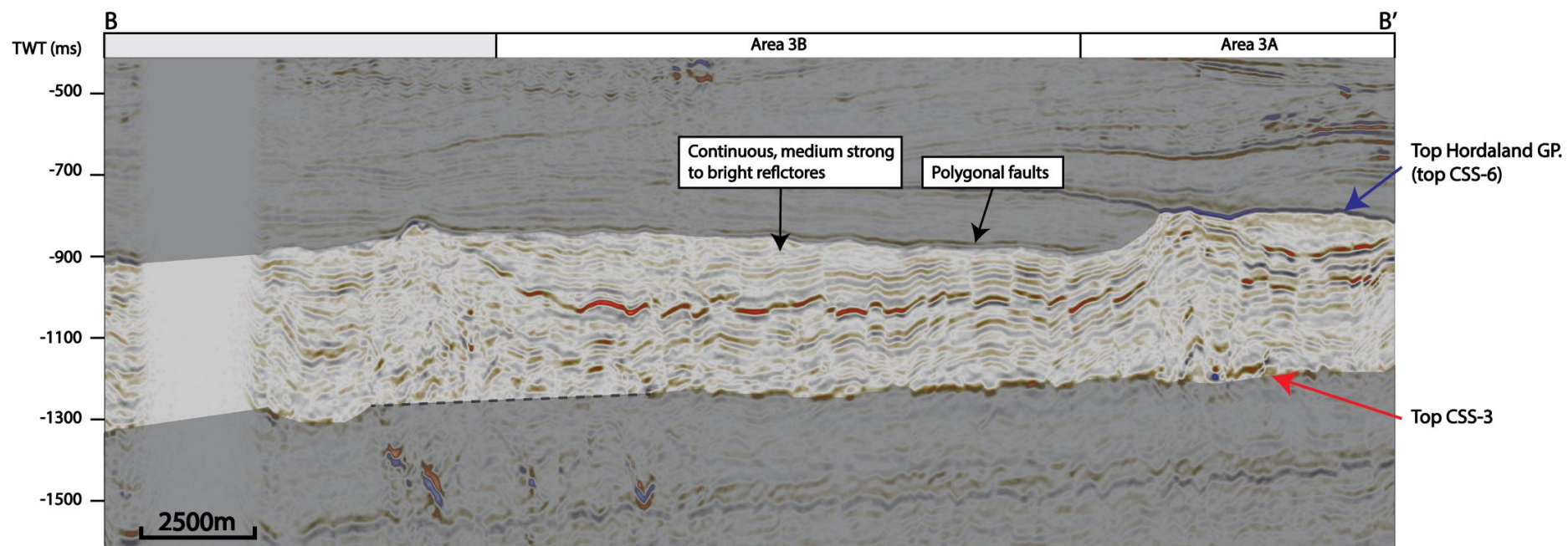


Figure 6-30: Elevation map displaying subarea 3B, which represent parts of the top Hordaland Group. The map shows the locations of Figure 6-31 and 6-32.



**Figure 6-31:** Seismic cross-section from the southern part of subarea 3B. The studied interval is characterized by continuous, parallel reflectors, disturbed by chaotic reflectors and a mound in southwest. On each side of the mound continuous reflectors are observed. The studied interval is highlighted. The location of the seismic profile is displayed in Figure 6-30.



**Figure 6-32:** Seismic cross-section through the southernmost part of area 3B. It extends into adjacent areas in west and east. The area of interest is highlighted, and displays continuous, polygonally faulted and medium strong to bright reflectors. The location of the seismic profile is displayed in Figure 6-30.

## 6.7 Lithology distribution in mounds and in unmounded areas

The previous chapters described several mounds in the northern North Sea basin. For further interpretation of the observations, in terms of the formation of the mounds, it is essential to get an understanding of lithology distribution in mounds versus unmounded areas. Consequently, several wells from the study area were examined. Figure 6-35 displays the released wells included in the study. It also provides an overview of which wells that contained sand in the studied interval. A lithological description of the unreleased wells is provided in Appendix C.

Wells from three types of areas were included in the study: 1) Wells penetrating mounds, 2) Wells penetrating unmounded areas in the basin centre, and 3) Wells penetrating unmounded areas on the eastern basin flank. The interval is defined by top Hordaland (top CSS-6) and top CSS-3.

### 6.7.1 Lithology distribution in mounds vs. unmounded areas in the basin

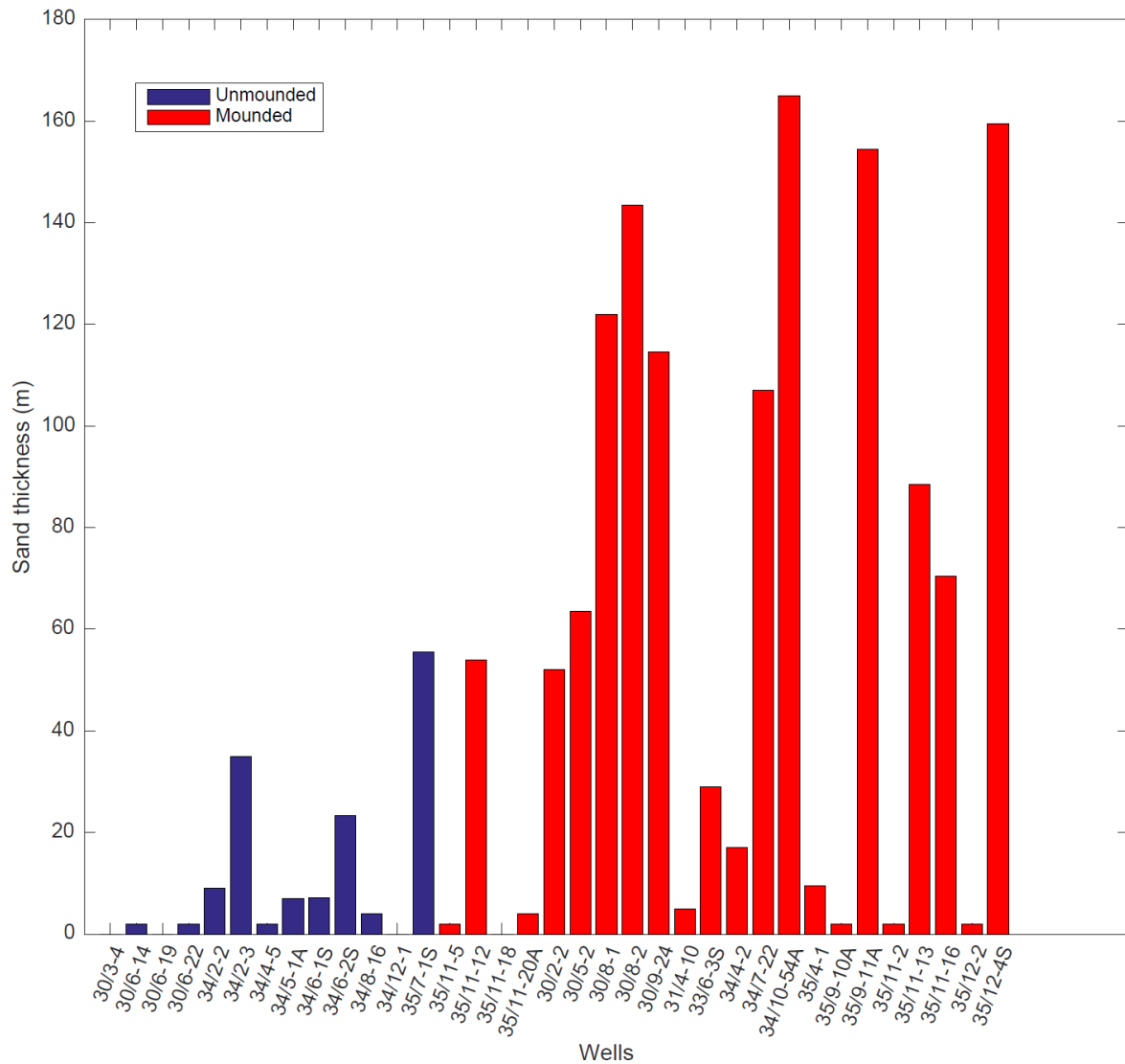
Mounds occur along the margins and on the flank of the basin. The sand content in the interval bound by top CSS-6 (top Hordaland) and top CSS-3 in the Hordaland Group (the same interval as investigated in the rest of chapter 6), was investigated with information from 34 wells.

Figure 6-33 displays the total amount of sand in each well within the given interval. Wells that penetrate unmounded areas are shown in dark blue, and wells penetrating mounds are viewed in light blue. The analyses show that wells penetrating mounds show larger total sand thicknesses in the studied interval, compared to the wells penetrating unmounded areas in the more central parts of the basin. A comparison of Figure 6-33 and 6-35 reveals a larger amount of sand in each well in the west compared to the east.

Figure 6-34 shows a comparison of the total amount of sand in unmounded (light green) and mounded (yellow) areas. The y-axis represents the total amount of sand, expressed in percent. The x-axis shows the sand in metres for both unmounded and mounded areas, and is divided into seven intervals based on sand thickness. The input of the plot is showed in Table 6-1, where the percent of total amount of sand registered in each interval is also expressed in meters. The number of wells belonging to the different intervals for unmounded and mounded areas is also shown.

The investigations demonstrate that sand is present in both mounded and unmounded areas, within the studied interval. It is also clear that much larger occurrences of sand is observed within the mounded areas. The analysis shows that all together 1359,5m sand was registered, and 1152,5m of the sand was observed in mounded areas. Hence, 945,5m more sand is

registered in mounded areas than in unmounded areas in the studied interval. In terms of the sand distribution between the mounds, 71,4% of the sand occur in mounds that contain more than 67m sand in total (Table 6-1). Four of the wells in unmounded areas show only claystone and none of the wells show a total amount of sand thicker than 67m. In mounded areas none of the wells show only claystone, and 8 wells show more than 67m sand (Table 6-1).



**Figure 6-33:** Displays the occurrence of sand in the investigated wells. The red bars represent the wells penetrating mounds, and the dark blue bars represent the wells penetrating unmounded areas.

**Table 6-1:** Displays the relationship between the total amount of sand in all wells combined (expressed in percent and meters) and how many wells that are included in the different intervals. The parameters marked in grey are used as input in Figure 6-34.

Interval (total amount of sand in meters)	Percentage of total amount of sand amount		Number of wells		Total sand thickness (meters), which equals percentage of total amount of sand	
	Unmounded areas	Mounds	Unmounded areas	Mounds	Unmounded areas	Mounds
<b>0 meter</b>	0	0	4	0	0	0
<b>Traces and stringers of sand (&lt;2m)</b>	0,6	0,5	4	3	8	6
<b>2-18m</b>	2,3	2,3	5	2	31,2	14,5
<b>19-34m</b>	1,7	2,1	1	2	23,3	46
<b>35-50m</b>	2,6	0	1	0	35	0
<b>51-66m</b>	8	8,5	2	2	109,5	115,5
<b>&gt;67m</b>	0	71,4	0	8	0	1125
<b>Total amount of sand</b>	<b>15,2%</b>	<b>84,8%</b>			<b>207m</b>	<b>1152,5m</b>

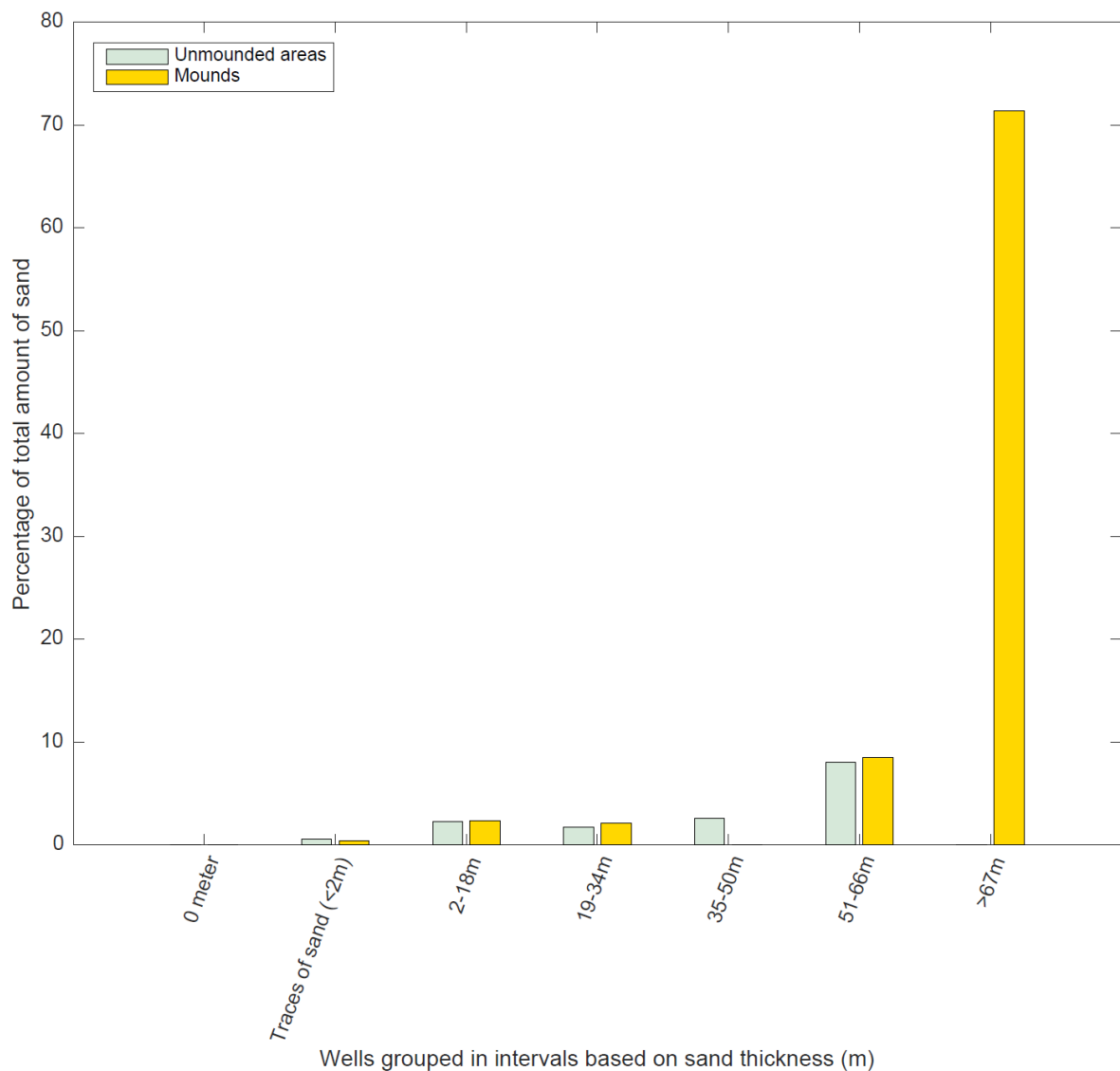


**Figure 6-34:** Sand thickness in wells that penetrates mounded (yellow) and unmounted (light green) areas. The x-axis shows wells grouped in intervals based on total sand thickness within the studied interval in the well (meters). The y-axis shows percent of total sand thickness. The plot shows that most of the sand is located within mounds.

### 6.7.2. Distribution of sand in unmounted areas at the flank

Observations from chapter 6.5 show that mounds are absent on the flank in area 3A. Several wells were examined to decide if the lack of mounds could be connected to absence of sand. The results are presented in Table 6-2, and show that:

- 1) 8 out of the 13 investigated wells show no evidence of sand in the studied interval.
- 2) 3 out of the 13 investigated wells show traces of sand in the studied interval.
- 3) 2 of the 13 investigated wells show sand in the studied interval (>47m sand).



Sand was also observed within deeper part of the Hordaland Group, but deeper than the studied interval (well 35/11-4). An overview of the location of the wells, together with lithology in the studied interval (top CSS-6 to top CSS-3), are displayed in Figure 6-35.

**Table 6-2:** Overview of distribution of sand in wells penetrating the unrounded areas on the eastern basin flank

Wells	Year drilled	Sand is present in interval of interest	Sand is not present in interval of interest	Sand present within the Hordaland Group	Total thickness of sand (meter) in the interval of interest	Comments
31/2-7	1982		X	No		Area 2, Troll
31/2-8	1982		X	No		Area 2, Troll
31/2-14	1984	(X)		(Yes)	Traces of sand	Area 2, Troll, Traces of sand in the upper part of the Hordaland Group (studied interval)
31/2-15	1984	(X)		(Yes)	Traces of sand	Area 2, Troll, Traces of sand in the upper part of the Hordaland Group (studied interval)
31/3-3	1984		X	No		Area 2
35/11-4	1990		X	Yes, 1100m RKB deep		Area 2, Fram, top Hordaland Group is located 734m RKB deep
35/11-7	1992		X	No		Area 2, Fram
31/2-1	1979		X	No		Area 3A, Troll
31/5-5	1992	(X)		(Yes)	Traces of sand	Area 3A, Troll, Claystone with traces of sand
31/6-1	1983	X		Yes	47,5m	Area 3A, Troll, Top Hordaland Group is located 531m RKB deep, Sand occur from 531 to 578,5m RKB. The main part of the Hordaland Group is characterized by claystoned.
31/6-2R	1984		X	No		Area 3A, Troll
31/6-6	1984		X	No		Area 3A, Troll
31/6-8R	1985	X		Yes	100m	Area 3A, Troll, Top Hordaland is located 538m RKB deep, sand 538-638m RKB.

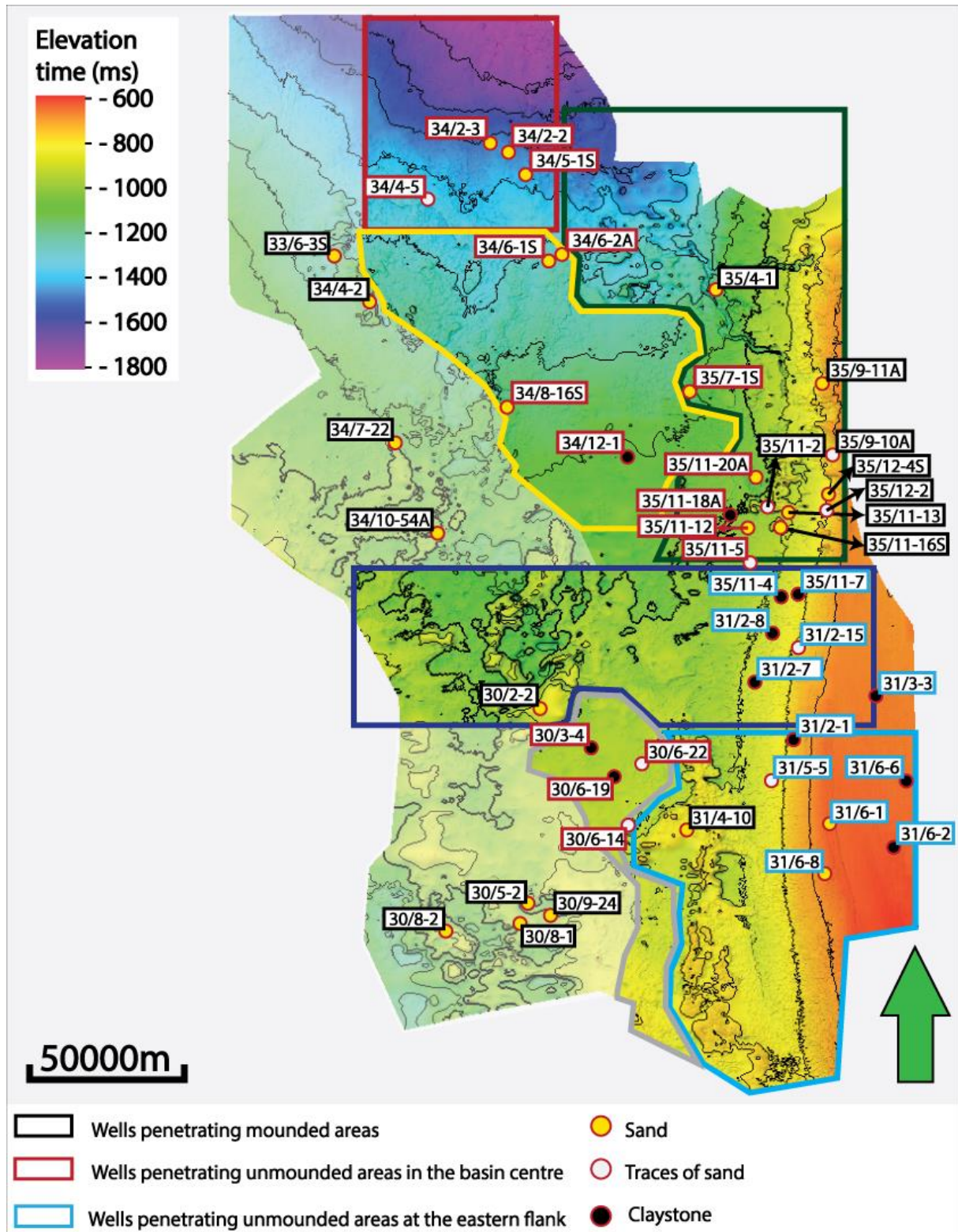


**Figure 6-35:** Elevation map of top Hordaland, displaying an overview of the location of the wells utilized to explore the lithology distribution in the study area. The colour-fill of the circles describe the lithology in the studied interval. The subareas are also displayed.

### 6.7.3 Uplift vs. sand thickness

The relationship between uplift observed in a mound (m) and sand thickness (m) was examined. How the uplift and sand thickness was measured is demonstrated in chapter 4.3. 9 mounds were

investigated and resulted in three observations. The first observation shows mounds where there are observed more uplift than sand, e.g. well 35/11-2 (marked with red in Table 6-3). The second observation shows two mounds where the total sand thickness in the well in the studied interval is larger than the uplift of the mound, e.g. 35/9-11A (marked with blue in Table 6-3). The third observation shows a well where the uplift almost corresponds to the total sand thickness in well 35/11-16S (marked with black in Table 6-3) This demonstrates that most of the investigated wells show less sand than uplift, although the sand thickness is measured based on a larger interval (top CSS-6 to top CSS-3) compared to the uplift (Figure 6-36).

**Table 6-3:** The table shows the relationship between uplift of the mounds in meters and the thickness of the studied interval (top CSS-6 to top CSS-3). The area marked with grey is used as input in Figure 6-36.

Well	Uplift (m)	Thickness of sand in studied interval (m)
31/4-10	98	5
35/4-1	32	9,5
35/9-10A	34	2
35/9-11A	40	155,5
35/11-2	121	2
35/11-13	62	87,5
35/11-16S	78	70,5
35/12-2	32	2
35/12-4S	35	159,5

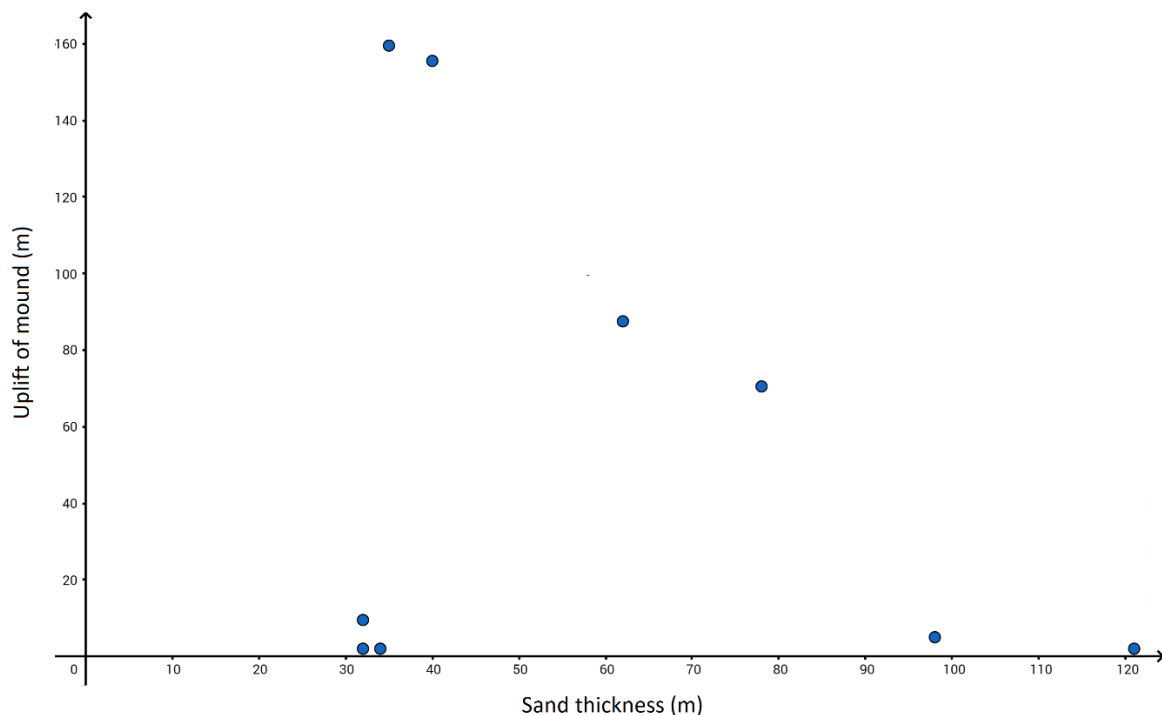


**Figure 6-36:** The plot shows uplift of the mounds (m) vs. sand thickness (m). The input is displayed in Table 6-3.



## **7. Interpretation**

Sand intrusions occur worldwide (Figure 5-1 and Table 5-1). However, based on observations in chapter 5, the sand intrusions do not appear to be randomly distributed. The results show an overrepresentation of sand intrusion at convergent margins and at inverted passive margins. The examination of literature data in chapter 5 shows that inclined parent beds are common at convergent and transform margins where sand intrusions occur. Inclined beds are also present along thrust faults that contain injected sand, as well as in folded parent beds. The importance of these inclined beds for triggering of sand injections will be presented in chapter 7.1. Chapter 6 shows that the mounded features mainly occur along the basin-flank transition. In the northeastern part of the study area (subarea 1A), the mounds are also present at the slope. Accordingly, chapter 6 shows a certain distribution of mounded features, observed at the top Hordaland surface. Chapter 7.2 contains interpretations of the distribution of the mounds in the Hordaland Group (chapter 6), with reference to previously described sand intrusions at inverted passive margins (chapter 5).

### **7.1 Suggested trigger mechanisms for sand intrusions at convergent and transform margins**

14 locations where sand intrusions occur at convergent and transform margins were presented in chapter 5, and 10 of these locations apparently have inclined parent units. The remaining of the investigated locations consist of one location where the literature describes a relatively flat parent sand (Frey-Martinez et al. (2007) in the Levant basin), and the other three locations lack a description of how the parent sand was oriented at the time of injection (Table 5-1). A model that suggests how subsurface remobilization occurred at convergent and transform margins was developed. The model is consistent with the observations presented in chapter 5.

Model one (Figure 7-1) was developed with the intention of explaining triggering of sand intrusions at settings characterized by sloping parent beds along convergent and transform margins. In such settings step-wise movements are expected to occur along the convergent or transform margin, and hence rapid sediment compaction occur as pulses. In water saturated sands, the rapid compaction will lead to rapid overpressure build-up. Overpressure build-up and fluid transport is not able to stop the compaction in this kind of tectonic setting. Such fluid transport results in overpressuring of the up-dip parts of the inclined layers. As Figure 7-1 illustrates, the compaction pulses lead to elevated pore fluid pressures in the deep parts of the inclined layer, and these overpressures are transferred to shallower depths by the centroid effect

(assuming that the aquifer is sealed by a low permeable rock). Overpressure is capable of preventing further mechanical compaction, when the mechanical compaction is a result of increased overburden thickness. Whereas, in tectonic settings dominated by lateral compaction due to large-scale tectonic plate movement, the overpressures cannot prevent the compaction. Assuming that inclined layers are present, and that the same amount of overpressure occur in deep and shallower sediments. In the shallowest parts of the inclined beds, the overpressures will most likely exceed the lithostatic stress and cause subsurface sediment remobilization (Figure 7-1). One example of this observation is observed at Dana Point, in California (Bouroullec et al., 2010).

The step-wise compression caused by the subduction of the plate, trigger earthquakes. The earthquakes cause shear movement in the sand, resulting in reorganization of the grains and rapid compaction. Such local grain rearrangements are presumably what causes changes in the ground water table after earthquakes (Coble, 1965; Roeloffs, 1998). This observation is considered as supporting evidence of the proposal of this thesis: that local grain rearrangements result in rapid pore pressure changes that can trigger sand injections in inclined layers.

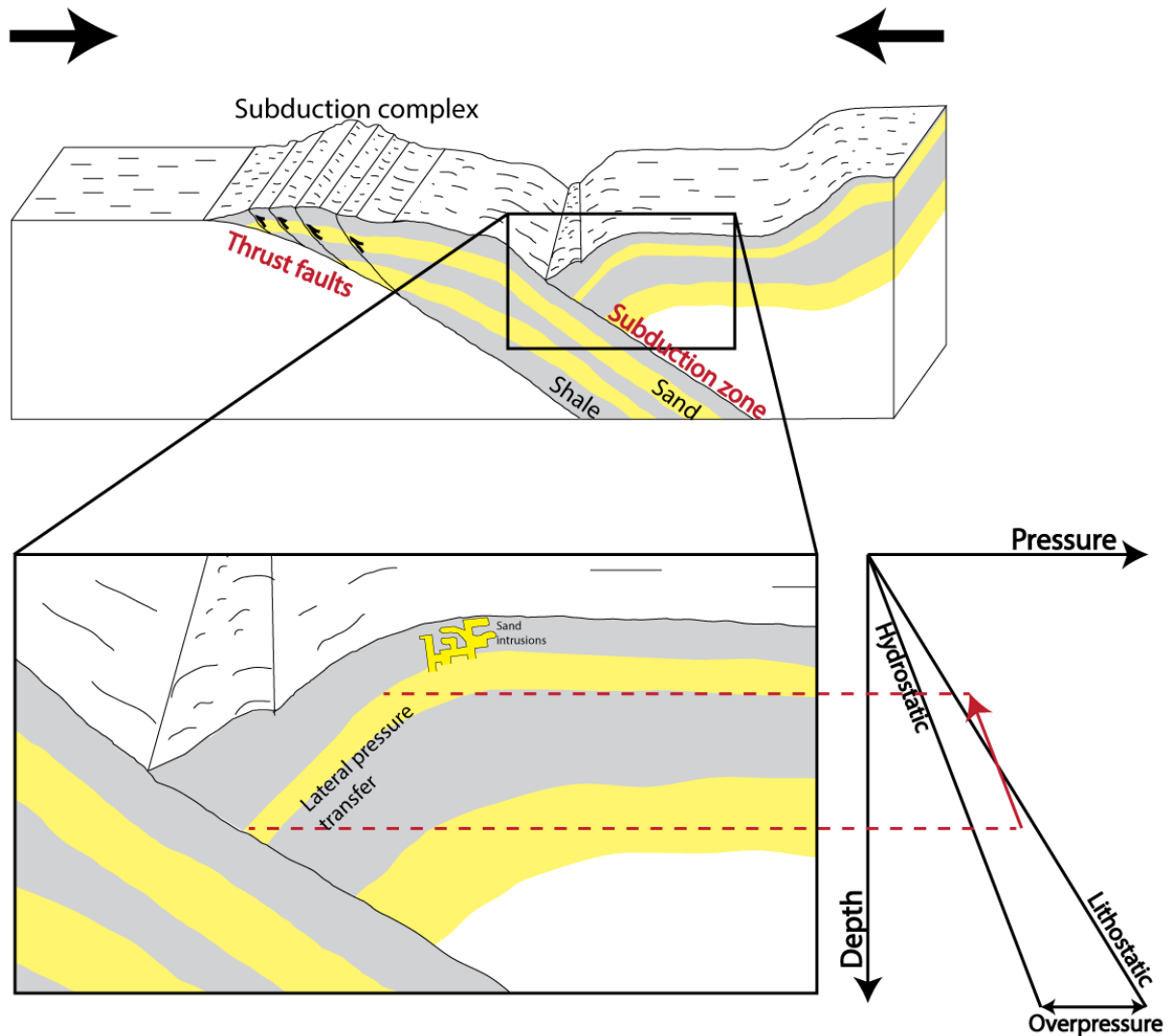


**Figure 7-1:** Sketch of model one. The model describes a possible explanation of how subsurface remobilization of sand occurs at active margins, originating from an inclined parent body. The step-wise plate movement linked to the subduction of the oceanic plate causes rapid pressure build-up. In an inclined parent body, deep parts of the sand layer are in pressure communication with shallower parts of the sand layer. The two red dashed lines represent the same overpressure, when it is equalized within the inclined layer. The red arrow emphasizes how the pore pressure in the shallowest part of the sand layer, exceeds the lithostatic pressure, whereas the pore pressure in the deepest parts of the sand layer only exceeds the hydrostatic pressure. Since the lateral pressure transfer happens rapidly, it represents a good candidate to trigger remobilization of sand at convergent margins.

Winslow (1983) suggested a model (model 2) that describes sand remobilization that occurs in relation to thrust folds, overturned limbs and at the crest of anticlines near the thrusts in a foreland fold and thrust belt. Model two resembles model one in terms of the tectonic regime and release of high pore pressure as an important trigger mechanism. What separates the two, is the observation of sand intrusions occurring in already existing fractures, in addition to sand injectites intruding into the hanging wall at the toe of the thrust faults, which are both reflected in model two (Figure 7-2).

In this thesis, it is suggested that the step-wise movements during the folding cause rapid fluid migration within the parent sand, located at the base of the fold (Figure 7-2). Due to the intermittently compression and folding of the strata, it may result in remobilization of sand as the compression forces fluids to migrate upwards, in addition to the folding causing weakness zones within the overburden. Winslow (1983) also concluded that the clastic intrusions were onset by regional shortening of the crust, and emphasize that the subsurface remobilization most likely was associated to the release of high pore pressures caused by rapid tectonic loading due to the generation of thrusts.

When model two is evaluated in terms of lateral pressure transfer, the parent body is also here gently inclined. Hence the principle explained in model one is also applicable here. Due to the already existing fractures, it is easier for the sand to enter the low permeable seal compared to in model one.

Shearing occurs along the thrust faults, and can potentially contribute in the process of triggering sand intrusions. If sand is present within the fault plane, the shearing results in reorganization of grains into a more compact lattice structure, forcing fluids to escape. Based on the observations illustrating that the thrust fault cross-cut the parent, it is likely that reorganization of sand grains has occurred (Figure 7-2). Sand intrusions occurring along the fault plane of thrust faults are also described in Panoche and Tumey Hills by Palladino et al. (2016).

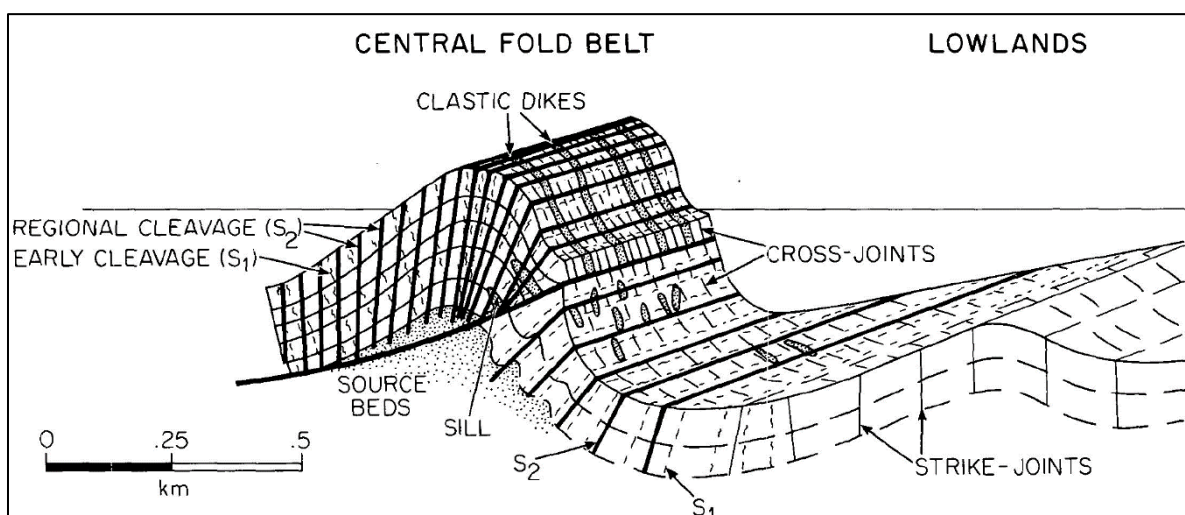


**Figure 7-2:** Schematic sketch that illustrates the distribution of sand intrusions in relation to the structure of the fold, in addition to the relationship between the parent sand and the sand intrusions (Figure 3 in Winslow, 1983).

The two models represent two different situations, though controlled by the same tectonic regime. The latter is here associated to different parts of the convergent margin. Model two is



associated to the subduction complex, and hence the oceanic plate. Model one is associated to inclined areas close to the trough, in addition to the continental slope. Figure 7-3 displays an overview of how the models describe the events in the different parts of the convergent margin.

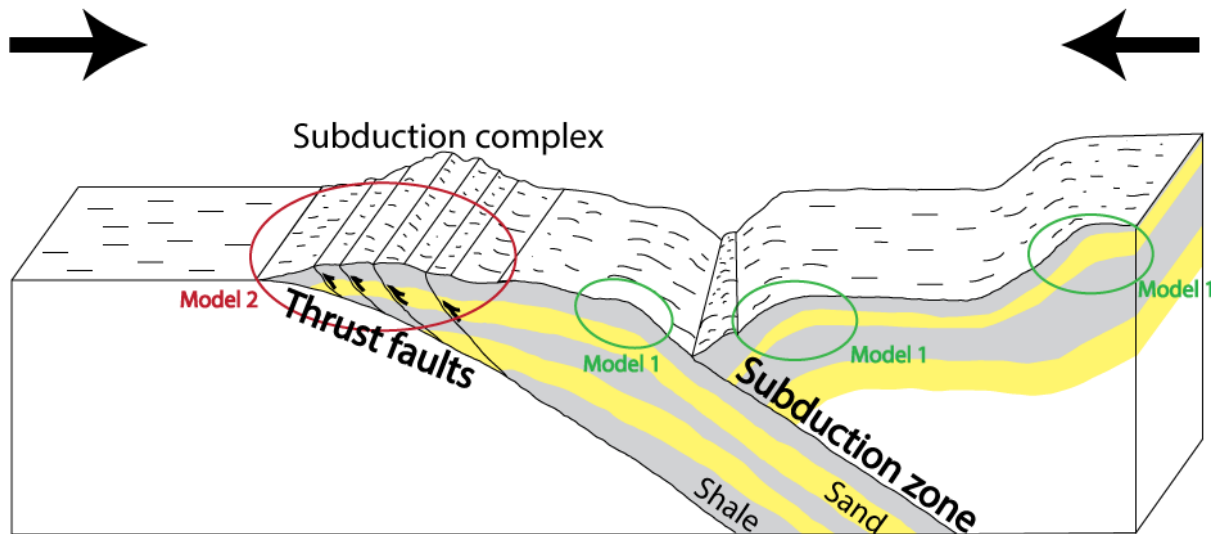


**Figure 7-3:** Sketch of a convergent margin, where the two different models are assigned to the corresponding areas.

Convergent and transform margins are tectonically active areas, and hence numerous authors have suggested earthquakes as the main trigger mechanism causing sand remobilization. What is suggested here is that the step-wise plate movements might have an indirectly impact on the remobilization process rather than a direct impact (e.g. earthquake induced shearing). It is important to stress that there is a possibility that different and several trigger mechanisms could have triggered sand injection at convergent and transform margins. Especially at locations where large volumes of sand has been remobilized and the remobilization has occurred in several phases.

The suggested theory is consistent with what Winslow (1983) suggested (model two), and it is also supported by the experiment conducted by Hermanrud et al. (2010), where remobilization of sand was triggered in an inclined tube. Whether the theory explains what happened in each of the included basins at convergent and transform margins is more uncertain, both in terms of identification of the parent bed and the inclination of the parent bed.

## **7.2 Post-depositional subsurface remobilization at inverted passive margins, based on the case study from the northern North Sea**

The northern North Sea is located at an inverted passive margin. Here, the results from the CSS-4 to CSS-6 of the Cenozoic succession in the northern North Sea, will be utilized to understand the formation processes of subsurface remobilization at inverted passive margins. The results

from the northern North Sea is considered applicable to other inverted passive margins worldwide, as the processes discussed in the forthcoming chapter are linked to the tectonic setting of the basin and not the specific location of the basin.

### **7.2.1 Evidence of subsurface remobilization in the northern North Sea**

Evidences of subsurface remobilization of sand are frequently observed in the northern North Sea basin. Mounds are observed at the top Hordaland Group in subarea 1A, 2 and 3A. When the mounds were investigated in profile view, they revealed chaotic and bright reflectors. Since chaotic and bright reflectors coincided with the mounds, it strongly suggests that the mounds developed due to sand remobilization.

Mounds, chaotic and bright reflectors have been described in the literature as evidences of sand intrusions (e.g. Lonergan et al., 2000; Cartwright et al., 2007; Huuse et al., 2007; Ackers and Bryn, 2015). To verify the interpretation, an analysis of the amount of sand in the studied interval versus uplift of the mounds was conducted. It was expected that the amount of sand versus uplift would display a linear relationship, where increased uplift would reflect increased amount of sand. The well analysis proved that most of the investigated mounds showed more uplift than sand content. Hence, the theory was disproved and it was understood that mud is remobilized together with the sand.

### **7.2.2 Slope failure and submarine slab slides**

Huvenne et al. (2002) described a slope failure observed in the Porcupine basin, located southwest offshore Ireland. The Porcupine basin shows a geological setting much like what is seen in the northern North Sea. The results and interpretations presented by Huvenne et al. (2002) have been used as an analogue in the interpretation of the observations from the northern North Sea. The following is a direct quote from the Huvenne et al. (2002) paper:

“Slope failures occur generally when the external forces (combination of gravity, seismic loading, seepage, etc., i.e. the shear stress) acting on the sediment package exceed the internal shear strength of the sediments (Lee et al., 1999). This shear strength is inversely related to the pressure in the pore fluids (Hampton et al., 1996). Prevention of necessary dewatering after deposition allows excess pore pressures to build up and causes a decrease in sediment strength (Gardner et al., 1999). Hence, while pore water pressures had time to accommodate and reduce in the upper horizons, a deeper-lying stratum probably retained higher internal pore pressures and became a weak layer. Once the failure was triggered, this weak layer liquefied and

collapsed, and became the failure plane of the slide, while the overlying, more consolidated material broke up along tension cracks” (Huvenne et al., 2002, p. 37).

Huvenne et al. (2002) present two main arguments, leading to the classification of the slide in the Porcupine Basin as a submarine slab slide: 1) the presence of a headwall scarp, and 2) the detachment surface being parallel to the bedding. They also identified the slide toe and the slide plane, which they use as supporting evidence for their arguments. What separates a submarine slab slide from a regular submarine slide, is that the slide plane is parallel to the bedding, for the entire or a significant length of the displacement. Hence, a submarine slab slide is also referred to as a translational slide. The displaced strata is normally recognized as consolidated to overconsolidated strata (Huvenne et al., 2002)

A headwall scarp has not been identified in the northern North Sea in the course of this thesis. If a headwall scarp once was present in the northern part of the eastern margin (subarea 1A), it has potentially been hid by mounds occurring at the slope. In the southeastern part of the study area (subarea 2 and 3A) a headwall scarp might be present, but it has not yet been identified.

Top CSS-3 represents a clear detachment surface, and the base of the remobilized sand. Only one detachment surface is interpreted within the studied interval in the northern North Sea (Figure 7-4). The detachment surface is parallel to the bedding, and the strata within the slide shows little evidence of deformation except the subsurface sediment remobilization. This coincides with how Huvenne et al. (2002) described a submarine slab slide. The studied interval in the northern North Sea (top CSS-3 to top CSS-6) is of Early Oligocene to Mid Miocene age. Christensen (2015) did research on subsurface remobilization in the Johan Sverdrup area, and observed two detachment surfaces within the same interval as investigated in this thesis. Her first detachment surface coincides with top CSS-2 (D1) and the second coincides with top CSS-5 (D2) (Figure 7-5). Accordingly, it is understood that the location of detachment surfaces varies within the North Sea, but they tend to coincide with the boundary between two layers.

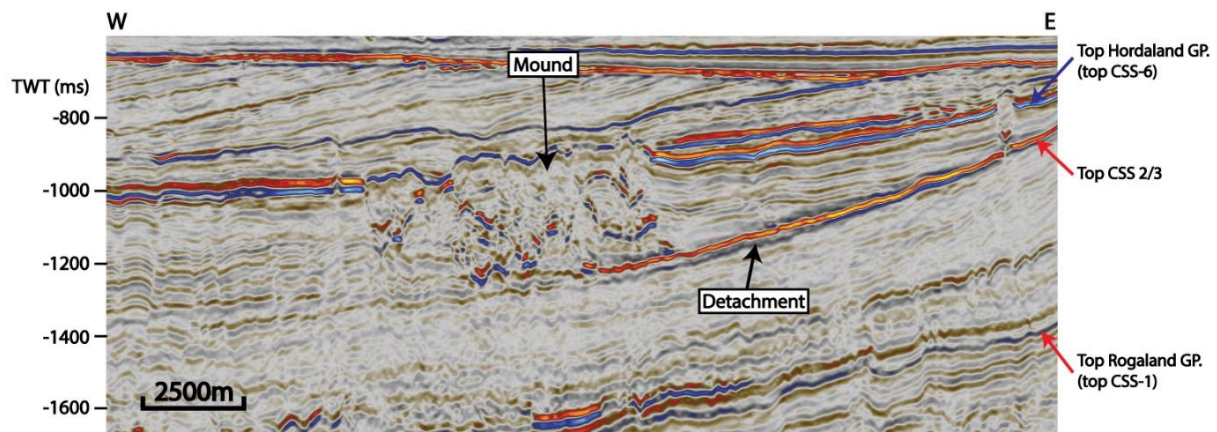


**Figure 7-4:** E-W oriented cross-section that points out the detachment surface in the study area in the northern North Sea. It also shows subsurface sediment remobilization at the basin-flank transition.

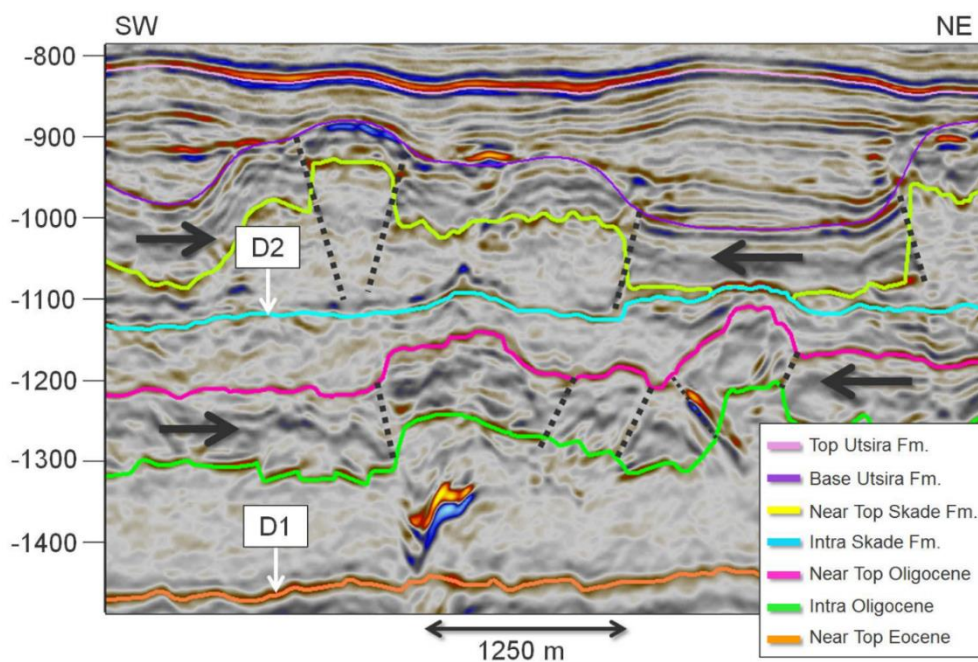


**Figure 7-5:** Detachment surfaces from the Johan Sverdrup area (D1 and D2). Near Top Eocene coincides with top CSS-2 and Intra Skade FM. coincides with top CSS-4. The vertical scale is given in TWT (ms). (Figure 6-25 in Christensen (2015)).

### 7.2.3. Distribution of mounds

A clear distribution of mounds is observed on the top Hordaland Group. The highest concentration of mounds is observed at the basin flank transition, but also at the flank. Mounds are absent in the central parts of the basin. Assuming that a submarine slab slide triggered the subsurface sediment remobilization in the northern North Sea, the slide would have been expected to freeze close to the basin-flank transition. Such a sequence of events would have explained the lack of sand intrusions in the basin center.

Lykousis et al. (2002) described a submarine slab slide in the Aegean Trough, in the Mediterranean. They observe chaotic reflectors and mounding at the basin-flank transition (toe of slope), similar to what is observed in the northern North Sea (Figure 7-6). As displayed in chapter 6, mounds that occur close to the basin flank transition (toe of slope) are either arranged in ridges or in clusters. The ridges are oriented N-S, and hence parallel to the eastern basin margin (subarea 1A and 3A). A potential headwall scarp would also be expected to be oriented N-S. The distribution of mounds in the investigated area fits well with the theory of a submarine slab slide triggering remobilization, and intrusions being observed along the slide toe. One could speculate that the seismic expressions of the slide toe is obscured by the deformation caused by sand remobilization. The mounds arranged in N-S trending and continuous ridges are consistent with a model of liquidization occurring along the entire slide plan (detachment surface).

The mounds arranged in clusters close to the basin-flank transition are observed in the northern part of subarea 1A. The largest clusters are located close to a well-defined channel (Figure 6-13), but there are not seen any evidence indicating that the formation of the mounds is related to the submarine channels. The channels rather seem to erode into the mounds, and hence it is inferred that the channels were active after the remobilization ceased.

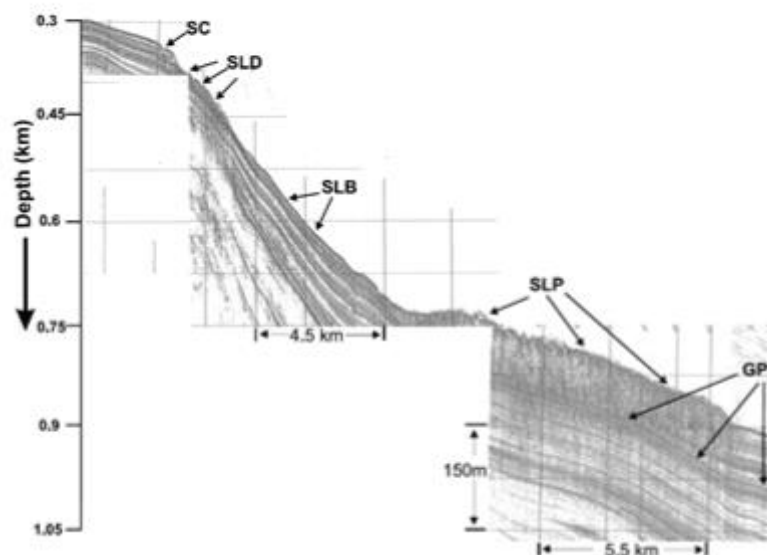


**Figure 7-6:** Submarine slide from in the Aegean Trough, in the Mediterranean area. The seismic profile shows the slab slide (SLB), the glide plane of the slide (GP), the headwall scarp (SC), slide scarp debris (SLD) and mounded features at the toe of the slide (SLP) (Slightly modified after Lykousis et al. (2002)).

Kirkham et al. (2017) and Kirkham et al. (2018) present figures of rim synclines surrounding mud volcanoes. When the depth of the rim synclines equal the amount of uplift, it is a good indication of the sediments being sourced from strata below and close to the mound. The mounds observed in the study of the northern North Sea do not show any rim synclines, and hence it is unlikely that the mounds are sourced from the layer below.

Single mounds and smaller clusters of mounds occur on the slope in subarea 1A. These mounds do not show a preferred orientation. The lack of orientation may be a result of the position of the mounds. Since the single mounds and smaller clusters of mounds occur further east compared to the ridges, they were formed closer to the headwall scarp. Hence, one can speculate that these mounds formed soon after the submarine slab slide was initiated.

#### **7.2.4 Lithology distribution in CSS-4 to CSS-6**

The lithology distribution in the study area gives important information about where sand intrusions possibly could occur. Since the central parts of the basin show occurrence of sand, although less sand than close to the flank, mounds are not absent because of lack of sand. This observation strengthens the theory of subsurface remobilization being triggered by submarine slab slides.

In area 2 and 3A, mounds only occur along the basin-flank transition. One alternative is that the lack of sand intrusions on the slope in area 2 and 3A is a result of lack of sand at the time of injection. Today, the wells in the area show no sand or only traces of sand, but this was not necessarily the case at the time of injection. Due to the ridge-shaped and N-S trending mounds, it is more likely that the liquidization process involved the entire detachment surface. This explains both the large volumes of remobilized sand, and the orientation of the mounds. It also fits with the thickness difference observed in Figure 6-28, where the sequence west of the mound is thicker than the sequence east of the mound. This feature may be caused by sediments from the detachment being fed to the mound along the basin-flank transition. If this was the case, it remains to be explained why subsurface remobilization occur at the flank in the northern part of the study area and are absent on the flank in the southern part of the study area.

Most of the mounds show less sand in the CSS-4 to CSS-6 interval than the amount of uplift of the top Hordaland surface (top (CSS-6). This observation shows that mud was remobilized together with the sand, and helps explaining how such large amounts of sand have been remobilized. Liquidized sand shows higher porosity compared to “regular” sand (Pabis and Magiera, 2002). Consequently, more fluids are required to remobilize an entire layer of sand

than what is already accessible in the pores of the sand. Liquefied mud can act as an external fluid source, and would also explain the non-linear relationship between the uplift and the amount of sand in the mounds. Liquidization of mud and sand is triggered by shearing. Such shearing can have been triggered by the shearing along the detachment of a submarine slab slide.

Some of the mounds (Figure 6-6 and 6-8) clearly show chaotic reflectors in the lowermost part of the mound, and continuous reflectors in the upper part of the mound. Common for these mounds are that they are located close to the basin floor (Figure 7-7). One could speculate that the lack of remobilization of the shallowest part of CSS-4 to CSS-6 occurs due to decreasing energy in the submarine slab slide. As the slide approaches the basin floor, the progress of the slide slows down and the shear stress along the slide plane declines. Accordingly, remobilization is expected to occur within the entire studied interval in areas where the submarine slab slide has high energy, and a lack of remobilization of the shallowest parts of the studied interval in areas where the submarine slab slide was characterized by low energy.

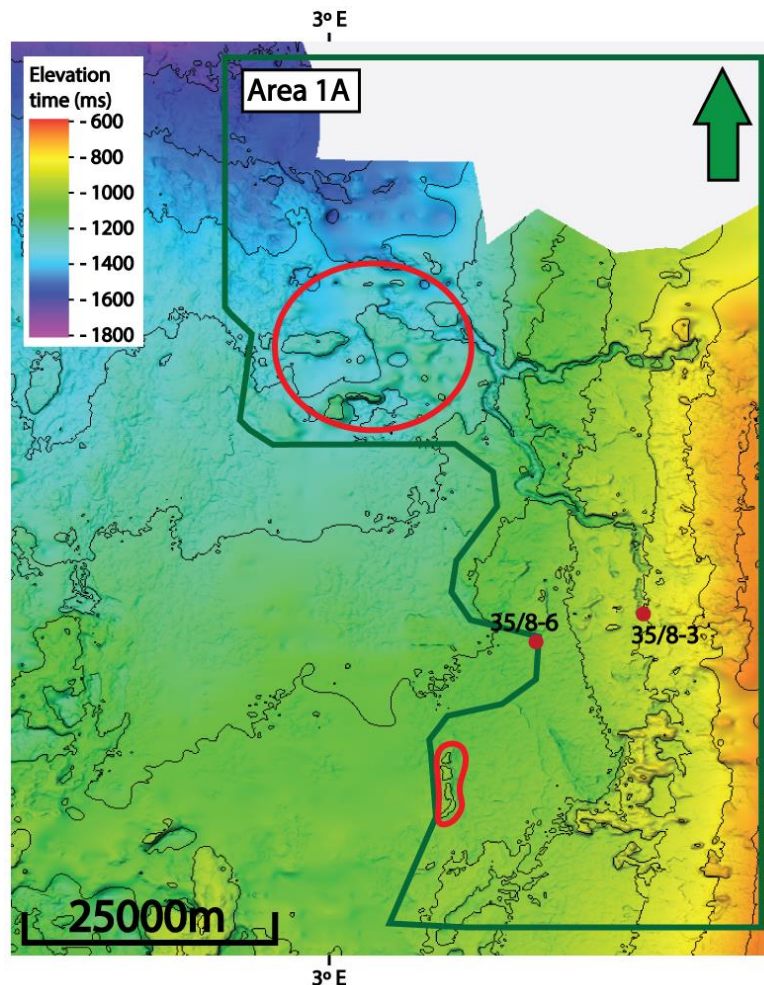


**Figure 7-7:** Elevation map of parts of top Hordaland Group (subarea 1A), which shows the mounds located closest to the basin floor (marked with a red circle).

### 7.2.5 Formation of sand intrusions in the northern North Sea basin

Based on the observations described in chapter 6, it seems likely that a submarine slab slide has triggered the subsurface sediment remobilization in the northern North Sea. The observations and interpretations were utilized to develop a model that describes the link between the submarine slab slide and subsurface sediment remobilization at inverted passive margins (Figure 7-8). The model shows where a potential headwall scarp would have been located, how the detachment represents the slide plane, which is parallel to the bedding, and how mounds are created at the basin-flank transition, close to the slide toe.



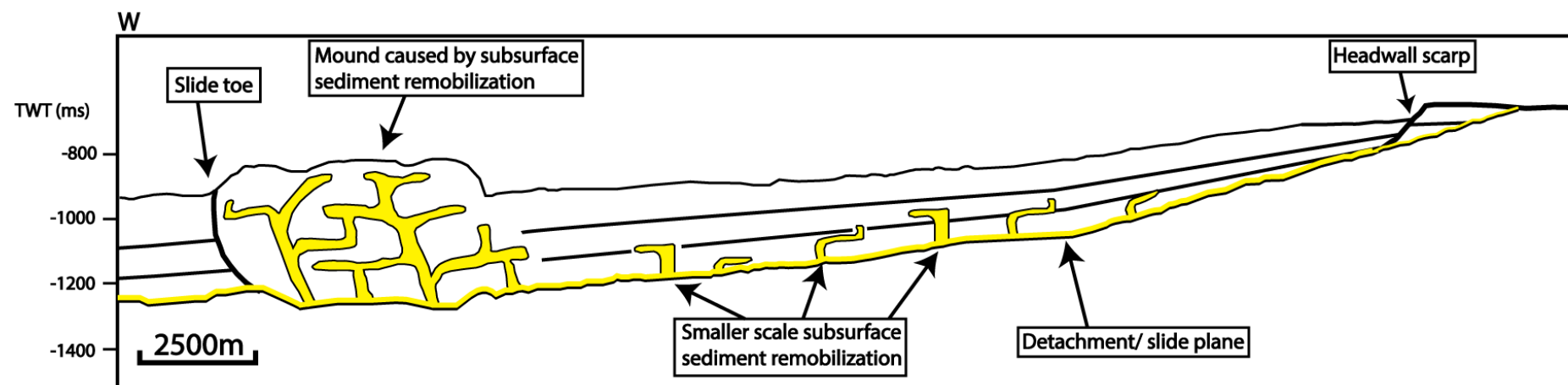


**Figure 7-8:** Model developed based on observations presented in chapter 6. It shows the link between the submarine slab slide and subsurface sediment remobilization. Liquefaction of sand and mud occur due to shearing along the slide plane. The thin yellow drape above the slide plane represents the parent bed of the sand intrusions.

The lack of observed headwall scarp can have different causes: 1) the headwall scarp is represented by a very small step along a seismic reflector, e.g. the height of the headwall scarp described by Huvenne et al. (2002) varies between a few to 25m, 2) it is challenging to identify the headwall scarp when the surface is mounded, especially if subsurface sediment remobilization occur below the headwall scarp, and hides it.

Lateral pressure transfer is here proposed as the most likely trigger mechanism at convergent and transform margins. Subsurface sediment remobilization happens in an inclined environment also in the northern North Sea. The reason why lateral pressure transfer is presumably not applicable here, is that the eastern margin of the northern North Sea is represented by a low-angled slope, i.e. almost horizontal. Active margins on the other hand, normally show a steeper slope and a narrower shelf compared to passive margins (Doyle, 2017). Also, the horizontal compression during tectonic events (earthquakes caused by the compression) presumably results in rapid compaction and pore pressure build-up. Such events were not present at typical inverted passive margins. This implies that neither the inclination of the slope, nor the difference in overburden weight would cause a significantly high pore pressure gradient. Hence, the subsurface sediment remobilization happens across sedimentary layers, rather than along the porous media (towards east) to the upper slope.

In summary, the following model for subsurface remobilization of the CSS-4 to CSS-6 is suggested:

1. Basin margin uplift in the Oligocene supplied primary sand input to the basin (the Skade Formation), and resulted in a slope gradient increase. The uplift caused sliding along the shear planes between the Grid Formation and the over- or underlying mudstones. The submarine slab slide triggered subsurface sediment remobilization.
2. A new phase of basin margin uplift in the Mid Miocene supplied more sand to the basin (the Utsira Formation), and resulted in an increase of the slope gradient. The uplift created the detachment surface on top of the Skade Formation, which acted as the slide plane. The submarine slab slide triggered subsurface sediment remobilization.

This suggested two-step model is applicable to the observations of Christensen (2015), where two detachment surfaces were observed within the Oligocene and Miocene succession. The study area of Christensen (2015) is located in the Johan Sverdrup area, i.e. south of the study area examined in this thesis. Only one detachment surface was identified in the study area of this thesis. Faleide et al. (2002) describe regional differences within the North Sea basin, which

could explain why only one generation of subsurface sediment remobilization was observed in the Early Oligocene to Mid Miocene succession in the northern North Sea, compared to the Johan Sverdrup area. Hence, only the second step of the two-step model is applicable to the study area in this thesis.



## 8. Future work

This thesis has provided new information about trigger mechanisms for subsurface sediment remobilization at convergent and inverted passive margins. With such a regional study, there are still features that should be investigated in more detail. Ideas for future work are listed in the following two subchapters.

### 8.1 The literature study

- Study every basin in Table 5-1 more closely.
- Include more locations where sand intrusions are observed in Table 5-1.
- Develop alternative formation models for subsurface remobilization at convergent and transform margins.

### 8.2 The case study from the northern North Sea

- Do more detailed seismic interpretation of the eastern basin flank to search for more evidence for the occurrence of a submarine slab slide (e.g. search for a headwall scarp and compression along the basin-flank transition).
- For subsurface remobilization to occur, the slab slide must have been initiated quite abrupt. It would have been interesting to model how fast a slide has to move to generate liqudization along the slide plane.
- Compare the lateral extent of the Grid and Skade Formations versus subsurface remobilization. The relationship between the three could give information about the parent unit of the sand intrusions.
- Examine if the model is applicable to other parts of the North Sea, and in the rest of the Hordaland Group.
- Examine if there is anything (geometrically) that separates the mounds containing mostly sand versus the mounds containing more mud than sand.

## 9. Conclusion

The aim of this study was to investigate a possible link between trigger mechanisms of sand intrusions, and the tectonic setting of the basin where they occur. The literature study that was performed as a part of this thesis, revealed an overrepresentation of sand intrusions at convergent margins (including transform margins) and inverted passive margins.

The main conclusion from the literature study is that lateral pressure transfer, caused by the centroid effect, represents an important trigger mechanism at convergent and transform margins. This was suggested on the basis of local grain rearrangements occurring due to step-wise compression of sediments in the deep. The step-wise compression may result in rapid pore pressure changes that can trigger sand injectites in shallower parts of inclined and permeable layers.

The case study from the northern North Sea was utilized to investigate trigger mechanisms for subsurface sediment remobilization at inverted passive margins. Seismic interpretation of 3D seismic data, combined with well analyses of 34 wells was used to examine the study area. The main conclusions from studies of the interval (top CSS-3 to top CSS-6) of Early Oligocene to Mid Miocene age are:

- Submarine slab slides are likely to have triggered the subsurface sediment remobilization. This model was based on the following:
  - Remobilization took place at the slope and along the basin-flank transition, but not in the basin center.
  - The detachment surface interpreted along top CSS-3 encompasses a good candidate for the slide plane. A continuous strong reflector was observed along the base of the remobilized interval. This reflector represents the interpreted detachment surface.
  - Mounds created by subsurface sediment remobilization are arranged in N-S trending ridges along the basin-flank transition, and are hence parallel to the eastern margin and a potential headwall scarp.
  - Mud was remobilized together with the sand. This was reflected in the non-linear relationship between total sand thickness in the remobilized interval versus the uplift of the mound.

The model presented in this thesis, is the same as the one presented in Huvenne et al. (2002), where it is suggested that:

- The slope failure occurred in a weak layer, when external forces surpassed the shear strength of the weak layer.
- Liquidization of sand and mud occurred as a result of shearing along the slide plane of the submarine slab slide.

The submarine slab slide was identified based on the interpreted slide plane being parallel to the bedding. What separated the two case studies was that a headwall scarp was not identified in the northern North Sea.

Based on observations from the literature and the 3D seismic dataset from the northern North Sea, it was understood that one trigger mechanism cannot explain the formation of sand intrusions and extrudites worldwide. The main trigger mechanisms of large-scale sand intrusions appear to be linked to the tectonic setting of the basin. However, other trigger mechanisms cannot be ruled out as local trigger mechanisms.





## References

- Abbassene, F., Chazot, G., Bellon, H., Bruguier, O., Ouabadi, A., Maury, R. C., Déverchère, J., Bosch, D., and Monié, P., 2016, A 17Ma onset for the post-collisional K-rich calc-alkaline magmatism in the Maghrebides: Evidence from Bougaroun (northeastern Algeria) and geodynamic implications: *Tectonophysics*, v. 674, p. 114-134.
- Ackers, M. A., and Bryn, B. K. L., 2015, Common characteristics of remobilised sand mounds from seismic attributes: *First break*, v. 33, p. 39-49.
- Allen, J. R. L., 1982, *Sedimentary Structures: Their Character and Physical Basis*, v. 1, Elsevier, Amsterdam, 593 pp.
- Allen, J. R. L., 1985, *Physical Sedimentology*, Allen & Unwin, London, 272 pp.
- Allen, M. B., Macdonald, D. I. M., Xun, Z., Vincent, S. J., and Brouet-Menzies, C., 1997, Early Cenozoic two-phase extension and late Cenozoic thermal subsidence and inversion of the Bohai Basin, northern China: *Marine and petroleum Geology*, v. 14, p. 951-972.
- Allen, M. B., Macdonald, D. I. M., Xun, Z., Vincent, S. J., and Brouet-Menzies, C., 1998, Transtensional deformation in the evolution of the Bohai Basin, northern China, *in* Holdsworth, R. E., Strachan, R. A., and Dewey, J. F., eds., *Continental Transpressional and Transtensional Tectonics*, Geological Society, London, Special Publications, v. 135, p. 215-229.
- Almagor, G., 1980, Halokinetic deep-seated slumping on the mediterranean slope of northern Sinai and southern Israel: *Marine Georesources & Geotechnology*, v. 4, p. 83-105.
- Almagor, G., 1984, Salt-controlled slumping on the Mediterranean slope of central Israel: *Marine Geophysical Research*, v. 6, p. 227-243.
- Almagor, G., 1986, Mass transport on the continental slope of Israel: *Geo-Marine Letters*, v. 6, p. 29-34.
- Alsop, G. I., and Marco, S., 2011, Soft-sediment deformation within seismogenic slumps of the Dead Sea Basin: *Journal of Structural Geology*, v. 33, p. 433-457.
- Archer, J. B., 1984, Clastic intrusions in deep-sea fan deposits of the Rosroe Formation, Lower Ordovician, western Ireland: *Journal of Sedimentary Research*, v. 54, p. 1197-1205.
- Atwater, T., and Molnar, P., 1973, Relative motion of the Pacific and North American plates deduced from sea-floor spreading in the Atlantic, Indian, and South Pacific Oceans, *in* Proceedings Conference on Tectonic Problems of the San Andreas Fault System, v. 13, Stanford University Publication of Geological Science, p. 136-148.
- Beyer, J., 2015, Sandstone injectites record pre-, syn-, and post-folding deformation at Sheep Mountain Anticline, Wyoming, PhD thesis: The University of Texas at Arlington.
- Bloet, J. P., Imbert, P., and Foubert, A., 2017, Mechanisms of biogenic gas migration revealed by seep carbonate paragenesis, Panoche Hills, California: *American Association of Petroleum Geology Bulletin*, v. 101, p. 1309-1340.
- Boehm, A., and Moore, J., 2002, Fluidized sandstone intrusions as an indicator of paleostress orientation, Santa Cruz, California: *Geofluids*, v. 2, p. 147-161.
- Bouroullec, R., Pyles, R., and Bouroullec, R., 2010, Sandstone Extrusions and Slope Channel Architecture and Evolution: Mio-Pliocene Monterey and Capistrano Formations, Dana Point Harbor, Orange County, California, USA: *Journal of Sedimentary Research*, v. 80, p. 376-392.
- Braccini, E., de Boer, W., Hurst, A., Huuse, M., Vigorito, M., and Templeton, G., 2006, Sand injectites: *Geology*, v. 186, p. 67-88.
- Briedis, N. A., Bergslien, D., Hjellbakk, A., Hill, R. E., and Moir, G. J., 2007, Recognition criteria, significance to field performance, and reservoir modeling of sand injections in the Balder field, North Sea, *in* Hurst, A., and Cartwright, J., eds., *Sand Injectites:*

- Implications for hydrocarbon exploration and production: American Association of Petroleum Geologists Memoir, v. 87, p. 91-102.
- Brooke, C. M., Trimble, T. J., and Mackay, T. A., 1995, Mounded shallow gas sands from the Quaternary of the North Sea: analogues for the formation of sand mounds in deep water Tertiary sediments?, *in* Hartley, A. J., and Prosser, D. J., eds., *Characterisation of Deep Marine Clastic Systems*, Geological Society, London, Special Publications, v. 94, p. 95-101.
- Bruce, B., and Bowers, G., 2002, Pore pressure terminology: *The Leading Edge*, v. 21, p. 170-173.
- Carruthers, R. G., Caldwell, W., and Steuart, D. R., 1912, *The oil-shales of the Lothians*, 2nd edn., Memoir of the Geological Survey of Scotland, Her Majesty's Stationary Office, Edinburgh.
- Cartwright, J., 2007, The impact of 3D seismic data on the understanding of compaction, fluid flow and diagenesis in sedimentary basins: *Journal of the Geological Society*, London, v. 164, p. 881-893.
- Cartwright, J., 2010, Regionally extensive emplacement of sandstone intrusions: a brief review: *Basin Research*, v. 22, p. 502-516.
- Cartwright, J., Huuse, M., and Aplin, A., 2007, Seal bypass systems: *American Association of Petroleum Geologists Bulletin*, v. 91, p. 1141-1166.
- Cartwright, J., James, D., and Bolton, A., 2003, The genesis of polygonal fault systems: a review, *in* Van Rensbergen, P., Hillis, R. R., Maltman, A. J., and Morley, C. K., eds., *Subsurface Sediment Mobilization*, Geological Society, London, Special Publications, v. 216, p. 223-243.
- Cartwright, J., James, D., Huuse, M., Vetel, W., and Hurst, A., 2008, The geometry and emplacement of conical sandstone intrusions: *Journal of Structural Geology*, v. 30, p. 854-867.
- Chan, M., Netoff, D., Blakey, R., Kocurek, G., and Alvarez, W., 2007, Clastic-injection Pipes and Syndepositional Deformation Structures in Jurassic Eolian Deposits: Examples from the Colorado Plateau, *in* Hurst, A., Cartwright, J., ed., *Sand injectites: Implications for hydrocarbon exploration and production*, American Association of Petroleum Geologists Memoir v. 87, p. 233-244.
- Christensen, E., 2015, The geological evolution of the Oligocene to Middle Miocene Hordaland Group, from deposition to present day geometries, based on data from the Johan Sverdrup area, Master thesis: University of Bergen.
- Clausen, J. A., Gabrielsen, R. H., Reksnes, P. A., and Nysæther, E., 1999, Development of intraformational (Oligocene–Miocene) faults in the northern North Sea: influence of remote stresses and doming of Fennoscandia: *Journal of Structural Geology*, v. 21, p. 1457-1475.
- Cobain, S., Peakall, J., and Hodgson, D. M., 2015, Indicators of propagation direction and relative depth in clastic injectites: Implications for laminar versus turbulent flow processes: *Geological Society of America Bulletin*, v. 127, p. 1816-1830.
- Cobain, S. L., Hodgson, D. M., Peakall, J., and Shiers, M. N., 2017, An integrated model of clastic injectites and basin floor lobe complexes: implications for stratigraphic trap plays: *Basin Research*, v. 29, p. 816-835.
- Coble, R., 1965, The effects of the Alaskan earthquake of March 27, 1964, on ground water in Iowa: *Proceedings of the Iowa Academy of Science*, v. 72, p. 323-332.
- Cole, D., Stewart, S. A., and Cartwright, J. A., 2000, Giant irregular pockmark craters in the Palaeogene of the outer Moray Firth basin, UK North Sea: *Marine and Petroleum Geology*, v. 17, p. 563-577.

- Cosgrove, J. W., and Hillier, R. D., 2000, Forced-fold development within Tertiary sediments of the Alba Field, UKCS: evidence of differential compaction and post-depositional sandstone remobilization, *in* Cosgrove, J. W., and Ameen, M. S., eds., *Forced Folds and Fractures*, Geological Society, London, Special Publications, v. 169, p. 61-71.
- Coward, M. P., Dewey, J., Hempton, M., and Holroyd, J., 2003, Tectonic evolution, *The Millennium Atlas: Petroleum Geology of the central northern North Sea*: London, The Geological Society, p. 17-33.
- Davies, R., Cloke, I., Cartwright, J., Robinson, A., and Ferrero, C., 2004, Post-breakup compression of a passive margin and its impact on hydrocarbon prospectivity: An example from the Tertiary of the Faeroe Shetland Basin, United Kingdom: *American Association of Petroleum Geologist Bulletin*, v. 88, p. 1-20.
- Davies, R. J., 2003, Kilometer-scale fluidization structures formed during early burial of a deep-water slope channel on the Niger Delta: *Geology*, v. 31, p. 949-952.
- Davies, R. J., Huuse, M., Hirst, P., Cartwright, J., and Yang, Y., 2006, Giant clastic intrusions primed by silica diagenesis: *Geology*, v. 34, p. 917-920.
- Delaney, P. T., Pollard, D. D., Ziony, J. I., and McKee, E. H., 1986, Field relations between dikes and joints: emplacement processes and paleostress analysis: *Journal of Geophysical Research: Solid Earth*, v. 91, p. 4920-4938.
- Dharmayanti, D., Tait, T., and Evans, R., 2006, Deep-water Reservoir Facies of the Late Jurassic Angel Fan, Dampier Sub-Basin, Australia, Extended abstract, Annual Convention, American Association of Petroleum Geologists, p. 1-3.
- Dickinson, W. R., and Seely, D. R., 1979, Structure and stratigraphy of forearc regions: *American Association of Petroleum Geologists Bulletin*, v. 63, p. 2-31.
- Diggs, T. N., 2007, An Outcrop Study of Clastic Injection Structures in the Carboniferous Tesnus Formation, Marathon Basin, Trans-Pecos Texas, *in* Hurst, A., and Cartwright, J., eds., *Sand injectites: Implications for hydrocarbon exploration and production*: American Association of Petroleum Geologists Memoir, v. 87, p. 209-219.
- Diller, J. S., 1890, Sandstone dikes: *Geological Society of America Bulletin*, v. 1, p. 411-442.
- Dixon, R. J., Schofield, K., Anderton, R., Reynolds, A. D., Alexander, R. W. S., Williams, M. C., and Davies, K. G., 1995, Sandstone diapirism and clastic intrusion in the Tertiary submarine fans of the Bruce-Beryl Embayment, Quadrant 9, UKCS, *in* Hartley, A. J., and Prosser, D. J., eds., *Characterization of Deep Marine Clastic Systems*: Geological Society, London, Special Publications, v. 94, p. 77-94.
- Doyle, L. J., 2017, Continental margin, *Encyclopædia Britannica*, Encyclopædia Britannica, inc., downloaded January 2018 from: <https://www.britannica.com/science/continental-margin>
- Dreimanis, A., and Rappol, M., 1997, Late Wisconsinan sub-glacial clastic intrusive sheets along Lake Erie bluffs, at Bradville, Ontario, Canada: *Sedimentary Geology*, v. 111, p. 225-248.
- Duranti, D., 2007, Large-scale Sand Injection in the Paleogene of the North Sea: Modeling of Energy and Flow Velocities, *in* Hurst, A., and Cartwright, J., eds., *Sand Injectites: Implications for Hydrocarbon Exploration and Production*: American Association of Petroleum Geologists Memoir, v. 87, p. 129-139.
- Duranti, D., and Hurst, A., 2004, Fluidization and injection in the deep-water sandstones of the Eocene Alba Formation (UK North Sea): *Sedimentology*, v. 51, p. 503-529.
- Duranti, D., Hurst, A., Bell, C., Groves, S., and Hanson, R., 2002, Injected and remobilized Eocene sandstones from the Alba Field, UKCS: cores and wireline log characteristics: *Petroleum Geoscience*, v. 8, p. 99-107.

- Eidvin, T., Jansen, E., Rundberg, Y., Brekke, H., and Grogan, P., 2000, The upper Cenozoic of the Norwegian continental shelf correlated with the deep sea record of the Norwegian Sea and the North Atlantic: *Marine and Petroleum Geology*, v. 17, p. 579-600.
- Eidvin, T., and Riis, F., 1992, En biostratigrafisk og seismo-stratigrafisk analyse av tertiære sedimenter i nordlige deler av Norskerenna, med hovedvekt på øvre pliocene vifteavsetninger: *Norwegian Petroleum Directorate Contribution*, v. 32, 40 pp.
- Eidvin, T., Riis, F., and Rasmussen, E. S., 2014, Oligocene to Lower Pliocene deposits of the Norwegian continental shelf, Norwegian Sea, Svalbard, Denmark and their relation to the uplift of Fennoscandia: A synthesis: *Marine and Petroleum Geology*, v. 56, p. 184-221.
- Eidvin, T., Riis, F., Rasmussen, E. S., and Rundberg, Y., 2013, Investigation of Oligocene to Lower Pliocene deposits in the Nordic offshore area and onshore Denmark: *Norwegian Petroleum Directorate Bulletin*, v. 10, 62 pp.
- Faleide, J. I., Kyrkjebø, R., Kjennerud, T., Gabrielsen, R. H., Jordt, H., Fanavoll, S., and Bjerke, M. D., 2002, Tectonic impact on sedimentary processes during Cenozoic evolution of the northern North Sea and surrounding areas, *in* Doré, A.G. et al. ed., *Exhumation of the North Atlantic Margin: Timing, Mechanism and Implications for Petroleum Exploration: Geological Society, London, Special Publications*, v. 196, p. 235-269.
- Flemings, P. B., Stump, B. B., Finkbeiner, T., and Zoback, M., 2002, Overpressure and flow focusing in the Eugene Island 330 field (offshore Louisiana, USA): Theory, examples, and implications: *American Journal of Science*, v. 302, p. 827-855.
- Frey-Martinez, J., Cartwright, J., Hall, B., and Huuse, M., 2007, Clastic intrusion at the base of deep-water sands: A trap-forming mechanism in the eastern Mediterranean, *in* Hurst, A., and Cartwright, J., eds., *Sand Injectites: Implications for Hydrocarbon Exploration and Production: American Association of Petroleum Geologists Memoir*, v. 87, p. 49-63.
- Frey Martinez, J., Cartwright, J., and Hall, B., 2005, 3D seismic interpretation of slump complexes: examples from the continental margin of Israel: *Basin Research*, v. 17, p. 83-108.
- Fuller, M. L., 1912, The new Madrid earthquake, *U.S. Geological Survey Bulletin*, v. 494, 119 pp.
- Færseth, R. B., 1996, Interaction of Permo-Triassic and Jurassic extensional fault-blocks during the development of the northern North Sea: *Journal of the Geological Society of London*, v. 153, p. 931-944.
- Galli, P., 2000, New empirical relationships between magnitude and distance for liquefaction: *Tectonophysics*, v. 324, p. 169-187.
- Galloway, W. E., Garber, J. L., Liu, X., and Sloan, B. J., 1993, Sequence stratigraphic and depositional framework of the Cenozoic fill, Central and Northern North Sea Basin, *in* Parker, R., ed., *Petroleum geology of northwest Europe: The Geological Society of London*, v. 1, p. 33-43.
- Gamberi, F., 2010, Subsurface sediment remobilization as an indicator of regional-scale defluidization within the upper Tortonian Marnoso-arenacea formation (Apenninic foredeep, northern Italy): *Basin Research*, v. 22, p. 562-577.
- Gardner, J. V., Prior, D. B., and Field, M. E., 1999, Humboldt slide - a large shear-dominated retrogressive slope failure: *Marine Geology*, v. 154, p. 323-338.
- Garfunkel, Z., 1984, Large-scale submarine rotational slumps and growth faults in the eastern Mediterranean: *Marine Geology*, v. 55, p. 305-324.
- Garfunkel, Z., and Almagor, G., 1985, Geology and structure of the continental margin off northern Israel and the adjacent part of the Levantine Basin: *Marine Geology*, 62, p. 105-131.

- Garfunkel, Z., and Almagor, G., 1987, Active salt dome development in the Levant Basin, southeast Mediterranean, *in* Lerche, I., and O'Brien, J., eds., *Dynamical Geology of Salt and Related Structures*: Academic Press, New York, v., p. 263-300.
- Gautier, D. L., 2005, Kimmeridgian shales total petroleum system of the North Sea graben province: *Geological Survey Bulletin (US) 2204-C*, 24 pp.
- Gill, W. D., and Kuenen, P. H., 1957, Sand volcanoes on slumps in the Carboniferous of County Clare, Ireland: *Quarterly Journal of the Geological Society*, v. 113, p. 441-460.
- Gradstein, F., and Backstrøm, S., 1996, Cainozoic biostratigraphy and palaeobathymetry, northern North Sea and Haltenbanken: *Norsk Geologisk Tidsskrift*, v. 76, p. 3-32.
- Gradstein, F. M., Anthonissen, E., Brunstad, H., Charnock, M., Hammer, O., Hellem, T., and Lervik, K. S., 2010, Norwegian offshore stratigraphic lexicon (NORLEX): *Newsletters on Stratigraphy*, v. 44, p. 73-86.
- Gras, R., and Cartwright, J. A., 2002, Tornado Faults: the seismic expression of the Early Tertiary on PS-data, Chestnut Field, UK North Sea, 64th European Association Geologists Engineers Conference & Exhibition: Florence (Extended Abstract H020).
- Greensmith, J. T., 1957, A sandstone dyke near Queensferry, West Lothian: *Transactions of the Edinburgh Geological Society*, v. 17, p. 54-59.
- Gregersen, U., and Johannessen, P. N., 2007, Distribution of the Neogene Utsira Sand and the succeeding deposits in the Viking Graben area, North Sea: *Marine and Petroleum Geology*, v. 24, p. 591-606.
- Gregersen, U., Michelsen, O., and Sørensen, J. C., 1997, Stratigraphy and facies distribution of the Utsira Formation and the Pliocene sequences in the northern North Sea: *Marine and Petroleum Geology*, v. 14, p. 893-914.
- Hall, A., and Bishop, P., 2002, Scotland's denudational history: an integrated view of erosion and sedimentation at an uplifted passive margin, *in* Doré, A. G., Cartwright, J. A., Stoker, M. S., Turner, J. P., and White, N., eds., *Exhumation of the North Atlantic Margin: Timing, Mechanisms and Implications for Petroleum Exploration*: Geological Society, London, Special Publications, v. 196, p. 271-290.
- Hampton, M. A., Lee, H. J., and Locat, J., 1996, Submarine landslides: *Reviews of Geophysics*, v. 34, p. 33-59.
- Hartmann, L. A., Baggio, S. B., and Duarte, S. K., 2013, Decoding geochemical and gamma-spectrometric signatures from lavas and sand injectites at the base of the Paraná volcanic province, Novo Hamburgo, Brazil: *International Geology Review*, v. 55, p. 510-524.
- Helland-Hansen, W., Ashton, M., Lømo, L., and Steel, R., 1992, Advance and retreat of the Brent delta: recent contributions to the depositional model: Geological Society, London, Special Publications, v. 61, p. 109-127.
- Hermanrud, C., Teige, G. M. G., Iding, M., Eiken, O., Rennan, L., and Østmo, S., 2010, Differences between flow of injected CO<sub>2</sub> and hydrocarbon migration: Geological Society, London, Petroleum Geology Conference v. 7, p. 1183-1188.
- Hesse, R., and Reading, H. G., 1978, Subaqueous clastic fissure eruptions and other examples of sedimentary transposition in the lacustrine Horton Bluff Formation (Mississippian), Nova Scotia, Canada, *in* Matter, A., and Tucker, M., eds., *Modern and Ancient Lake Sediments* International Association of Sedimentologists Special Publications, v. 2, p. 241-257.
- Hillier, R. D., and Cosgrove, J. W., 2002, Core and seismic observations of overpressure-related deformation within Eocene sediments of the Outer Moray Firth, UKCS: *Petroleum Geoscience*, v. 8, p. 141-149.
- Hiscott, R. N., 1979, Clastic sills and dikes associated with deep-water sandstones, Tourelle Formation, Ordovician, Quebec: *Journal of Sedimentary Research*, v. 49, p. 1-10.

- Huang, Q., 1988, Geometry and tectonic significance of Albian sedimentary dykes in the Sisteron area, SE France: *Journal of Structural Geology*, v. 10, p. 453-462.
- Hubbard, S. M., Romans, B. W., and Graham, S. A., 2007, An Outcrop Example of Large-scale Conglomeratic Intrusions Sourced from Deep-water Channel Deposits, Cerro Toro Formation, Magellanes Basin, Southern Chile, *in* Hurst, A., and Cartwright, J., eds., Sand injectites: Implications for Hydrocarbon Exploration and Production, v. American Association of Petroleum Geologists Memoir 87, p. 199-207.
- Hurst, A., and Cartwright, J., 2007, Relevance of sand injectites to hydrocarbon exploration and production, *in* Hurst, A., and Cartwright, J., eds., Sand injectites: Implications for Hydrocarbon Exploration and Production: American Association of Petroleum Geologists, Memoir, v. 87, p. 1-19.
- Hurst, A., Cartwright, J., and Duranti, D., 2003a, Fluidization structures produced by upward injection of sand through a sealing lithology, *in* Van Rensbergen, P., Hillis, R. P., Maltman, A. J., and Morley, C. K., eds., Subsurface sediment mobilization: Geological Society, London, Special Publications, v. 216, p. 123-137.
- Hurst, A., Cartwright, J., Huuse, M., Jonk, R., Schwab, A., Duranti, D., and Cronin, B., 2003b, Significance of large-scale sand injectites as long-term fluid conduits: evidence from seismic data: *Geofluids*, v. 3, p. 263-274.
- Hurst, A., Cartwright, J. A., Huuse, M., and Duranti, D., 2006, Extrusive sandstones (extrudites): A new class of stratigraphic trap?, *in* Allen, M. R., Goffey, G. P., Morgan, R. K., and Walker, I. M., eds., The deliberate search for stratigraphic traps: Where are they now?: Geological Society, London, Special Publications, v. 254, p. 289-300.
- Hurst, A., Scott, A., and Vigorito, M., 2011, Physical characteristics of sand injectites: *Earth Science Reviews*, v. 106, p. 215-246.
- Hurst, A., and Vigorito, M., 2017, Saucer-shaped sandstone intrusions: An underplayed reservoir target: *American Association of Petroleum Geologists* v. 101, p. 625-633.
- Huuse, M., Cartwright, J., Hurst, A., and Steinsland, N., 2007, Seismic characterization of large-scale sandstone intrusions, *in* Hurst, A., and Cartwright, J., eds., Sand Injectites: Implications for Hydrocarbon Exploration and Production: American Association of Petroleum Geologists v. 87, p. 21-35.
- Huuse, M., Cartwright, J. A., Gras, R., Hurst, A., Dore, A. G., and Vining, B. A., 2005, Kilometre-scale sandstone intrusions in the Eocene of the outer Moray Firth (UK North Sea); migration paths, reservoirs and potential drilling hazards, *in* Dore, A. G., and Vining, B. A., eds., Petroleum Geology: North-West Europe and Global Perspectives - Proceedings of the 6th Petroleum Geology Conference: The Geological Society of London, p. 1577-1594.
- Huuse, M., Jackson, C. A. L., Van Rensbergen, P., Davies, R. J., Flemings, P. B., and Dixon, R. J., 2010, Subsurface sediment remobilization and fluid flow in sedimentary basins: an overview: *Basin Research*, v. 22, p. 342-360.
- Huvenne, V. A., Croker, P. F., and Henriot, J. P., 2002, A refreshing 3D view of an ancient sediment collapse and slope failure: *Terra Nova*, v. 14, p. 33-40.
- Hyam, D. M., Marshall, J. E. A., and Sanderson, D. J., 1997, Carboniferous diamictite dykes in the Falkland Islands: *Journal of African Earth Sciences*, v. 25, p. 505-517.
- Isaksen, D., and Tonstad, K., 1989, A Revised Cretaceous and Tertiary lithostratigraphic nomenclature for the Norwegian North Sea. *Norwegian Petroleum Directory*, v. 5.
- Ito, M., Ishimoto, S., Ito, K., and Kotake, N., 2016, Geometry and lithofacies of coarse-grained injectites and extrudites in a late Pliocene trench-slope basin on the southern Boso Peninsula, Japan: *Sedimentary Geology*, v. 344, p. 336-349.
- Jackson, C. A., 2007, The geometry, distribution, and development of clastic injections in slope systems: seismic examples from the Upper Cretaceous Kyrre Formation, Måløy Slope,

- Norwegian Margin, *in* Hurst, A., and Cartwright, J., eds., *Sand Injectites: Implications for Exploration and Production: American Association of Petroleum Geologists*, v. 87, p. 37-48.
- Jenkins, O. P., 1930, Sandstone dikes as conduits for oil migration through shales: *American Association of Petroleum Geologists*, v. 14, p. 411-421.
- Jenssen, A. I., Bergslien, D., Rye-Larsen, M., and Lindholm, R. M., 1993, Origin of complex mound geometry of Paleocene submarine-fan sandstone reservoirs, Balder Field, Norway, *in* Parker, R., ed., *Petroleum Geology of northwest Europe: The Geological Society of London*, v. 1, p. 135-143.
- Jiang, Z., Liu, H., Zhang, S., Su, X., and Jiang, Z., 2011, Sedimentary characteristics of large-scale lacustrine beach-bars and their formation in the Eocene Boxing Sag of Bohai Bay Basin, East China: *Sedimentology*, v. 58, p. 1087-1112.
- Jolly, R. J. H., and Lonergan, L., 2002, Mechanisms and controls on the formation of sand intrusions: *Journal of the Geological Society*, v. 159, p. 605-617.
- Jonk, R., 2010, Sand-rich injectites in the context of short-lived and long-lived fluid flow: *Basin Research*, v. 22, p. 603-621.
- Jonk, R., Cronin, T., and Hurst, A., 2007a, Variations in Sediment Extrusion in Basin-Floor, Slope, and Delta-front Settings: Sand Volcanoes and Extruded Sand Sheets from the Namurian of County Clare, Ireland, *in* Hurst, A., Cartwright, J., ed., *Sand injectites: Implications for hydrocarbon exploration and production: American Association of Petroleum Geologists Memoir*, v. 87, p. 221-226.
- Jonk, R., Duranti, D., Hurst, A., Parnell, J., and Fallick, A. E., 2007b, Aqueous and Petroleum Fluids Associated with Sand Injectites Hosted by Lacustrine Shales from the Oil-shale Group (Dinantian), Midland Valley, Scotland, *in* Hurst, A., Cartwright, J., ed., *Sand injectites: Implications for hydrocarbon exploration and production: American Association of Petroleum Geologists*, v. 87, p. 265-274.
- Jonk, R., Hurst, A., Duranti, D., Parnell, J., Mazzini, A., and Fallick, A. E., 2005a, The origin and timing of sand injection, petroleum migration, and diagenesis: the Tertiary petroleum system of the South Viking Graben, North Sea: *American Association of Petroleum Geologists Bulletin*, v. 89, p. 329-357.
- Jonk, R., Parnell, J., and Hurst, A., 2005b, Aqueous and petroleum fluid flow associated with sand injectites: *Basin Research*, v. 17, p. 241-257.
- Jordt, H., Faleide, J. I., Bjørlykke, K., and Ibrahim, M. T., 1995, Cenozoic sequence stratigraphy of the central and northern North Sea Basin: tectonic development, sediment distribution and provenance areas: *Marine and Petroleum Geology*, v. 12, p. 845-879.
- Jordt, H., Thyberg, B. I., and Nøttvedt, A., 2000, Cenozoic evolution of the central and northern North Sea with focus on differential vertical movements of the basin floor and surrounding clastic source areas: *Geological Society Special Publications*, v. 167, p. 219-243.
- Kirkham, C., Cartwright, J., Hermanrud, C., and Jebsen, C., 2017, The genesis of mud volcano conduits through thick evaporite sequences: *Basin Research*, p. 1-20.
- Kirkham, C., Cartwright, J., Hermanrud, C., and Jebsen, C., 2018, The formation of giant clastic extrusions at the end of the Messinian Salinity Crisis: *Earth and Planetary Science Letters*, v. 482, p. 434-445.
- Le Heron, D. P., and Etienne, J. L., 2005, A complex subglacial clastic dyke swarm, Sólheimajökull, southern Iceland: *Sedimentary Geology*, v. 181, p. 25-37.
- Lee, H., Locat, J., Dartnell, P., Israel, K., and Wong, F., 1999, Regional variability of slope stability: application to the Eel margin, California: *Marine Geology*, v. 154, p. 305-321.

- Lien, T., 2017, Geological constraints on the position of oil-water contacts in the Oseberg and Frigg areas of the northern North Sea, Master thesis: The University of Bergen
- Lonergan, L., and Cartwright, J. A., 1999, Polygonal faults and their influence on deep-water sandstone reservoir geometries, Alba Field, United Kingdom Central North Sea: *American Association Petroleum Geologists Bulletin*, v. 83, p. 410-432.
- Lonergan, L., Lee, N., Johnson, H. D., Cartwright, J. A., and Jolly, R. J. H., 2000, Remobilisation and injection in deepwater depositional systems: implications for reservoir architecture and prediction, *in* Wiemer, P. et al., *Deep-Water Reservoirs of the World: GCSSEPM Foundation 20th Annual Bob F. Perkins Research Conference*, p. 515-532.
- Lowe, D. R., 1979, Sediment gravity flows: their classification and some problems of application to natural flows and deposits, *in* Doyle, L. J., and Pilkey, O. H., eds., *Geology of Continental Slopes: Society of Economic Paleontologists and Mineralogists, Special Publications v. 27*, p. 75-82.
- Lykousis, V., Roussakis, G., Alexandri, M., Pavlakis, P., and Papoulia, I., 2002, Sliding and regional slope stability in active margins: North Aegean Trough (Mediterranean): *Marine Geology*, v. 186, p. 281-298.
- Løseth, H., Raulline, B., and Nygård, A., 2013, Late Cenozoic geological evolution of the northern North Sea: development of a Miocene unconformity reshaped by large-scale Pleistocene sand intrusion: *Journal of the Geological Society*, v. 170, p. 133-145.
- Løseth, H., Rodrigues, N., and Cobbold, P. R., 2012, World's largest extrusive body of sand?: *Geology*, v. 40, p. 467-470.
- Løseth, H., Wensaas, L., Arntsen, B., and Hovland, M., 2003, Gas and fluid injection triggering shallow mud mobilization in the Hordaland Group, North Sea, *in* Van Rensbergen, P., Hillis, R. R., Maltman, A. J., and Morley, C. K., eds., *Subsurface Sediment Mobilization: Special Publications, Geological Society, London*, v. 216, p. 139-157.
- Macdonald, D., and Flecker, R., 2007, Injected sand sills in a Strike-slip Fault Zone: a case Study from the Pil'sk Suite (Miocene), Southeast Schmidt Peninsula, Sakhalin, *in* Hurst, A., Cartwright, J., ed., *Sand injectites: Implications for hydrocarbon exploration and production, American Association of Petroleum Geologist Memoir*, v. 87, p. 253-263.
- Macleod, M. K., Hanson, R. A., Bell, C. R., and McHugo, S., 1999, The Alba Field ocean bottom cable seismic survey: Impact on field development: *The Leading Edge*, v. 18, p. 1306-1312.
- Maltman, A., 1994, *The Geological Deformation of Sediments*, Chapman and Hall, London, 362 pp.
- Maltman, A. J., and Bolton, A., 2003, How sediments become mobilized, *in* Van Rensbergen, P., Hillis, R. R., Maltman, A., and Morley, C. K., eds., *Subsurface Sediment Mobilization: Geological Society, London, Special Publications*, v. 216, p. 9-20.
- Marco, S., Katz, O., and Dray, Y., 2014, Historical sand injections on the Mediterranean shore of Israel: evidence for liquefaction hazard: *Journal of the International Society for the Prevention and Mitigation of Natural Hazards*, v. 74, p. 1449-1459.
- Martel, A. T., and Gibling, M. R., 1993, Clastic dykes of the Devonian-Carboniferous Horton Bluff Formation, Nova Scotia: storm-related structures in shallow lakes: *Sedimentary Geology*, v. 87, p. 103-119.
- Martinsen, O. J., Bøen, F., Charnock, M. A., Mangerud, G., Nøttvedt, A., Fleet, A. J., and Boldy, S. A. R., 1999, Cenozoic development of the Norwegian margin 60-64 degrees N: sequences and sedimentary response to variable basin physiography and tectonic setting, *in* Fleet, A. J., and Boldy, S. A. R., eds., *Petroleum geology of Northwest Europe; proceedings of the 5th conference: Geological Society of London*, p. 293-304.



- McGuire, D. J., 1988, Depositional framework of the Upper Cretaceous-lower Tertiary Moreno Formation, central San Joaquin basin, California, *in* Graham, S. A., and Olson, H. C., eds., *Studies of the geology of the San Joaquin Basin: Los Angeles, Pacific Section, Society of Economic Paleontologists and Mineralogists*, v. 60, p. 173-188.
- Michelsen, O., Danielsen, M., Heilmann-Clausen, C., Jordt, H., Laursen, G. V., and Thomsen, E., 1995, Occurrence of major sequence stratigraphic boundaries in relation to basin development in Cenozoic deposits of the southeastern North Sea, *in* Steel, R. J., Felt, V. L., Johannessen, E. P., and Mathieu, C., eds., *Sequence stratigraphy on the Northwest European Margin: Norwegian Petroleum Society Special Publications*, v. 5, p. 415-427.
- Milton, N. J., Bertram, G. T., and Vann, I. R., 1990, Early Paleogene tectonics and sedimentation in the central North Sea, *in* Hardman, R. F. P., and Brooks, J., eds., *Tectonic Events Responsible for Britain's Oil and Gas Reserves: Geological Society of London*, v. 55, p. 339-351.
- Minisini, D., and Schwartz, H., 2007, An Early Paleocene cold seep system in the Panoche and Tumey Hills Central California (United States), *in* Hurst, A., Cartwright, J., ed., *Sand injectites: Implications for hydrocarbon exploration and production, American Association of Petroleum Geologists Memoir*, v. 87, p. 185-197.
- Mitchell, C., Graham, S. A., and Suek, D. H., 2010, Subduction complex uplift and exhumation and its influence on Maastrichtian forearc stratigraphy in the Great Valley Basin, northern San Joaquin Valley, California: *Geological Society of America Bulletin*, v. 122, p. 2063-2078.
- Mitchell, S. M., Beamish, G. W. J., Wood, M. V., Malacek, S. J., Armentrout, J. A., Damuth, J. E., and Olson, H. C., 1993, Paleocene sequence stratigraphic framework of the Faeroe Basin, *in* Parker, R., ed., *Petroleum Geology of Northwest Europe: Proceedings of the 4th Conference: Geological Society, London*, p. 1011-1023.
- Monnier, D., Imbert, P., Gay, A., Mourgues, R., and Lopez, M., 2014, Pliocene sand injectites from a submarine lobe fringe during hydrocarbon migration and salt diapirism: a seismic example from the Lower Congo Basin: *Geofluids*, v. 14, p. 1-19.
- Moore, J. G., and Shannon, P. M., 1991, Slump structures in the Late Tertiary of the Porcupine Basin, offshore Ireland: *Marine and Petroleum Geology*, v. 8, p. 184-197.
- Moreau, J., Ghienne, J. F., and Hurst, A., 2012, Kilometre-scale sand injectites in the intracratonic Murzuq Basin (South-west Libya): an igneous trigger?: *Sedimentology*, v. 59, p. 1321-1344.
- Morley, C. K., and Naghadeh, D. H., 2017, Tectonic compaction shortening in toe region of isolated listric normal fault, North Taranaki Basin, New Zealand: *Basin Research*, p. 1-13.
- Murchison, R., 1827, Supplementary remarks on the oolitic series in the counties of Sutherland and Ross, and in the Hebrides: *Transactions of the Geological Society*, v. 2, 353 pp.
- Nardin, T. R., Hein, F. J., Gorsline, D. S., and Edwards, B. D., 1979, A review of mass movement processes sediment and acoustic characteristics, and contrasts in slope and base-of-slope systems versus canyon-fan-basin floor systems, *in* Doyle, L. J., and Pilkey, O. H., eds., *Geology of Continental Slopes SEPM Special Publications*, v. 27, p. 61-73.
- Neuwerth, R., Suter, F., Guzman, C. A., and Gorin, G. E., 2006, Soft-sediment deformation in a tectonically active area: The Plio-Pleistocene Zarzal Formation in the Cauca Valley (Western Colombia): *Sedimentary Geology*, v. 186, p. 67-88.
- Nøttvedt, A., Gabrielsen, R. H., and Steel, R. J., 1995, Tectonostratigraphy and sedimentary architecture of rift basins, with reference to the northern North Sea: *Marine and Petroleum Geology*, v. 8, p. 881-901.

- Obermeier, S. F., 1989, The New Madrid earthquakes: An engineering-geologic interpretation of relict liquefaction features: Geological Survey professional paper, v. 1336-B, 114 pp.
- Olabode, S. O., 2006, Siliciclastic slope deposits from the Cretaceous Abeokuta Group, Dahomey (Benin) Basin, southwestern Nigeria: *Journal of African Earth Sciences*, v. 46, p. 187-200.
- Olafiranye, K., Jackson, C. A. L., and Hodgson, D. M., 2013, The role of tectonics and mass-transport complex emplacement on upper slope stratigraphic evolution; a 3D seismic case study from offshore Angola: *Marine and Petroleum Geology*, v. 44, p. 196-216.
- Oluboyo, A. P., Gawthorpe, R. L., Bakke, K., and Hadler-Jacobsen, F., 2014, Salt tectonic controls on deep-water turbidite depositional systems: Miocene, southwestern Lower Congo Basin, offshore Angola: *Basin Research*, v. 26, p. 597-620.
- Pabis, A., and Magiera, J., 2002, Measurements of porosity of a gas-solid fluidized bed: *Advanced Powder Technology*, v. 13, p. 347-362.
- Palladino, G., Grippa, A., Bureau, D., Alsop, G. I., and Hurst, A., 2016, Emplacement of sandstone intrusions during contractional tectonics: *Journal of Structural Geology*, v. 89, p. 230-249.
- Parize, O., 1988, Sills et Dykes Gréseux sédimentaires: paléomorphologie, fracturation précoce, injection et compaction, PhD thesis: Ecole des Mines de Paris.
- Parize, O., Beaudoin, B., Eckert, S., Friès, G., Hadj-Hassan, F., Schneider, F., Su, K., Tijani, M., Trouiller, A., de Fouquet, C., and Vandromme, R., 2007, The Vocontian Aptian and Albian syndepositional clastic sills and dikes: A field-based mechanical approach to predict and model the early fracturing of marly-limy sediments, *in* Hurst, A., Cartwright, J., ed., *Sand injectites: Implications for hydrocarbon exploration and production*, American Association for Petroleum Geologists Memoir, v. 87, p. 163-172.
- Parize, O., and Friès, G., 2003, The Vocontian clastic dykes and sills: a geometric model, *in* Van Rensbergen, P., Hillis, R. P., Maltman, A., and Morley, C. K., eds., *Subsurface Sediment Mobilization: Geological Society, London, Special Publications*, v. 216, p. 51-71.
- Parnell, J., Boyce, A. J., Hurst, A., Davidheiser-Kroll, B., and Ponicka, J., 2013, Long term geological record of a global deep subsurface microbial habitat in sand injection complexes: *Scientific Reports*, v. 3, 1828 pp.
- Passchier, S., 2000, Soft-sediment deformation features in core from CRP-2/2A, Victoria Land Basin, Antarctica: *Terra Antarctica*, v. 7, p. 401-412.
- Pennington, W. D., 1981, Subduction of the eastern Panama Basin and seismotectonics of northwestern South America: *Journal of Geophysical Research: Solid Earth*, v. 86, p. 10753-10770.
- Peterson, G. L., 1966, Structural interpretation of sandstone dikes, northwest Sacramento Valley, California: *Geological Society of America Bulletin*, v. 77, p. 833-842.
- Pinto, V. M., Hartmann, L. A., Santos, J. O. S., and McNaughton, N. J., 2015, Zircon ages delimit the provenance of a sand extrudite from the Botucatu Formation in the Paraná volcanic province, Iraí, Brazil: *Anais da Academia Brasileira de Ciências*, v. 87, p. 1611-1622.
- Pollard, D. D., and Johnson, A. M., 1973, Mechanics of growth of some laccolithic intrusions in the Henry Mountains, Utah, II: Bending and failure of overburden layers and sill formation: *Tectonophysics*, v. 18, p. 311-354.
- Porat, N., Levi, T., and Weinberger, R., 2007, Possible resetting of quartz OSL signals during earthquakes - Evidence from late Pleistocene injection dikes, Dead Sea basin, Israel: *Quaternary Geochronology*, v. 2, p. 272-277.
- Price, N. J., and Cosgrove, J. W., 1990, *Analysis of geological structures*, Cambridge, Cambridge University Press.

- Qi, J. F., and Yang, Q., 2010, Cenozoic structural deformation and dynamic processes of the Bohai Bay basin province, China: *Marine and Petroleum Geology*, v. 27, p. 757-771.
- Ravnås, R., Nøttvedt, A., Steel, R. J., and Windelstad, J., 2000, Syn-rift sedimentary architectures in the northern North Sea, *in* Nøttvedt, A., ed., *Dynamics of the Norwegian Margin*, Geological Society, London, Special Publications, v. 167, p. 133-177.
- Reimnitz, E., and Marshall, N. F., 1965, Effects of the Alaska earthquake and tsunami on recent deltaic sediments: *Journal of Geophysical Research*, v. 70, p. 2363-2376.
- Ribeiro, C., and Terrinha, P., 2007, Formation, deformation and chertification of systematic clastic dykes in a differentially lithified carbonate multilayer. SW Iberia, Algarve Basin, Lower Jurassic: *Sedimentary Geology*, v. 196, p. 201-215.
- Rodrigues, N., Cobbold, P. R., and Løseth, H., 2009, Physical modelling of sand injectites: *Tectonophysics*, v. 474, p. 610-632.
- Roeloffs, E. A., 1998, Persistent water level changes in a well near Parkfield, California, due to local and distant earthquakes: *Journal of Geophysical Research*, v. 103, p. 869-889.
- Rundberg, Y., 1989, Tertiary sedimentary history and basin evolution of the Norwegian North Sea between 60°N and 62°N an integrated approach, PhD: University of Trondheim.
- Rundberg, Y., and Eidvin, T., 2005, Controls on depositional history and architecture of the Oligocene-Miocene succession, northern North Sea Basin, *in* Wandaas, B., ed., *Onshore-Offshore Relationships on the North Atlantic Margin*, Norwegian Petroleum Society Special Publications, v. 12, p. 207-239.
- Rundberg, Y., and Eidvin, T., 2016, Discussion on 'Late Cenozoic geological evolution of the northern North Sea: development of a Miocene unconformity reshaped by large-scale Pleistocene sand intrusion', *Journal of the Geological Society*, 170, 133-145: *Journal of the Geological Society*, v. 173, p. 384-393.
- Saucier, R. T., 1989, Evidence for episodic sand-blow activity during the 1811-1812 New Madrid (Missouri) earthquake series: *Geology*, v. 17, p. 103-106.
- Schwartz, H., Sample, J., Weberling, K. D., Minisini, D., and Moore, J. C., 2003, An ancient linked fluid migration system: cold-seep deposits and sandstone intrusions in the Panoche Hills, California, U.S.A.: *Geo-Marine Letters*, v. 23, p. 340-350.
- Scott, A., Vigorito, M., and Hurst, A., 2009, The process of sand injection: internal structures and relationships with host strata (Yellowbank Creek Injectite Complex, California, U.S.A.): *Journal of Sedimentary Research*, v. 79, p. 568-583.
- Shaker, S. S., 2002, Causes of disparity between predicted and measured pore pressure: The Leading Edge (Society of Exploration Geophysicists), v. 21, p. 756-760.
- Shaker, S. S., 2005, Geopressure centroid: perception and pitfalls, SEG Technical Program Expanded Abstracts 2005, Society of Exploration Geophysicists, p. 1247-1249.
- Shanmugam, G., Shrivastava, S. K., and Das, B., 2009, Sandy debrites and tidalites of Pliocene reservoir sands in upper-slope canyon environments, offshore Krishna-Godavari Basin (India): implications: *Journal of Sedimentary Research*, v. 79, p. 736-756.
- Sherry, T. J., Rowe, C. D., Kirkpatrick, J. D., and Brodsky, E. E., 2012, Emplacement and dewatering of the world's largest exposed sand injectite complex: *Geochemistry, Geophysics, Geosystems*, v. 13, 1-17 p.
- Shoulders, S. J., and Cartwright, J., 2004, Constraining the depth and timing of large-scale conical sandstone intrusions: *Geology*, v. 32, p. 661-664.
- Shoulders, S. J., Cartwright, J., and Huuse, M., 2007, Large-scale conical sandstone intrusions and polygonal fault systems in Tranche 6, Faroe-Shetland Basin: *Marine and Petroleum Geology*, v. 24, p. 173-188.
- Sims, J. D., and Garvin, C. D., 1995, Recurrent liquefaction induced by the 1989 Loma Prieta earthquake and 1990 and 1991 aftershocks: implications for paleoseismicity studies: *Bulletin of the Seismological Society of America*, v. 85, p. 51-65.

- Steel, R. J., 1993, Triassic-Jurassic megasequence stratigraphy in the Northern North Sea: rift to post-rift evolution: Geological Society, London, Petroleum Geology Conference series, v. 4, p. 299-315.
- Stump, B. B., and Flemings, P. B., 2000, Overpressure and fluid flow in dipping structures of the offshore Gulf of Mexico (E.I.330 field): *Journal of Geochemical Exploration*, v. 69-70, p. 23-28.
- Surlyk, F., Gjelberg, J., and Noe-Nygaard, N., 2007, The Upper Jurassic Hareelv Formation of East Greenland: a giant sedimentary injection complex, *in* Hurst, A., Cartwright, J., ed., Sand injectites: Implications for hydrocarbon exploration and production, American Association of Petroleum Geologists Memoir, v. 87, p. 141-149.
- Surlyk, F., and Noe-Nygaard, N., 2003, A giant sand injection complex: The Upper Jurassic Hareelv Formation of East Greenland: *Geologia Croatica*, v. 56, p. 69-81.
- Swarbrick, R. E., and Osborne, M. J., 1998, Mechanisms that generate abnormal pressures: an overview. In: Law, B.E., Ulmishek, G.F and Slavin U.I. (eds.), *Abnormal pressures in hydrocarbon environments: American Association of Petroleum Geologists Memoir*, v. 70, p. 13-34.
- Szarawarska, E., Huuse, M., Hurst, A., De Boer, W., Lu, L., Molyneux, S., and Rawlinson, P., 2010, Three-dimensional seismic characterisation of large-scale sandstone intrusions in the lower Palaeogene of the North Sea: completely injected vs. in situ remobilised sandbodies: *Basin Research*, v. 22, p. 517-532.
- Sørensen, J. C., Gregersen, U., Breiner, M., and Michelsen, O., 1997, High-frequency sequence stratigraphy of Upper Cenozoic deposits in the central and southeastern North Sea areas: *Marine and Petroleum Geology*, v. 14, p. 99-123.
- Taboada, A., Rivera, L. A., Fuenzalida, A., Cisternas, A., Philip, H., Bijwaard, H., Olaya, J., and Rivera, C., 2000, Geodynamics of the northern Andes: Subductions and intracontinental deformation (Colombia): *Tectonics*, v. 19, p. 787-813.
- Taj, R. J., Aref, M. A. M., and Schreiber, B. C., 2014, The influence of microbial mats on the formation of sand volcanoes and mounds in the Red Sea coastal plain, south Jeddah, Saudi Arabia: *Sedimentary Geology*, v. 311, p. 60-74.
- Thomas, M. F. H., 2011, Sedimentology and basin context of the Numidian Flysch Formation; Sicily and Tunisia, Doctor of Philosophy in the Faculty of Engineering and Physical Sciences: University of Manchester, 277 p.
- Thompson, B. J., Garrison, R. E., and Moore, J. C., 1999, A late Cenozoic sandstone intrusion west of Santa Cruz, California: fluidized flow of water and hydrocarbon-saturated sediments, *in* Garrison, R. E., Aiello, I. W., and Moore, J. C., eds., *Late Cenozoic Fluids Seeps and Tectonics along the San Gregorio Fault Zone in the Monterey Bay Region, California*, American Association of Petroleum Geologists, Pacific Section, volume and Guide Book, GB-76, p. 53-74.
- Thompson, B. J., Garrison, R. E., and Moore, J. C., 2007, A Reservoir-scale Miocene Injectite near Santa Cruz, California, *in* Hurst, A., Cartwright, J., ed., *Sand injectites: Implications for Hydrocarbon Exploration and Production*, v. American Association of Petroleum Geologists Memoir 87, p. 151-162.
- Thyberg, B. I., Jordt, H., Bjørlykke, K., and Faleide, J. I., 2000, Relationships between sequence stratigraphy, mineralogy and geochemistry in Cenozoic sediments of the northern North Sea: Geological Society, London, Special Publications, v. 167, p. 245-272.
- Traugott, M., 1997, Pore/fracture pressure determinations in deep water: *Deepwater Technology*, v. 4, p. 68-70.
- Tremblay, A., and Pinet, N., 2016, Late Neoproterozoic to Permian tectonic evolution of the Quebec Appalachians, Canada: *Earth-Science Reviews*, v. 160, p. 131-170.

- Truswell, J. F., 1972, Sandstone sheets and related intrusions from Coffee bay, Transkei, South Africa: *Journal of Sedimentary Petrology*, v. 42, p. 578-583.
- Underhill, J. R., Monaghan, A. A., and Browne, M. A. E., 2008, Controls on structural styles, basin development and petroleum prospectivity in the Midland Valley of Scotland: *Marine and Petroleum Geology*, v. 25, p. 1000-1022.
- Vétel, W., and Cartwright, J., 2010, Emplacement mechanics of sandstone intrusions: Insights from the Panoche Giant Injection Complex, California: *Basin Research*, v. 22, p. 783-807.
- Vigorito, M., Hurst, A., Cartwright, J., and Scott, A., 2008, Regional-scale subsurface sand remobilization: geometry and architecture: *Journal of the Geological Society*, v. 165, p. 609-612.
- Whipp, P. S., Jackson, C. A. L., Gawthorpe, R. L., Dreyer, T., and Quinn, D., 2014, Normal fault array evolution above a reactivated rift fabric; a subsurface example from the northern Horda Platform, Norwegian North Sea: *Basin Research*, v. 26, p. 523-549.
- Wild, J., and Briedis, N., 2010, Structural and stratigraphic relationships of the Palaeocene mounds of the Utsira High: *Basin Research*, v. 22, p. 533-547.
- Winslow, M. A., 1983, Clastic dike swarms and the structural evolution of the foreland fold and thrust belt of the southern Andes: *Geological Society of America Bulletin*, v. 94, p. 1073-1080.
- Yardley, G., and Swarbrick, R., 2000, Lateral transfer: A source of additional overpressure?: *Marine and Petroleum Geology*, v. 17, p. 523-537.
- Zhang, J., Jiang, Z., Liang, C., Wu, J., Xian, B., and Li, Q., 2016, Lacustrine massive mudrock in the Eocene Jiyang Depression, Bohai Bay Basin, China: Nature, origin and significance: *Marine and Petroleum Geology*, v. 77, p. 1042-1055.
- Ziegler, P. A., 1975, Geologic evolution of North Sea and its tectonic framework: *American Association of Petroleum Geologists Bulletin*, v. 59, p. 1073-1097.
- Ziegler, P. A., 1990, *Geological atlas of Western and Central Europe*. Shell International Petroleum, Mij, Den Haag, 239 pp.
- Ziegler, P. A., and Van Hoorn, B., 1989, Evolution of the North Sea rift system, *in* Tankard, A. J., and Balkwill, H. R., eds., *Extensional Tectonics and Stratigraphy of the North Atlantic Margins*: *American Association of Petroleum Geologists Memoir*, v. 46, p. 471-500.



## **Appendix**

### **Appendix A: Field report**

#### **Field report: Field work in Panoche Hills and Tumey Hills**



20<sup>th</sup> of September to 8<sup>th</sup> of October

The University of Bergen (together with the University of Aberdeen)

Iselin T. Tjensvold (field assistant for research fellow Antonio Grippa)

## Introduction

The Panoche and Tumey Hills represent one of the best exposed sandstone intrusion networks in the world (Cartwright, 2010). This report will present observations from the field, interpretations based on the observations and how these observations have been valuable for the progress of the work of my master thesis.

In my master thesis, I am exploring the possibility of categorizing sand injectites based on the basin setting they occur. The study is based on literature, and there have been found evidence suggesting that two basin settings dominate:

1. Sand injectites at convergent margins
2. Sand injectites at inverted passive margins

At the University of Bergen, I have regional 3D broadband seismic data available (acquired by CGG) from the Northern North Sea. In this dataset I will study sand injectites formed at inverted passive margins.

In the Panoche and Tumey Hills, deep water depositional sands were remobilized at a convergent basin setting (Dickinson and Seely, 1979; McGuire, 1988) and hence the observations from this fieldtrip are most relevant to the first category. However, the observations are also very valuable in the context of the link between outcrop and seismic interpretation.

## Sandstone intrusions in Panoche and Tumey Hills

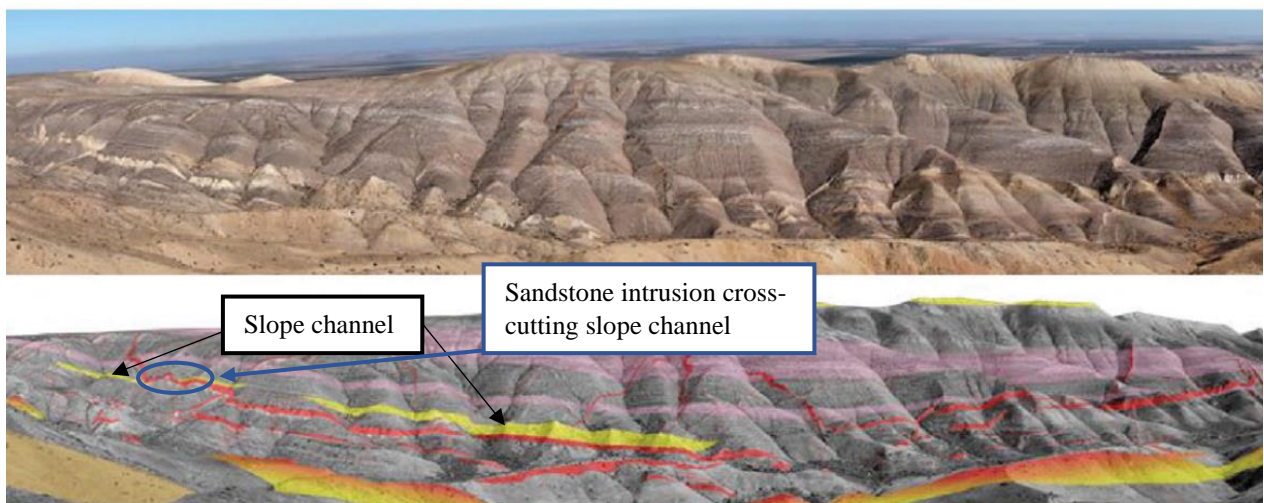


**Figure 1:** Sand injectites in the Right Angle Canyon, California (modified after Hurst and Vigorito (2017)).



During the remobilization events, the Great Valley forearc basin was located at an active margin. An active margin is characterized by a narrow shelf, steep slope, and a relative narrow basin before the basin floor becomes a part of the accretionary prism (Fig. 2) (McGuire, 1988). In Panoche Hills and Tumey Hills there are found injectites formed during two phases of remobilization. The first remobilization phase happened during Danian (Early Paleocene) (e.g. Fig. 1) and the second phase happened during Eocene.

Before the field trip in California I was convinced that the sand injectites in Panoche and Tumey Hills occurred directly related to the compression and thrusting within the accretionary prism. Based on observations in the field and discussion with Antonio Grippa, from the University of Aberdeen, I realize that the remobilization did not happen in direct relation to the accretionary prism, but rather at the continental margin (Fig. 2). There were made several observations of large scale channel-complex (turbiditic channels) being the parent sand of the injectites. However, Winslow (1983) describes dike swarms at the toe of the thrust faults, intruding into the hanging wall in Chile. Based on her observations, sand injectites occurring in direct relation to compression within the accretionary prism should not be excluded from the possible settings where injectites occur.

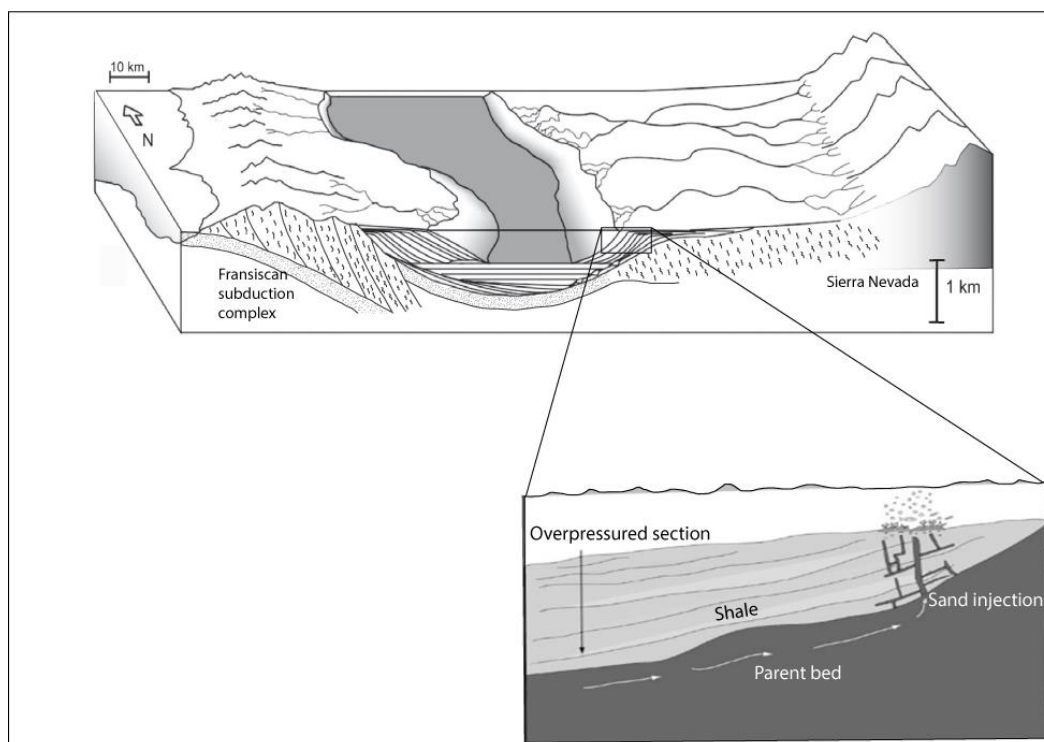


**Figure 2:** The figure shows a schematic diagram showing the general tectonic setting of the San Joaquin Basin during the first injection event (modified after Mitchell et al. (2010) and Schwartz et al. (2003)).

### The link between sand injectites in outcrop and in seismic

Sand injectites represent complex networks (Fig. 3). To understand the link between outcrop and subsurface data, it is crucial to get a good picture of the pressure communication between different sand bodies, and hence the possible fluid migration routes through the system. Sandstone intrusions are connected to their parent unit, they form a network of dikes and sills and they may also cross-cut pristine depositional sandstone units. I think this is one of the most important lessons I learned during the fieldtrip. There is a very good example in Right Angle canyon, where a slope channel-fill deposit cross-cut by a meter-scale sandstone intrusion (Fig. 1). Consequently, there is pressure communication between the depositional sand and the injectite, even though the slope channel deposit is not the parent unit.

Another important lesson learnt was that if a large dike (seismic scale) is observed in the field it will not be visible if it is steep (vertical). In other words, once may overlook huge fluid pathways, which may be crucial for the interpretation and understanding of a petroleum system. Figure 4 shows another important observation; dikes are not just a pipe. They might be large sheets, interconnected with other sand injectites in the horizontal dimension, making the sandstone intrusions networks even more complex to understand.



**Figure 3:** The picture shows a large sandstone intrusion network in the Dosados Canyon, Panoche Hills, California. Most of these injectites would not be visible in seismic.

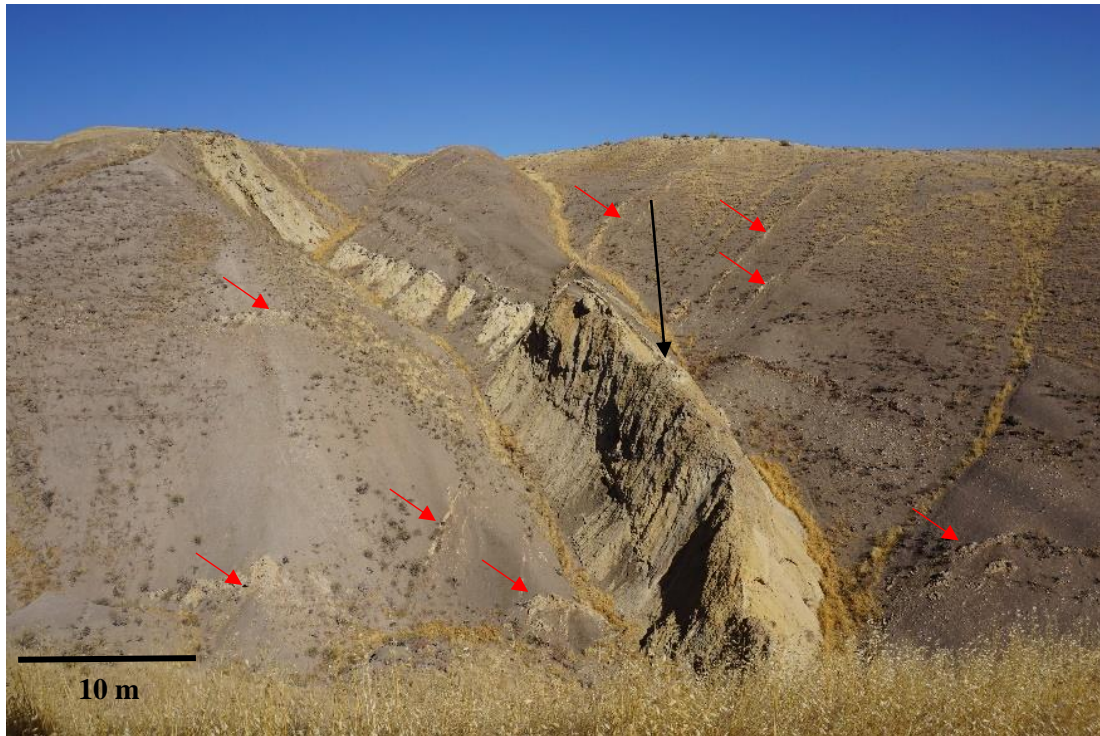


**Figure 4:** The picture shows a sand injectite dike (marked with a black arrow). The main injectite is very thick (tens of meters), and would be visible in seismic where it would show a wing structure. Smaller injectites can also be observed (red arrows) on the picture, but these will not be visible in seismic. The picture is taken in Dosados Canyon, Panoche Hills, California.

## Conclusion

- Sandstone intrusions create large networks, establishing pressure communication between sand bodies that were not connected originally, and hence new migration routes for gas or fluids are constructed.
- It is important to keep in mind that sandstone intrusions may not only be interconnected to each other, but also other sand bodies which they cross-cut.
- Sandstone intrusions in the Panoche and Tumey Hills formed at the continental margin, and not within the accretionary prism. However, based on observations from Winslow (1983) in Chile, injectites occurring in relation to the compression within the accretionary prism should not be excluded from possible geological settings where sand injectites occur.

## Acknowledgements

I gratefully acknowledge Antonio Grippa (research fellow at The University of Aberdeen, UK) for inviting me to be his field assistant. I value our good discussions and his eagerness to explain different geological features and processes when we were in the field.

## References

Discussion with post doc Antonio Grippa, The University of Aberdeen

Cartwright, J., 2010, Regionally extensive emplacement of sandstone intrusions: a brief review: Basin Research, v. 22, no. 4, p. 502-516.

Dickinson, W., and Seely, D., 1979, Structure and stratigraphy of forearc regions: AAPG Bulletin, v. 63, no. 1, p. 2-31.

Hurst, A., and Vigorito, M., 2017, Saucer-shaped sandstone intrusions: An underplayed reservoir target: AAPG Bulletin, v. 101, no. 4, p. 625-633.

McGuire, D. J., 1988, Depositional framework of the Upper Cretaceous-lower Tertiary Moreno Formation, central San Joaquin basin, California.

Winslow, M. A., 1983, Clastic dike swarms and the structural evolution of the foreland fold and thrust belt of the southern Andes: Geological Society of America Bulletin, v. 94, no. 9, p. 1073-1080.

**Appendix B: Complete version of Table 5-1**

<b>Location</b>	<b>Basin</b>	<b>Specific area</b>	<b>Inclined parent body</b>	<b>Time of remobilization</b>	<b>Basin setting at time of remobilization</b>	<b>Location of remobilized sands</b>	<b>Trigger mechanisms unrelated to basin type</b>	<b>References</b>
<b>South Africa</b>	Karoo basin				Inverted passive margin	Toe of slope (Proximal in the basin floor lobes, linked to pinchouts)		(Cobain et al., 2015; Cobain et al., 2017)
<b>Angola</b>	Lower Congo Basin		Yes	Miocene – Pliocene transition	Inverted passive margin (flank uplift generated by salt diapirism)	Toe of slope (Updip fringe of submarine lobe)		(Monnier et al., 2014; Oluboyo et al., 2014)
<b>Ross land, Antarctica</b>	Victorialand Basin			Lower Oligocene	Inverted passive margin		Glacial trigger	(Passchier, 2000; Parnell et al., 2013)
<b>Australia</b>	Dampier Sub-basin				Inverted passive margin			(Dharmayanti et al., 2006)
<b>California</b>	San Joaquin Basin	Panoche and Tumey Hills	Yes	Lower Palaeocene and Eocene	Convergent (Compressional) margin	Above crest of sloping permeable sediments (Cold-seep)		(Schwartz et al., 2003; Minisini and Schwartz, 2007; Vigorito et al., 2008; Cartwright, 2010; Vétel and Cartwright, 2010; Palladino et al., 2016)
<b>Southwestern California</b>		Dana Point	Yes	Miocene	Transform (Compressional) margin			(Bouroullec et al., 2010)

<b>California</b>	Santa Cruz Basin	Santa Cruz	Yes	Miocene	Transform (Compressional) margin	Basin margin	(Boehm and Moore, 2002; Thompson et al., 2007; Sherry et al., 2012)
<b>Canada</b>		Quebec	Yes		Inverted passive margin	Slope	(Hiscott, 1979)
<b>Southern Chile</b>	Magellanes basin		Yes		Retroarc foreland basin (Convergent regime)		(Winslow, 1983; Hubbard et al., 2007)
<b>Canada</b>		Lake Erie Bluffs, Bradtville, Ontario		Holocene		Glacial trigger	(Dreimanis and Rappol, 1997)
<b>China</b>	Bohai Bay Basin				Inverted Passive margin	Toe of slope	(Zhang et al., 2016)
<b>Western Colombia</b>		Colombian Andes		Plio-Pleistocene	Convergent (Compressional) margin		(Neuwerth et al., 2006)
<b>The Falkland Islands</b>						Glacial trigger	(Hyam et al., 1997)
<b>The North Sea (UK)</b>	The Faroe-Shetland Basin			Mid – Late Miocene	Inverted passive margin	Flank, Slope, toe of slope	(Mitchell et al., 1993; Hall and Bishop, 2002; Davies et al., 2004; Shoulders and Cartwright, 2004; Shoulders et al., 2007; Cartwright, 2010)
<b>South–East France</b>	Vocontian Basin			Cretaceous (Aptian to Mid Albian)	Inverted passive margin	Slope, toe of slope	(Parize and Friès, 2003; Parize et al., 2007)

					(channel banks)	
<b>East Greenland</b>	Southern part of the East Greenland rift basin	Jameson Land	Late Oxfordian to the Volgian	Inverted passive margin		(Surlyk and Noe-Nygaard, 2003; Surlyk et al., 2007)
<b>Southern Iceland</b>	Sólheimajökull		Holocene		Glacial trigger	(Le Heron and Etienne, 2005)
<b>India</b>	Krishna-Godwari basin	Bay of Bengal	Pliocene	Inverted passive margin	Slope and toe of slope	(Shanmugam et al., 2009)
<b>Ireland</b>	Western Irish Namurian basin	County Clare	Carboniferous	Inverted passive margin	Slope and toe of slope	(Gill and Kuenen, 1957; Jonk et al., 2007a)
<b>Western Ireland</b>		Rosroe Peninsula		Inverted passive margin	Toe of slope	(Archer, 1984)
<b>Israel</b>	Dead Sea Basin		Pleistocene-Holocene	Convergent (Compressional) margin		(Porat et al., 2007; Alsop and Marco, 2011)
<b>Eastern Mediterranean</b>	Levant Basin	Outside the coast of Israel	Pliocene and Pleistocene	Convergent (Compressional) margin		(Frey-Martinez et al., 2007)
<b>Italy</b>		Apennines,	Late Miocene	Convergent (Compressional) margin		(Gamberi, 2010; Huuse et al., 2010)
<b>Japan</b>		Boso Peninsula	Pliocene or later	Convergent (compressional) margin	At the toe of the trench-slope basin	(Ito et al., 2016)
<b>Libya</b>	Murzuque Basin		Devonian		Hydrothermal event	(Moreau et al., 2012)

<b>Southwestern Nigeria (Gulf of Guinea)</b>	Dahomey (Benin) Basin			Cretaceous or later	If the injection occurred during Cretaceous, it happened during rifting	Slope	(Davies, 2003; Olabode, 2006)
<b>The North Sea, (Norway)</b>	The North Sea Basin		Yes and no	Palaeocene, Early Eocene, Oligocene, Miocene	Inverted passive margin	Flank and toe of slope	(Jenssen et al., 1993; Lonergan et al., 2000; Faleide et al., 2002; Jonk et al., 2005a; Cartwright, 2010; Christensen, 2015; Rundberg and Eidvin, 2016)
<b>New Zealand</b>	Taranaki Basin						(Hurst et al., 2003b; Morley and Naghadeh, 2017)
<b>Portugal</b>	Algarve Basin	SW Iberia		Jurassic (Early Pliensbachian)	Extensional tectonics/rifting		(Ribeiro and Terrinha, 2007)
<b>Mainly covers Brazil, but also Uruguay, Argentina and Paraguay</b>	Paraná Basin	Paraná volcanic province		Cretaceous		Hydrothermal event	(Hartmann et al., 2013; Pinto et al., 2015)
<b>Russia</b>		Southeast Schmidt Peninsula, Sakhalin,	Yes	Miocene	Transform (compressional) margin		(Macdonald and Flecker, 2007)
<b>North Sea (UK)</b>	North Sea Basin	Outer Moray Firth		Eocene	Inverted passive margin		(Lonergan et al., 2000; Duranti and Hurst, 2004; Huuse et al.,



<b>Saudi Arabia</b>	Red Sea Coastal Plain	South Jeddah		Holocene	Peritidal setting	Coastal plain	Tidal pumping	2005; Cartwright, 2010) (Taj et al., 2014)
<b>Scotland</b>		Midland Valley	Yes		Convergent (compressional) margin			(Jonk et al., 2005b; Jonk et al., 2007b; Underhill et al., 2008)
<b>West Texas</b>	Marathon Basin		Yes	Carboniferous	Convergent (compressional) margin	In accretionary prism		(Diggs, 2007)
<b>Tunisia</b>	Maghrebian Flysch Basin	Tabarka	Yes	Oligo-Miocene	Convergent (compressional) margin	Lateral injection originating in channel complex in upper slope environment		(Thomas, 2011)
<b>The U.S.</b>	The Colorado Plateau	Utah		Jurassic	Convergent (compressional) margin		Volcanism?	(Chan et al., 2007)
<b>The U.S.</b>	Eastern Bighorn Basin	Wyoming		Cretaceous	Convergent (compressional) margin	The western flank and the nose of of the Sheep Mountain Anticline		(Beyer, 2015)